12-2013

SPECIES DISCRIMINATION, SYSTEMATICS, AND ONTOGENY OF BLASTOIDEA

James William Atwood
University of Tennessee - Knoxville, jatwood2@utk.edu

To the Graduate Council:

I am submitting herewith a dissertation written by James William Atwood entitled "SPECIES DISCRIMINATION, SYSTEMATICS, AND ONTOGENY OF BLASTOIDEA." I have examined the final electronic copy of this dissertation for form and content and recommend that it be accepted in partial fulfillment of the requirements for the degree of Doctor of Philosophy, with a major in Geology.

Colin D. Sumrall, Major Professor

We have read this dissertation and recommend its acceptance:

Michael L. McKinney, Robert Riding, Johnny A. Waters

Accepted for the Council:

Carolyn R. Hodges

Vice Provost and Dean of the Graduate School

(Original signatures are on file with official student records.)

SPECIES DISCRIMINATION, SYSTEMATICS, AND ONTOGENY OF BLASTOIDEA

A Dissertation Presented for the

Doctor of Philosophy

Degree

The University of Tennessee, Knoxville

James William Atwood

December 2013

DEDICATION

For Mom and Pop.

ACKNOWLEDGEMENTS

This dissertation would not have been possible without the help of many people. It is to these people that I owe a debt of gratitude. My sincerest apologies to anyone that I may have forgotten to mention, it was not my intention to slight you.

To my advisor Colin Sumrall, thank you for being an amazing mentor and teacher. I am grateful that a serendipitous set of events led me to you for an education, and I am truly honored to have been your student. You are an amazing scholar and friend.

To Johnny Waters, thank you for advice, knowledge, and the chance to work abroad with you. I am very appreciative for the opportunities and help along the way. To Michael McKinney, Brian O'Meara, and Robert Riding, thank you for sound advice and guidance through this process. I couldn't have asked for a better Committee.

Thank you to Brenda Hunda at the Cincinnati museum and Dan Levin/Mark Florence at the Smithsonian for your valuable time and assistance in collections. You have all made this process a lot less painful.

Thank you to René Lewis who was the best officemate ever. Thank you for advice, help, and putting up with me for years in a confined space. You made every day better. To Troy Fadiga, thank you for many lengthy discussions about systematics, morphometrics, and meatless food. Your help has been invaluable. You both are real friends.

To Mom and Pop, thank you for always being there, believing in me, and loving me. To Jay, you are the reason I started and stayed in college. To Tami and Kate, you are the reason I finished. I love you all.

To the following people who have helped me along the way, thank you, you have my gratitude: Charlie Mason, Eric Hogan, Geoff Gilleaudeau, Miles Henderson, Bobby Ford, Max Schnuck, Tim Paton, Hannah Johnson, Jackie Langille, Melody Branch, Teresa Parrott, Ryan

Roney, and Megan Ennis.

Lastly, I am indebted to those who provided financial support for this project: The University of Tennessee Department of Earth and Planetary Science, National Science Foundation Grant No. EAR-0745918, National Science Foundation - Assembling the Echinoderm Tree of Life Grant, DEB-1036260.

ABSTRACT

Blastoids are ideal model organisms with which to study evolutionary processes because nearly all of the skeletal elements are shared among all taxa, there have been recent advances in the understanding of blastoid homology, and they are more commonly preserved fully inflated than any other blastozoan. Because of this homology and preservation, blastoids are the perfect candidate for studies involving geometric morphometrics and systematics. But the potential of blastoids to be a model clade has been extremely hampered by the lack of a modern phylogenetics and classification.

The focus of this dissertation is to increase our understanding of blastoid species delineation, ontogeny, and systematics. The first chapter examines the blastoid population at one locality. Geometric morphometrics was used to show that four closely related blastoid species could be delineated statistically with very little error. Chapter two uses geometric morphometrics to examine the ontogenies of six different *Pentremites* species that were collected at four different localities in Indiana, Illinois, Kentucky, and Tennessee. It was possible using these techniques to describe similarities in their ontogenies and well as how individual plates develop. The final chapter of this dissertation focuses on systematics of blastoids. For this study, blastoids were examined from all over the world and were used to conduct a maximum parsimony analysis. These robust results were then compared to earlier work.

TABLE OF CONTENTS

List of Tables

List of Figures

I. INTRODUCTION

OVERVIEW

Over time, many problems have persisted in invertebrate paleontology including: how to quantitatively discriminate between closely related species, how to handle a lack of informative characters for phylogenetic analyses, and how specific elements of an organism vary in response to processes such as growth, evolution, or environment. This dissertation examines these processes by examining shape within and between closely related species, and through ontogeny. Furthermore, insights found while studying shape were used to reevaluate blastoid phylogeny in the light of new ideas concerning skeletal homologies and refined interpretations of character states. Blastoids, the study group for this work, are an extinct clade of stemmed echinoderms that originated by the Ordovician, reached their maximum diversity by the Mississippian, and went extinct during the End Permian extinction event. Blastoids are the most well-known, longest-lived, most diverse group of Blastozoa.

Geometric morphometrics as a branch of statistics has only been recognized for about two decades (Bookstein 1991). Geometric morphometrics is the combination of mathematical shape theory, descriptive statistics, and inferential statistics. Landmark analysis, within the framework of geometric morphometrics, has been used for shape analysis since its conception.

Shape is defined as all geometric information that remains when location, scale, and orientation effects are filtered from an object (Zelditch et al. 2004). Landmark analyses are commonly utilized in geometric morphometrics because they have the greatest statistical power, the lowest mean-squared error, and impose minimal constraints on the patterns of variation that can be detected (Adams, et al. 2004). Landmark analysis describes shape by

utilizing the spatial relationships of homologous points rather than linear measurements. This type of morphometrics allows for shape analysis by first utilizing a Procrustes alignment which, in this case, is a generalized least squares superimposition that uses a least squares fitting criterion to minimize the sum of squares distances over all landmarks over all specimens (Zelditch et al. 2004). Once points from individuals have been Procrustes aligned, all of the unneeded information including location, scale, and orientation has been removed leaving shape as the only variable.

Typically after the datasets have been Procrustes aligned, these data can be used to answer specific questions or in exploratory analyses to determine if any patterns in the dataset are initially evident. Questions may refer to individual diagnoses, detection of group differences or similarities, effects of growth (ontogeny), or covariances of form (Bookstein 1991; Zelditch et al. 2004).

To effectively use these powerful 3D methods, critical attributes must be present within the fossil population. Specimens must be: three dimensionally preserved, bear easily recognizable homologous traits, and the population must be unbiased with respect to shape. First, blastoids are notable among blastozoan echinoderms for bearing a robust skeletal structure that is often preserved fully inflated. Second, the highly conserved skeletal structure of blastoids results in a universal set of homologous landmarks in the form of three plate junctions that are type I landmarks. Finally, collecting methods used throughout this study were made specifically with the conservation samples that are unbiased with respect to shape.

A further aspect of blastoids that allowed this project to be completes is that numerous blastoid localities produce large numbers of specimens (Waters et al. 1985;

Dexter et al. 2009; Atwood and Sumrall 2012). As with all statistical arguments, geometric morphometrics is sensitive to sample size. By visiting the richly productive localities sufficient sample sizes were accumulated to provide robust statistical analyses. Because specimens were collected specifically for this study, it could be assured that unbiased samples were obtained with which to work.

In 1991, Foote was able to utilize geometric morphometrics to examine morphological diversity and taxonomic diversity to much success. It was my contention that much new information could be gleaned from utilizing these techniques as well as set a future stage for other work in Blastoidea as well as other invertebrate organisms. The advent of new technologies such as 3D laser scanning and new software packages such as XYZ facilitated the collection of large quantities of data rapidly for analysis.

Lastly, in order to move forward in placing blastoid shape into an evolutionary framework, a reasonable phylogenetic reconstruction needed to be completed. This will allow at the study of the evolution of shape and heterochronic change within the evolutionary history of the clade. The phylogenetic analyses will also be used in the ongoing Assembling the Echinoderm Tree of Life project. Blastoid systematics have been explored in the past but many question still persist because of earlier less robust methodologies, not being inclusive of all groups, and lack of traditional informative characters (Breimer & Macurda 1972; Waters & Horowitz 1993; Bodenbender 1995; Bodenbender & Fisher 2001; Sumrall & Brochu 2003; Sumrall & Waters 2012). In conjunction with recent studies on blastoid homology, it is believed that significant headway has been made in this problematic clade (Sumrall and Waters, 2012).

This dissertation examines species discrimination and the Ontogenies of

Pentremites blastoids with geometric morphometrics as well as the final chapter looking at blastoid systematics. It is divided into parts (II – IV), representing individual research papers, which either are or will be submitted to peer-reviewed journals. This dissertation has been prepared in a style and format consistent with the Journal of Paleontology.

Part II – Species discrimination of Glen Dean *Pentremites* blastoids

A three-dimensional (3D) analysis using geometric morphometrics allowed the reexamination of an old interpretation of species diversity at the Pennyrale Parkway locality and make breakthroughs in understanding blastoid morphology. This study examined four closely related species of blastoid using geometric morphometrics to discriminate between species. Specimens for this study were collected from a single shale unit in the Upper Mississippian Glen Dean Formation in Kentucky. A Next Engine laser scanner was used to acquire 3D images for all specimens. Data were analyzed using the R (language and environment for statistical computing and graphics). Mixture modeling allowed us to identify and separate all four apomorphically-separated species based on shape alone. Three new species were discovered during this study, including: *Pentremites fredericki*, *P. meganae and Diploblastus fadigai*. This chapter is already published in the Journal of Paleontology (Atwood and Sumrall, 2012).

Part III – Ontogeny of *Pentremites* blastoids

This study utilizes geometric morphometrics to examine the ontogeny of the blastoid genus *Pentremites*. Specimens of *Pentremites fredericki*, *P. godoni*, *P. pyriformis*, *P. spicatus, P. symmetricus*, and *P. tulipaformis* were collected from four Upper Mississippian localities in Kentucky, Indiana, Tennessee, and Illinois, USA. Three-dimensional images were acquired with the nextengine laser scanner from randomly selected specimens across the ontogeny

of each species and coordinates were collected for a series of homologous landmarks that fully describe blastoid morphology through ontogeny. Analysis of the data show that all species in this study share a common ontogenetic pathway and shape varies significantly with both size and by species. This result suggests that the initial shape of the theca just post metamorphosis has a strong influence on the mature thecal shape. This paper is to be submitted to the journal Lethaia.

Part IV – Blastoid systematics

Since the recognition of Blastoidea as a distinct echinoderm, paleontologists have proposed many different classification schemes and phylogenetic relationships for the clade. Until now, phylogenetic inferences have been made utilizing relatively few characters, limited taxon sampling, poor methodology, and a lack of rigorous methodologies. The aim of this chapter was to refine our understanding of blastoid phylogeny conducting a new maximum parsimony analysis with a fully revised set of characters. This ground-up phylogenetic study was conducted as part of the Assembling the Echinoderm Tree of Life project, to provide a robust, baseline phylogenetic hypothesis for the clade.

The maximum parsimony analysis included 21 ingroup taxa and three outgroup taxa coded for 49 characters and 139 informative character states. Taxa were coded using exemplar species drawn from across blastoids to cover most of the major proposed lineages. All characters were unordered and equally weighted. A branch and bound search retrieved two most parsimonious trees of a tree length of 107 steps, consistency index of 0.53, and retention index of 0.73.

In this study *Macurdablastus* codes as a fissiculate blastoid based on the manifestation of respiratory structures and lack of spiracles. Because *Macurdablastus* is sister taxon to Troosticrinidae, spiraculates are polyphyletic being derived twice on the tree from a paraphyletic Fissiculata. Non-troosticrinid spiraculates form a clade. Nucleocrinids, schizoblastids and the granatocrinid *Mesoblastus* form a clade that is sister taxon to a clade containing the granatocrinid *Granatoblastus* nested within Orbitremitidae (paraphyletic), Diploblastidae and Hyperoblastidae. These two clades form a monophyletic group that is sister taxon to a clade containing Ambolastomatidae and Pentremitidae. Non-*Macurdablastus* fissiculates form a clade. Astrocrinids and neoschismitids form a clade that is sister taxon to a clade containing codasterids nested within a paraphyletic Orophocrinidae. These relationships suggest that ordinal and familial classifications in Blastoidea are in need of revision. A comparison of tree topologies with previous studies (Bodenbender and Fisher 2001; Sumrall and Brochu, 2003) shown that given the revised matrix, the results presented here are significantly more parsimonious than previous studies. This paper is to be submitted to the journal Systematic Paleontology.

REFERENCES

ADAMS, D. C., F. J. ROHLF, AND D. E. SLICE. 2004. Geometric morphometrics: ten years of progress following the 'revolution'. Italian Journal of Zoology, 71(1):5-16.

ATWOOD, J. W., AND C. D. SUMRALL. 2012. Morphometric Investigation of the Pentremites Fauna from the Glen Dean Formation, Kentucky. Journal of Paleontology, 86(5):813-828.

BODENBENDER, B. 1995. Morphological, crystallographic, and stratigraphic data in cladistic analyses of blastoid phylogeny, Contributions from the Museum of Paleontology. University of Michigan, 201-257.

BODENBENDER, B. E., AND D. C. FISHER. 2001. Stratocladistic analysis of blastoid phylogeny. Journal of Paleontology, 75(2):351-369.

BOOKSTEIN, F. L. 1991. Morphometric tools for landmark data: geometry and biology. Cambridge University Press, Cambridge, New York etc, i-xvii, 1-435

BREIMER, A., AND B. MACURDA. 1972. The Phylogeny of Fissiculate Blastoids. Verhangelingen der Koninklijke Nederlandsche Akademie van Wetenschappen, Afdeeling Natuurkunde Eerste Reeks, Deel 26 (3):1-390.

DEXTER, T. A., C. D. SUMRALL, AND M. L. MCKINNEY. 2009. Allometric strategies for increasing respiratory surface area in the Mississippian blastoid Pentremites. Lethaia, 42(2):127-137.

FOOTE, M. 1991. Morphological and Taxonomic Diversity in a Clade's History: The Blastoid Record and Stochastic Simulations. Contributions from the Museum of Paleontology, 28(6):101-140.

SUMRALL, C. D., AND C. A. BROCHU. 2003. Resolution, sampling, higher taxa and assumptions in stratocladistic analysis. Journal of Paleontology, 77(1):189-194.

SUMRALL, C. D., AND J. A. WATERS. 2012. Universal Elemental Homology in Glyptocystitoids, Hemicosmitoids, Coronoids and Blastoids: Steps Toward Echinoderm Phylogenetic Reconstruction in Derived Blastozoa. Journal of Paleontology, 86(6):956-972.

WATERS, J. A., AND A. S. HOROWITZ. 1993. Ordinal-level evolution in the Blastoidea. Lethaia, 26(3):207-213.

WATERS, J. A., A. S. HOROWITZ, AND D. B. MACURDA. 1985. Ontogeny and Phylogeny of the Carboniferous Blastoid Pentremites. Journal of Paleontology, 59(3):701-712.

ZELDITCH, M. L., D. L. SWIDERSKI, D. H. SHEETS, AND W. L. FINK. 2004. Geometric Morphometrics for Biologists. Elsevier Academic Press (USA), San Diego.

II. MORPHOMETRIC INVESTIGATION OF THE *PENTREMITES* FAUNA FROM THE GLEN DEAN FORMATION, KENTUCKY

This chapter is a reformatted version of a paper, by the same name, published in the Journal of Paleontology.

ATWOOD, J. W., AND C. D. SUMRALL. 2012. Morphometric Investigation of the Pentremites Fauna from the Glen Dean Formation, Kentucky. Journal of Paleontology, 86(5):813-828.

ABSTRACT

New techniques involving three-dimensional (3D) data collection and landmark analysis provide an opportunity to make breakthroughs in understanding blastoid morphology. This pilot study examines four species (*Pentremites pyriformis*, *P. tulipaformis*, *P. fredericki* n. sp. and *P*. *meganae* n. sp.), using 3D morphological variation and geometric morphometrics to discriminate between species. All specimens were collected from a single shale unit within the Upper Mississippian Glen Dean Formation near Hopkinsville, Kentucky. A 3D laser scanner was used to acquire 3D images for all specimens. Conservative blastoid thecal plating allowed the collection of 3D coordinates for a series of homologous landmarks from these laser images that fully describe specimen morphology. Data were analyzed using the R (language and environment for statistical computing and graphics) packages SHAPES and MCLUST. Mixture modeling identified and separated all four species based on shape alone. In addition, three new species were uncovered during this study, including: *Pentremites fredericki*, *P*. *meganae and Diploblastus fadigai*.

INTRODUCTION

Morphometric techniques in invertebrate paleontology have many problems including: how to quantitatively discriminate species, handle a lack of informative characters for phylogenetic analysis of closely related species and how individual elements of an organism vary in response to growth, evolution, environment and injury. New techniques

involving three-dimensional (3D) data collection and landmark-based geometric morphometrics provide an opportunity to improve the understanding of these issues. Advances in shape theory, imaging and statistical analysis used in conjunction with proven traditional methods will allow the expansion of knowledge to almost any clade.

Although many studies of fossil invertebrates have examined morphology quantitatively, relatively few have utilized 3D landmark techniques. Three dimensional landmark studies have largely been limited to larger (vertebrate) organisms (Frost et al., 2003; Slice, 2007; Mitteroecker and Gunz, 2009) whereas 2D methods have been dominantly used for mostly smaller (invertebrate) organisms (Adrain and Westrop, 2006; Hollander et al., 2006; Webber and Hunda, 2007; Anderson et al., 2008). Thecae of blastoids, the focus of this manuscript, are bud-shaped to globular in gross morphology and best analyzed in a three-dimensional framework. Foote (1991) was the first to utilize 3D morphometrics in blastoids where he examined taxonomic richness and morphological diversity. The present study expands the use of 3D shape analysis in blastoids to species discrimination, using laser imaging and geometric morphometrics in conjunction with apomorphy-based methods. This combined approach provides more insight into blastoid variation and how species are delineated.

The blastoid *Pentremites* is an icon of North American Mississippian faunas, at times becoming the dominant macroscopic organism in a given environment. Morphologically, thecal shape, such as height-to-width ratios, is variable and multiple species of *Pentremites* commonly occur within a given community (Waters et al., 1985). It is, therefore, an excellent model organism with which to investigate population variation and species delineation using geometric morphometrics.

Geometric morphometric techniques rely on a robust series of landmarks for analysis. Blastoids are ideal for such studies because they have a very conservative thecal plate construction and thecae are commonly preserved in 3D. Blastoid thecae have multiple three-plate junctions providing almost entirely type 1 landmarks, defined as a discrete juxtaposition of tissues (Bookstein, 1991).

In this study three new blastoid species are described. *Pentremites meganae* n. sp. is a pyriform species diagnosed by a large stem facet, flat to convex ambulacra and summit plates that extend well above the deltoids. *Pentremites fredericki* n. sp. is a godoniform species that is diagnosed by convex ambulacra, large secondary deposits on the theca, and pits along the side plate/lancet suture. These two species are discrete apomorphically and morphometrically from the more common *P. pyriformis* and *P. tulipaformis* that occur at the study locality. *Diploblastus fadigai* n. sp. is diagnosed by strong ornamentation of the deltoid/radial plates, and large stem facet diameter.

PREVIOUS INVESTIGATIONS AND STRATIGRAPHY

The Upper Mississippian (Chesterian) Glen Dean Formation yields large numbers of extraordinarily well-preserved fossils (Butts, 1917; Nelson et al., 2002). This study focuses on blastoid collections derived from a single section of Glen Dean Formation exposed in a road cut along the Pennyrile Parkway in Christian County, southwestern Kentucky. The locality lies along the right hand side of the northbound lane. The lowermost 1-2m of the exposed section are highly weathered, fissile, fossiliferous, shale with minor limestone interbeds. The limestone is grayish brown on fresh faces and weathers light gray. The shale is light olive gray on fresh faces and weathers dark gray. The uppermost 3-4m of the

section are a thick, pale brown, oolitic limestone shoal. The Glen Dean Formation is overlain by the Tar Springs Sandstone and overlies the Hardinsburg Sandstone. This locality produces large quantities of echinoderms, in particular well-preserved *Pentremites*. The remainder of the fauna includes abundant fenestrate bryozoans and crinoids, with lesser amounts of ostrocods and brachiopods.

A previous investigation by Waters, et al. (1985) concluded that two blastoid species, *Pentremites tulipaformis* (a godoniform morphotype characterized by a short pelvis) and *P. pyriformis*, (a pyriform morphotype characterized by a long pelvis) are present at this locality. Waters, et al. (1985) utilized two-dimensional morphometrics, consisting of scatter plots of measured thecal dimensions to reach their conclusions (Fig. II-1). However, a high degree of variance in these data makes a clean separation of species difficult. This earlier study provides an opportunity to determine if advances in imaging techniques and shape analysis using geometric morphometrics allow higher precision in species identification.

Although Glen Dean fauna has two *Pentremites* morphotypes (Waters, et al., 1985), four species are present. The godoniform species *P. tulipaformis* bears small, incorporated spines at the ambulacral tips and flat interambulacra. It is separable from the godoniform *P. fredericki* n. sp. that lacks spines at the ambulacral tips and bears concave interambulacra. The pyriform *P. pyriformis* bears concave ambulacra and a very small stem facet. It is separable from the pyriform *P. meganae* n. sp. that bears convex ambulacra and a greatly enlarged stem facet. These four *Pentremites* species are separable by diagnostic apomorphic morphologies providing a framework to test whether geometric morphometrics can delineate these same four species by shape alone.

METHODOLOGY

Collection.—Variation within a species of organisms is multicausal and can confound the understanding of diversity, population dynamics and organismal relationships. Within populations, intrinsic sources of variability include: genetic variation, sexual dimorphism and ontogenetic state, whereas extrinsic sources may include ecophenotypic variation. In fossil species this is further complicated by variation resulting from temporal and geographic mixing of populations and preservational issues such as compaction. To simplify these issues for this study, the focus was limited to the phenotypic variation within a single population.

Museum collections were not used in this study because they are often biased samples of large and well-preserved specimens that may have been collected in a region rather than a single stratigraphic horizon. There are no methods to determine if the specimens were derived from culled lots that may be biased by shape to include "typical" examples of species from formations or localities. For this reason, new collections were assembled to assure that temporal and environmental mixing, environment, and shape could be controlled. Study of ontogenetic variation was left for a future manuscript.

Paramount to the collection of material was assuring that methodology did not bias the distribution of shape within the species populations. Specimens were collected from one locality thereby minimizing geographic and ecophenotypic variation. Since the locality was small and was limited to a single well-defined 1.5m stratigraphic interval, temporal and environmental variation is minimized. At this locality, all visible blastoid specimens (typically larger specimens) were surface collected and additional (typically smaller specimens) were collected in bulk samples of weathered shale. This bulk material was dry

sieved into five gallon buckets (18.92L) to remove any larger rock from the samples. Approximately 30 - 40 buckets of bulk material were collected yielding a sample weight of 600-800 Kg (1320-1760 lbs). Samples were washed in water and hydrogen peroxide to break down the shale matrix so that all contained blastoids could be retrieved via microscope and handpicking from the fossiliferous residue. This method allowed the collection of large numbers of blastoids including full ontogenies. By using this method, Pennyrile Parkway samples are not biased according to shape. Similar methods were used at the Sulphur, Indiana and Floraville, Illinois localities to great success (Dexter et al., 2009).

From the larger sample, of approximately 5,000 specimens, individual blastoids were screened for obvious deformation resulting from sediment compaction. This was accomplished visually by looking for deviation from the regular pentameral symmetry of specimens. If a blastoid showed nearly perfect radial symmetry, it was considered to be usable. Teratological specimens, including specimens with four ambulacra were also removed. Culling specimens in this manner leaves only phenotypic variation, sexual dimorphism and ontogenetic variation as the dominant sources of variance in the populations. External sexual dimorphism is unknown in *Pentremites*, but has been documented internally in the construction of the CD side hydrospires (Katz and Sprinkle, 1976). Ontogenetic variation was limited by removing, from consideration, all but the largest 10 percent of blastoid specimens in terms of thecal height. The resulting subsample, therefore, included specimens whose variation results predominantly from the natural phenotypic expression of the genome.

From all usable specimens, a study sample was selected for measurement. Specimens of each species based on apomorphic characters were chosen using a random number generator that was set to the population size and specimen numbers. Selected specimens were inspected under the microscope to insure that all of the landmarks could be identified. If a specimen was damaged so that a landmark was unrecordable, it was replaced by another specimen at random. A total of 52 specimens were analyzed in this study. Based on apomorphic characters, 40 of these were classified into the two dominant species (20 of each *P. tulipaformis* and *P. pyriformis*). Because of the scarcity of *P. fredericki* n. sp. and *P. meganae* only six specimens each were available for study. To aid in the recording of data, landmarks were marked with a micro pen on specimens under high magnification allowing their position to be seen on the 3D specimen images.

Analysis.—A 3D image of each specimen was acquired using the Nextengine 3D Laser Scanner at the University of Tennessee. Scans were made at the highest possible resolution, of 0.127mm. Only the A-ray was scanned on each specimen. Each image was composed of three scans that were 60 degrees apart to insure total coverage of the A-ray. From these 3D images X, Y, Z coordinates of landmarks (modified from Foote, 1991) were recorded. These landmarks are morphologically common to all species of known blastoids, and fully describe the morphology of the specimens in 3D (Fig. II-2). All landmarks were type I (sensu stricto Bookstein, 1991), being positioned at three plate junctions of thecal or ambulacral plates except landmark 6 which was type 2.

Landmark data were collected from the models using the imaging program MESHLAB (Cignoni et al., 2008) and analyzed using R (language and environment for statistical computing and graphics). Landmark configurations were aligned using a full

Procrustes superimposition that removed differences in location, scale, and orientation using the R package SHAPES (Bookstein, 1991; Zelditch et al., 2004; Dryden, 2007). This left shape variables as the only information being examined.

RESULTS

After implementing the Procrustes superimposition, the first five principal components from the SHAPES output file were used for the remainder of the analysis. These principal components explain 94.1 percent of the variation in the population and were deemed sufficient for the study. Morphological groupings were identified from a model based cluster analysis using these principle components in the R package MCLUST. The models assumed an underlying Gaussian distribution of the data set. Unlike canonical variate analyses and discriminant function analyses, mixture-modeling packages, such as MCLUST, need no prior specimen identification to classify clusters. Instead, MCLUST uses an expectation-maximization algorithm for maximum-likelihood estimation of multivariate mixture models (Fraley and Raferty, 2002). Model parameterizations utilized by MCLUST to search for morphological clusters include the distribution, volume, shape and orientation of the data in multivariate space.

Once the expectation-maximization procedure was completed, the choice between competing models was made using the Bayesian information criterion (BIC) and each individual specimen is assigned to a group with an estimated uncertainty. The BIC is the value of the maximized likelihood with a penalty for the number of parameters, and allows comparison of models with various parameterizations and clusters. The larger the BIC value (i.e. the value closest to zero in this case), the stronger the evidence is for the model

(Fraley and Raferty, 2002). Ninety models were examined during this process (10 different models with various combinations of parameterization and 1-9 components).

A list of the five most optimal models with their associated BIC scores and model parameterizations is shown in Table 1. The single most optimal model, (bold in Table 1), is the EII model with a BIC score of -545.818. This model of the study population confidently identified four subpopulations. All four apomorphy-based species are in separated clusters with a pyriform group and godoniform group. In this case, each subpopulation is identified as an individual *Pentremites* species with only three misclassified specimens (i.e. specimens which received different species assignments when assessed utilizing apomorphic characters). Four species are recovered by all of the best-supported models for the number of components in the dataset.

Specimens were plotted along the first two principal components with the optimal model (EII) species classification, represented by a different symbol (Fig. II-3.1). Axes 1 and 2 represent 74.80 percent and 8.41 percent of the variance, respectively. Component means are marked and ellipses with axes are drawn corresponding to their covariances. Three misclassified specimens are denoted by open symbols. Figure II-3.2 is the projection of the specimen data showing classification uncertainty with larger symbols indicating increasing uncertainty in species classification. In this model, the misclassified specimens are among the most uncertain, indicating suitability of the cluster model for the data as in the apomorphy classified.

SYSTEMATIC PALEONTOLOGY

Class BLASTOIDEA Say, 1825

Family PENTREMITIDAE d'Orbigny, 1852

Genus PENTREMITES Say, 1820

PENTREMITES MEGANAE n. sp.

Figs. II-4.1-4.18, 5.1-5.3

Pentremites pyriformis Say, 1825. GALLOWAY AND KASKA, 1957. pl. 4, figs. 33, 34 and 37.

Pentremites pyriformis Say, 1825. BEAVER, 1967. P. 304.

Diagnosis.—Large pyriform *Pentremites* with parabolic vault bearing flat to convex ambulacra; flat interambulacra; large stem facet diameter; vault/pelvis ratio approximately 0.6 for less mature specimens and 1.00-1.05 for mature specimens.

Description.—Theca large, up to 38 mm high on largest specimens, elongate with conical pelvis and parabolic vault in lateral view, occasionally slightly more inflated (Fig. II-4.1, 4.3, 4.9, 4.11); pelvis elongate, broad, conical with convex outline; vault elongate parabolic with straight to slightly convex outline; vault-pelvis ratio ranges from approximately 1.00 to 1.05 on mature larger to approximately 0.60 on smaller specimen; outline in oral view rounded pentagonal with slightly convex ambulacra on more mature specimens, flat ambulacra on juvenile specimens (Fig. II-4.2, 4.4, 4.10, 4.16); lateral edges of ambulacra seated slightly below surface of surrounding plates; summit flat, projecting above tips of deltoid bodies.

Basalia three, in normal position, with azygous basal in AB interray, elongate, confined to lower half of pelvis on theca (Figs. II-4.5, 4.7, 4.14, 4.17,6.2), conical in lateral

view with outline being slightly convex to slightly concave (Fig. II-6.2); azygous basal quadrate, with straight lateral sutures and convex radial sutures (Figs. II-4.5, 4.7, 4.14, 4.17, 6.2); zygous basals pentagonal with straight lateral sutures and convex radial sutures (Figs. II-4.5, 4.7, 4.14, 4.17, 6.2); secondary deposits bulbous above stem facet on all basal plates; stem facet diameter ranges from 3.5 mm for mature specimens to 2.5 mm for younger specimens, equivalent of one quarter to three quarters of the basal circlet respectively; on some specimens up to three columnals fused to stem facet by secondary deposits; crenulations present on periphery of stem facet; center smooth with small central lumen extending into thecal cavity.

Radials five, very large, extending from half way up pelvis to near summit covering the whole middle of the theca (Fig. II-4.1, 4.3, 4.9, 4.15); radial roughly hexagonal with very wide parabolic radial sinus penetrating about half plate length; basal sutures vary from straight to very slightly convex; radial-radial sutures straight dominating the length of the radial plate; radiodeltoid suture convex; RB sector large, convex parallel to RB axis; RR sector slightly concave parallel to axis and flattens near radial-radial suture; RD sector slightly convex. Radials ornamented by growth lines that are best seen in the RD sector.

Deltoids six, including epideltoid and hypodeltoid, make up 15-20 percent of length in mature thecae, much smaller in immature thecae, barely appearing on the thecal surface (Fig. II-4.13, 4.16), RDR suture makes angle of approximately 100 degrees; deltoid lips small, together with epideltoid form edge of peristome and proximal most medial food grooves; deltoid body diamond-shaped with aboral edges slightly concave; deltoids on CD side of theca include epideltoid and hypodeltoid; hypodeltoid similar to deltoid bodies of other deltoids; spiracles and anispiracle teardrop to diamond-shaped bordered by deltoid

lips proximally, lancet plates laterally, and side plates distally separated from deltoid body by approximately six pairs of side plates; anispiracle much larger than other spiracles (Fig. II-4.12, 4.18).

Peristome central on summit, formed by four deltoids lips and epideltoid on anal side, pentagonal to roughly star shaped, transversely elongate showing footprint of 2-1-2 symmetry, slightly smaller than anispiracle.

Ambulacra five, relatively wide and moderate in length, usually extend approximately half length of theca, moderately curved along length and convex in mature specimens, short, wide and flat in younger specimens (Fig. II-4.6, 4.8, 4.11, 4.15); in mature specimens, highest points on ambulacra seated slightly above level of surrounding thecal plates, in younger specimens ambulacra seated well below level of surrounding thecal plates, widest point of ambulacra just above radiodeltoid suture; lancet plates lie along ambulacral midline within radial sinus and occupy approximately one-half ambulacra width, median groove (main food groove) resides medially on the lancet and transverses entire length of ambulacrum, lateral grooves positioned between adjacent ridges on lancet plate and extends between two slightly curved adjacent side plates ending at brachiole socket which creates notch in roughly oval brachiole facet placed between two adjacent side plate sets (Fig. II-6.1); lateral groove ornamented on each side by articulation grooves positioned orthogonally with respect to lateral groove, side plates set against lancet edge angled slightly proximally, hydrospire pore positioned between two adjacent brachiole facets along suture between side plates and outer side plates of adjacent sets, hydrospire pore groove positioned from hydrospire pore through a single side plate shallowing and ending nearly at median groove on lancet, outer side plate small and roughly half moon

shaped (Fig. II-6.1); hydrospires examined in serially sectioned paratype CMC IP64798 (not figured here) in ten groups, five folds per ambulacral side, folds protruding short distance into thecal cavity.

No stems or brachioles known for this species.

Etymology.—The species is named for Megan Ennis.

Types.—Holotype CMC IP53373 and paratypes CMC IP53374-53376.

Occurrence.—*Pentremites meganae* n. sp. is known from Glen Dean Formation (Upper Mississippian, Chesterian), 10 m-15 m above the base of the formation, along Pennyrile Parkway in Christian County, southwestern Kentucky.

Remarks.—*Pentremites meganae* n. sp. differs from other species of *Pentremites* by the convex ambulacra in mature specimens. Convex ambulacra are present only on a few other species that are not within the pyriform group. The large stem facet and convex pelvis are also diagnostic as is a very pentagonal outline resulting from flat to slightly concave interambulacral areas. This species has been previously noted as *Pentremites pyriformis* but is markedly different in all described aspects (Galloway and Kaska, 1957; Beaver et al., 1967). One teratological specimen is known in type series. This specimen has an unidentified pathology seen on distal portions of ambulacra A, B, C, E, radial edge near the affected area on the ambulacra deformed by the pathology (Fig. II-5.2, 5.3).

PENTREMITES FREDERICKI n. sp.

Figs. II-2, 7.1-7.29

Diagnosis.—Medium-sized godoniform *Pentremites* with flat to concave ambulacra; slightly concave to concave interambulacra; distinctive pits along side plate/lancet plate suture, relatively small hydrospire groove; vault/pelvis ratio approximately 1.00 for smaller specimens, 3.00-3.05 for mature specimens.

Description.—Theca globular with wide pelvis that narrows distally and parabolic vault in lateral view, occasionally seen more inflated (Fig. II-7.5, 7.7, 7.10, 7.12, 7.13, 7.20, 7.22); pelvis short, broad, slightly bulbous with concave outline; theca ranges in height to approximately 21 mm on larger more mature known specimens; vault elongate parabolic with a convex outline; vault-pelvis ratio ranges from approximately 3.00 to 3.05 on mature larger specimens, approximately 1.00 on most immature juveniles; outline in oral view star-shaped pentagonal with strongly concave interambulacra (Fig. II-7.1, 7.8, 7.9, 7.16, 7.18, 7.19, 7.27); ambulacra weakly to moderately concave on older specimens (Fig. II-7.8) becoming nearly flat in younger specimens (Fig. II-7.16); lateral edges of ambulacra seated slightly below surface of surrounding plates; summit rounded juveniles (Fig. II-7.12, 7.22), flat and slightly projecting in mature specimens (Fig. II-7.5, 7.7, 7.10, 7.13).

Basalia three, in normal position with azygous basal in AB interray, confined to lower third of pelvis on theca (Fig. II-7.4, 7.6, 7.11, 7.14, 7.21, 7.26, 7.29) slightly bulbous in lateral view (Fig. II-7.3, 7.7); zygous basals pentagonal in aboral view, with slightly convex edges on basal-basal sutures and slightly concave edges on basal-radial edges (Figs. II-7.4, 7.6, 7.11, 7.14, 7.21, 7.26, 7.29, 8.2); azygous basal quadrate in aboral view, with slightly concave edges on basal-basal sutures and convex edges on basal-radial sutures (Figs. II-7.4, 7.6, 7.11, 7.14, 7.21, 7.26, 7.29, 8.2); secondary deposits bulbous on all basal plates around stem facet; stem facet shared equally between three basals; relatively large, diameter

ranges from 2.0 mm for mature specimens to 1.75 mm for younger specimens equivalent to one fifth to one third of the basal circlet respectively, surface is crenulated around margin with smooth platform centrally and very small lumen piercing theca centrally at three plate junction; on one large specimen one columnal fused proximally on theca (Fig. II-7.3, 7.4, 7.7); crenulations present proximally on columnals while center is smooth with very small central lumen.

Radials five, very large, extending from one third the way up pelvis to very near summit covering middle of theca (Figs. II-7.5, 7.7, 7.10, 7.12, 7.13, 7.20, 7.22, 8.2); radial roughly hexagonal with a wide v-shaped radial sinus penetrating most of plate length; radial-basal sutures vary from near straight to very slightly convex; radial-radial sutures straight dominating the length of the radial plate; radiodeltoid sutures slightly curved; RB sector small, convex parallel to RB axis; RR sector lightly convex parallel to axis and flattens near radial-radial suture; RD sector slightly convex; radials ornamented by growth lines that are seen in the RB, RR and RD sectors.

Deltoids six including epideltoid and hypodeltoid, small, comprising 10-15 percent of length in mature thecae, much less in immature thecae, RDR suture makes angle of approximately 60-75 degrees; deltoid lips small, together with epideltoid form edge of peristome and proximal most medial food grooves, innermost edge usually pointed (Fig. II-7.9, 7.24); deltoid body roughly diamond shaped with aboral edges s-shaped; CD side of theca with, epideltoid and hypodeltoid; hypodeltoid similar to deltoid bodies of other deltoids; spiracles and anispiracle teardrop shaped bordered by deltoid lips proximally, lancet plates laterally, and side plates distally separated from deltoid body by approximately four pairs of side plates; deltoid septa very thin, divided spiracles internally

(Fig. II-7.24); anispiracle much larger than other spiracles (Fig. II-7.1, 7.8, 7.9, 7.16, 7.18, 7.19, 7.24).

Peristome central on summit, formed by four deltoids lips and epideltoid on anal side, pentagonal to roughly star shaped, transversely elongate showing footprint of 2-1-2 symmetry, considerably smaller than anispiracle.

Ambulacra five, wide and long, usually extend greater than three quarters of thecal length, curved along length and convex in mature specimens, short, wide and flat in younger specimens (Fig. II-7.2, 7.3, 7.15, 7.17, 7.23, 7.25, 7.28); in mature specimens, highest points on ambulacra seated slightly below level of surrounding thecal plates, in younger specimens ambulacra seated well below level of surrounding thecal plates, widest point of ambulacra just below radiodeltoid suture; lancet plates lie along ambulacral midline within radial sinus and occupy approximately one-half ambulacra width, median groove resides medially on lancet and transverses entire ambulacral length, lateral grooves positioned between adjacent ridges on the lancet plate and extend between two slightly curved adjacent side plates ending at brachiole socket creating notch in roughly oval brachiole facet placed between two adjacent side plate sets (Fig. II-8.1); lateral groove ornamented on each side by articulation grooves positioned orthogonally with respect to lateral groove, side plates set against lancet edge angled slightly proximally, hydrospire pore positioned between two adjacent brachiole facets along suture between side plates and outer side plates of adjacent sets, hydrospire pore groove positioned from hydrospire pore approximately one third of the distance through a single side plate shallowing at end, small pit positioned where each side plate suture to lancet plate in mature specimens (Figs. II-7.7, 7.10, 8.1), outer side plate small and roughly half moon-shaped (Fig. II-8.1);

hydrospires observed in serially cut paratype CMC IP 54225 (not figured) in ten groups, five folds per ambulacral side, folds protruding into thecal cavity; no stems or brachioles known for this species.

Etymology.—Named for Daniel Frederick who suggested studying this fauna.

Types.—Holotype CMC IP64791 and paratypes CMC IP64792-64797.

Occurrence.— *Pentremites fredericki* n. sp. is known from Glen Dean Formation (Upper Mississippian, Chesterian), 10 m-15 m above the base of the formation, along Pennyrile Parkway in Christian County, southwestern Kentucky.

Remarks.—Pentremites fredericki n. sp. differs from other species of *Pentremites* by having slightly to very convex v-shaped interambulacral areas, relatively large stem facet, large secondary deposits on the basal plates as well as raised radial and deltoid edges alongside the ambulacra. Very distinct pits on the sideplate/lancet suture in conjunction with a very short hydrospire groove are also diagnostic.

PENTREMITES PYRIFORMIS Say, 1825

Figs. II-9.1-9.12, 11.9, 11.12

Pentremites pyriformis Say, 1825.

Synonymy in Galloway and Kaska, 1957, p. 56.

(*non*) *Pentremites pyriformis* Say, 1925. Galloway and Kaska, 1957. pl. 4, figs. 33, 34 and 37.

(non) Pentremites *pyriformis* Say, 1825. Beaver et al., 1967. P. 304.

Pentremites pyriformis Say, 1825. Waters et al., 1985. p. 704.

Pentremites pyriformis Say, 1825. Beaver, et al., 2000, p. 250.

Pentremites pyriformis Say, 1825. Dexter et al., 2009, p. 130, 133.

Diagnosis.—Medium-sized pyriform *Pentremites* with concave ambulacra at maturity; small stem facet diameter; vault/pelvis ratio approximately 0.80 to 0.90 in juvenile specimens and 1.00 to 1.05 for mature specimens.

Description.—Theca elongate with conical pelvis and parabolic vault in lateral view, (Fig. II-9.1, 9.8, 9.9); pelvis elongate, conical with concave outline; vault elongate parabolic with convex outline; vault-pelvis ratio ranges from approximately 1.00 to 1.05 on mature larger specimens to approximately 0.80 to 0.90 on smaller juvenile specimens; outline in oral view (Fig. II-9.4, 9.7, 9.11) rounded pentagonal with straight to slightly concave interambulacra; ambulacra slightly concave on mature specimens and flat on immature specimens; lateral edges of ambulacra seated below surface of surrounding plates; theca ranges in height to approximately 28 mm in more mature specimens; summit rounded in juvenile specimens, nearly flat and only slightly projecting in mature specimens.

Basalia three, in normal position with azygous basal in AB interray, elongate, confined to lower half of pelvis on theca (Figs. II-9.2, 9.3, 9.10, 10.2); azygous basal quadrate, with straight edges on basal-basal sutures and basal-radial sutures (Figs. II-9.2, 9.3, 9.10, 10.2); zygous basals pentagonal with straight edges on basal-basal sutures and convex edges on basal-radial edges (Figs. II-9.2, 9.3, 9.10, 10.2); secondary deposits well developed around stem facet on all basal plates thickening plates at base (Fig. II-9.3, 9.10); stem facet shared equally between three basals with crenulations around periphery, smooth to center with very small lumen that enters theca, diameter ranges up to 2.0 mm for mature specimens to 1.0 mm for juvenile specimens, equivalent to one sixth to one

quarter of the basal circlet respectively; some very large specimens show up to two columnals fused proximally on theca.

Radials five, large, extending from half way up the pelvis to near the summit covering the whole middle of the theca (Figs. II-9.1, 9.8, 9.9, 10.2), roughly hexagonal with wide parabolic radial sinus penetrating approximately half plate length; radial-basal sutures roughly straight; radial-radial sutures straight dominating the length of the radial plate; radiodeltoid suture straight to slightly convex; RB sector large, convex parallel to RB axis; RR sector slightly convex parallel to axis and flattens near radial-radial suture; RD sector slightly convex; radials ornamented by growth lines strongest in RR sector.

Deltoids six including epideltoid and hypodeltoid, small, comprise 5-10 percent of length in mature thecae, DR suture makes angle of approximately 60 degrees; deltoid lips small, together with epideltoid form edges of peristome and proximal most medial food grooves; deltoid bodies diamond-shaped with aboral edges flat; CD side of theca bearing, epideltoid and hypodeltoid; hypodeltoid similar to deltoid bodies of other deltoids; spiracles and anispiracle teardrop shaped bordered by deltoid lips proximally, lancet plates laterally and side plates distally separated from deltoid body by approximately five pairs of side plates; anispiracle much larger than other spiracles (Fig. II-9.4, 9.7, 9.11).

Peristome central on summit, formed by four deltoids lips and epideltoid on anal side, roughly star shaped, transversely elongate, shows footprint of 2-1-2 symmetry, much smaller than anispiracle (Fig. II-9.4, 9.8, 9.11).

Ambulacra five, wide, relatively short in length, usually extend approximately half length of theca, slightly concave in mature specimens, short, wide and flat in younger specimens (Fig. II-9.5, 9.6, 9.12); in mature specimens, highest points on ambulacra seated

below level of surrounding thecal plates, in younger specimens ambulacra seated well below level of surrounding thecal plates, widest point of ambulacra at radiodeltoid suture; lancet plates lie along ambulacral midline within radial sinus and occupy approximately one-half ambulacra width, median groove resides medially on the lancet and transverses the entire plate length, lateral grooves positioned between adjacent ridges on the lancet plate, extending between two slightly curved adjacent side plates, ending at the brachiole socket which creates notch in oval brachiole facet positioned between two adjacent side plate sets (Fig. II-10.1); lateral groove ornamented on each side by articulation grooves positioned orthogonally with respect to lateral groove, side plate set against lancet edge angled slightly proximally; hydrospire pore positioned between two adjacent brachiole facets along suture between side plates and outer side plates of adjacent sets; hydrospire pore groove positioned from hydrospire pore through a single side plate, shallowing and ending half way between side plate and median groove on lancet, outer side plates small and roughly half moon shaped (Fig. II-10.1); hydrospires in ten groups, up to eight folds per ambulacral side, folds protruding into thecal cavity (Dexter et al., 2009).

Summit structures cover spiracles and peristome (Fig. II-11.9, 11.12); spiracle cover plates type 1 (Beaver, 2000) cylindrical widening as they reach spiracles and extend well above summit; individual spiracles cannot be identified; cover plates over median groove biserial, quadrate, greatly enlarged and highly elevated with respect to lateral cover plates (Fig. II-11.9); later cover plates biserial, extremely small (Fig. II-11.9).

Brachioles poorly known, of unknown length, formed from biserial brachiolar plates and small cover plates (Fig. II-11.12).

Material.—CMC IP 66821-66823, 66830.

Remarks.—Pentremites pyriformis Say has not been formally described in detail since its original designation (Say, 1825). Unfortunately, the holotype specimen (PANS-30428) is lost. This paper follows current usage of *Pentremites pyriformis* and basing this description on Glen Dean material and accompanied by plate diagrams, photographs and a modern description.

Pentremites pyriformis differs from other pyriform *Pentremites* by the concave ambulacra at maturity; small stem facet diameter; and the nearly 1 to 1 vault to pelvis ratio.

PENTREMITES TULIPAFORMIS Hambach, 1903

Figs. II-9.13-24, 11.1-8, 11.10-11

Synonymy in Galloway and Kaska, 1957, p. 67.

Pentremites tulipaformis Hambach, 1903. Beaver, 1968. P. 304.

Pentremites tulipaformis Hambach, 1903. Waters et al., 1985. p. 705.

Pentremites tulipaformis Hambach, 1903. Beaver, 1998, p. 336.

Pentremites tulipaformis Hambach, 1903. Beaver et al., 2000, p. 250.

Diagnosis.—Medium-sized, globular *Pentremites* with wide, slightly concave ambulacra, flat to slightly concave interambulacra, small stem facet diameter with bulbous secondary deposits around facet, and vault/pelvis ratio that is approximately 2.75-3.00 for mature specimens 1.00 for immature specimens; in some populations incorporated spine present at base of radial sinus.

Description.—Theca globular with broadly conical pelvis and parabolic vault in lateral view, occasionally seen more inflated (Fig. II-9.13, 9.22, 9.23); pelvis short, broad,

slightly bulbous with slightly concave to slightly convex outline; vault elongate parabolic with convex outline; vault-pelvis ratio ranges from approximately 2.75 to 3.00 on mature larger specimens to approximately 1.00 on immature specimen; outline in oral view (Fig. II-9.14, 9.16, 9.20) rounded pentagonal with interambulacral areas flat to slightly concave, spines at ambulacral tips give corners of outline a double notch appearance (Fig. II-9.15, 9.17, 9.24); lateral edges of ambulacra seated well below surface of surrounding plates; theca ranges in height to approximately 20 mm on largest specimens; summit slightly rounded and slightly projecting.

Basalia three, in normal position with azygous basal in AB interray, short, confined to lower half of pelvis on theca (Figs. II-9.15, 9.17, 9.24, 11.2); azygous basal quadrate, with straight edges on basal-basal and basal-radial sutures (Figs. II-9.15, 9.17, 9.24, 11.2); zygous basals pentagonal with straight edges on basal-basal sutures and concave edges on basal-radial edges (Figs. II-9.15, 9.17, 9.24, 11.2); secondary deposits bulbous on all basal plates around stem facet; lobes extend proximally along BB sutures forming a rounded triangular deposit (Fig. II-9.15, 9.17, 9.24); stem facet circular, shared equally between three basals, diameter ranges from 2.0 mm for mature specimens to 0.5 mm for juvenile specimens, equivalent of one fifth to one sixth of the basal circlet respectively, outer edge crenulated with crenulations present proximally on columnals while center is smooth with small central lumen.

Radials five, very large, extending from half way up the pelvis to very near the summit covering the whole middle of the theca (Fig. II-9.13, 9.22, 9.23); radial roughly hexagonal with very wide roughly v-shaped radial sinus penetrating about two thirds plate length; small spine located at the bottom of radial sinus (Fig. II-12.1) that is not seen in

other occurrences, which could be a local pathology; radial-basal sutures slightly convex; radial-radial sutures straight dominating the length of the radial plate; radiodeltoid suture slightly s-shaped (Fig. II-12.2); RB sector moderate in size, slightly convex parallel to RB axis; RR sector slightly convex to straight parallel to axis; RD sector slightly convex; radials ornamented by growth lines in all sectors; radials overlap deltoids.

Deltoids six including epideltoid and hypodeltoid, small, make up 20-25 percent of length in mature thecae, DR suture makes angle of approximately 70 degrees; deltoid lips moderate, together with epideltoid form edge of peristome and proximal most medial food grooves; deltoid bodies diamond-shaped with aboral edges slightly s-shaped, deltoid septae thin, easily seen bisecting spiracles (Fig. II-9.14, 9.16, 9.20), hypodeltoid; hypodeltoid similar to deltoid bodies of other deltoids; spiracles and anispiracle teardrop to round shaped bordered by deltoid lips proximally, lancet plates laterally and side plates distally separated from deltoid body by approximately three pairs of side plates; anispiracle slightly larger than other spiracles (Fig. II-9.14, 9.16, 9.20).

Peristome central on summit, formed by four deltoids lips and epideltoid on anal side, pentagonal, transversely slightly elongate showing footprint of 2-1-2 symmetry, slightly smaller than anispiracle.

Ambulacra five, wide and moderate in length, usually extend approximately three-quarters of theca terminating at radial spine described above, moderately curved along length and slightly concave in mature specimens, short, wide and very slightly convex in younger specimens (Fig. II-9.18, 9.19, 9.21); in mature and less mature specimens, highest points on ambulacra seated slightly above level of surrounding thecal plates, widest point of ambulacra above radiodeltoid suture; lancet plates lie along ambulacral midline within

radial sinus and occupy approximately one-half ambulacra width, median groove positioned medially on lancet, transverses the entire ambulacral length, lateral grooves positioned between adjacent ridges on lancet plate extending between two slightly curved adjacent side plates, ending at brachiole socket forming notch in roughly oval brachiole facet that positioned between two adjacent side plate sets; lateral groove ornamented on each side by articulation grooves positioned orthogonally with respect to lateral groove, side plates set against lancet edge angled slightly proximally, hydrospire pore positioned between two adjacent brachiole facets along suture between side plates and outer side plates of adjacent sets (Fig. II-12.1), hydrospire pore groove positioned from hydrospire pore through a single side plate shallowing and ending half way through the plate, outer side plate small and roughly half moon shaped (Fig. II-12.1); hydrospires in ten groups, five folds per ambulacral side, folds protruding short distance into thecal cavity.

Summit Structures cover spiracles and peristome (Fig. II-11.1-8, 11.10). Spiracle cover plates (Fig. II-11.8) type 3 (Beaver, 2000) very thick rectangular extending well above summit and resemble a domelike structure (Fig. II-11.1, 11.7); anispiracle plates same as other spiracles but bear spall anal pyramid within block-like spiracle cover plate series (Fig. II-11.5); small block-like plates cover peristome and areas in between spiracles, ambulacral cover plates (Fig. II-11.1, 11.7) very small biserial undifferentiated between medial and lateral food grooves, not well preserved (Fig. II-11.4).

Brachioles and stem not preserved.

Material.— USNM S-3592; CMC IP 66824-66829.

Remarks.—Pentremites tulipaformis has not been sufficient redescribed since the original description of Hambach (1903) with accompanied plate diagrams and

photographs. Specimens from the Pennyrile Parkway locality uniformly have ambulacral spines, but this is not universal for the specimens (Galloway and Kaska, 1957; Beaver et al., 1968). Although the type series (USNM S-3592) lacks spines, in all other respects it conforms well to the Pennyrile Parkway population. Macurda (1980) considered this an anomaly to be local but did not attribute a specific cause.

Pentremites tulipaformis differs from other godoniform *Pentremites* by bearing wide, slightly concave ambulacra, flat to slightly concave interambulacra, small stem facet diameter with bulbous secondary deposits around facet.

Family DIPLOBLASTIDAE Fay, 1964

Genus DIPLOBLASTUS Fay, 1961

DIPLOBLASTUS FADIGAI new species

Figs. II-13.1-13.4

Diagnosis.—*Diploblastus* with convex ambulacra, relatively large stem facet diameter with very large secondary deposits, and strong thecal ornamentation.

Description.—Theca barrel-shaped with slightly convex pelvis and inverted u-shaped vault in lateral view (Fig. II-13.3-4); pelvis short, broad, nearly flat with slightly convex outline; stem facet slightly raised with respect to basal circlet; vault-pelvis ratio ranges from approximately 7.0 on presumed mature holotype specimen; outline in oral view rounded pentagonal with convex ambulacra (Fig. II-13.1); lateral edges of ambulacra seated slightly below surface of surrounding plates; interambulacral areas slightly concave to slightly convex; theca height approximately 4.5 mm.

Basalia three, azygous basal in DE interray as normal for *Diploblastus*, short, confined to lower half of pelvis on theca (Figs. II-13.2, 14.2); azygous basal quadrate, with straight edges on basal-basal and basal-radial sutures (Figs. II-13.2, 14.2); zygous basals pentagonal with straight basal-basal and basal-radial sutures (Figs. II-13.2, 14.2); secondary deposits large and flat on all basal plates; stem facet diameter 0.3mm for holotype specimen equivalent of one quarter to one third of the basal circlet; single proximal columnal fused proximally on theca; crenulations present distally on columnal, center is smooth with small circular central lumen (Fig. II-13.2).

Radials five, proportionately very large, extending from half way up the pelvis to near top of theca, covering middle three-quarters of theca (Fig. II-13.3-4); radial roughly u-shaped with wide roughly parabolic radial sinus penetrating most of plate length; radial-basal sutures slightly convex; radial-radial sutures straight dominating the length of the radial plate; radiodeltoid suture flat; RB sector small, slightly convex parallel to RB axis; RR sector roughly flat parallel to axis; RD sector convex; radials ornamented by very heavy growth line ridges strongest along radiodeltoid suture best expressed in RD sector (Fig. II-13.3-4).

Deltoids eight including superdeltoid, hypodeltoid and two cryptodeltoids, wide, make up 10-15 percent of length in mature theca, hypodeltoid slightly larger than regular deltoids, RDR angle approximately 110 degrees; deltoid lips small, v-shaped, together with superdeltoid form edge of peristome and proximal most medial food grooves; deltoid body roughly diamond shaped with aboral edges flat, ornamented with multiple small bulbous lumps proximally and heavy growth lines distally (Fig. II-13.3-4); CD side of theca bearing four, superdeltoid, hypodeltoid and two cryptodeltoids; hypodeltoid similar to deltoid

bodies of other deltoids but larger adoral surface parabolic; cryptodeltoids poorly exposed in holotype, lie along edges of periproct; eight somewhat paired u-shaped spiracles bordered by deltoid lips proximally, lancet plates laterally, hypodeltoid body distally by deltoid lips, incompletely split by slightly protuberant deltoid septum; anispiracle irregularly paired, bordered by superdeltoid lip proximally, cryptodeltoid plates laterally, hypodeltoid body distally; anispiracle larger and more elongate than other spiracles (Figs. II-13.1, 14.2).

Peristome central on summit, formed by four deltoid lips and superdeltoid on anal side, pentagonal to roughly star shaped, transversely elongate showing footprint of 2-1-2 symmetry, slightly larger than anispiracle.

Ambulacra five, narrow and moderate in length, extend most of the length of theca, moderately curved along length and convex (Fig. II-13.3-4); highest points on ambulacra seated roughly even or slightly above level of surrounding thecal plates; lancet plates concealed, lying fully under side plates along ambulacral midline within radial sinus and occupy approximately one-half ambulacra width (Figs. II-13.4, 14.1), median groove positioned medially along suture between side plates from right and left sides of ambulacrum, transverses entire ambulacral length, lateral grooves positioned between adjacent ridges on side plates extending between two straight adjacent side plates ending at the brachiole socket which abuts a roughly oval brachiole facet positioned between two adjacent side plate sets; lateral groove ornamented on each side by articulation grooves positioned medially with respect to median groove, side plate set against opposing side plates and angled slightly proximally, hydrospire pore positioned between but slightly abmedial to two adjacent brachiole facets along suture between side plates and outer side

plates of adjacent sets, short hydrospire pore groove positioned from hydrospire pore through a single side plate shallowing and ending near the hydrospire pore (Fig. II-14.1), outer side plate small and roughly half u-shaped (Fig. II-14.1). Only one attached columnal and no brachioles known for this species.

Etymology.—Named for Troy Fadiga who discovered this species.

Types.—Holotype CMC IP 66831.

Occurrence.—*Diploblastus fadigai* n. sp. is known from Glen Dean Formation (Upper Mississippian, Chesterian), 10 m-15 m above the base of the formation, along Pennyrile Parkway in Christian County, southwestern Kentucky.

Remarks.—Diploblastus fadigai n. sp. differs from other species of *Diploblastus* by the strong surface ornamentation present on the deltoids and radials, and very large, flat, secondary deposits on the basal plates, azygous basal in the DE position, and convex outline. Consequently, further description is tentative pending on discovery of more specimens.

CONCLUSIONS

For these data, the model-based clustering algorithm of MCLUST chose a model with four components. The corresponding four-group classification matches the four empirically diagnosed groups with 94.23 percent accuracy. It is likely that the misclassifications result from the small sample size of the two lesser-represented species. If these species were better represented in the sample set, it is likely that their morphospace would have been more precisely defined resulting in significantly smaller classification error. These methods can be used in any clade with a set of homologous points or as an exploratory population

where the number of subpopulations is unknown. The only problem that may occur is that underrepresented organisms could fail to be identified or identified incorrectly. Ideally these methods will be used on all known species of *Pentremites* to help identify synonymies and validate classifications where possible.

The geometric morphometry employed during the present study demonstrated its usefulness in separating closely related species that, in the past, have been difficult to identify using conventional apomorphies. Even in genera that have a high degree of variability, such as *Pentremites* (Waters et al., 1985), 3-D geometric morphometrics recovers species groups with a high degree of accuracy. The evidence presented here justifies continuation of the use of traditional and geometric morphometric techniques to achieve the maximum degree of discrimination among species of blastoids. Future plans are to expand these methods to the fields of systematics and ontogenetics in Blastoidea.

ACKNOWLEDGEMENTS

We thank T. Fadiga for invaluable advice in morphometrics and with help in sample collections. We also thank Daniel Frederick for introducing us to this locality and aiding in sample collection. Assistance in the field was provided by B. Ford, R. Shroat-Lewis, G. Gilleaudeau, and E. Hogan. Assistance with museum collections was provided by Brenda Hunda, Cincinnati Museum Center; Mark Florence and Daniel Levin US National Museum. Reviewers Johnny Waters and James Sprinkle provided valuable reviews that greatly improved this manuscript. The laser scanner was acquired through NSF grant EAR-0745918. Financial assistance for this study was provided by the NSF - Assembling the Echinoderm Tree of Life Grant, DEB-1036260.

REFERENCES

ADRAIN, J. M., AND S. R. WESTROP. 2006. New earliest Ordovician trilobite genus *Millardicurus*: The oldest known hystricurid. Journal of Paleontology, 80:650-671.

ANDERSON, F. E., A. PILSITS, S. CLUTTS, V. LAPTIKHOVSKY, G. BELLO, E. BALGUERIAS, M. LIPINSKI, C. NIGMATULIN, J. M. F. PEREIRA, U. PIATKOWSKI, J. P. ROBIN, A. SALMAN, AND M. G. TASENDE. 2008. Systematics of *Alloteuthis* (cephalopoda:loliginidae) based on molecular and morphometric data. Journal of Experimental Marine Biology and Ecology, 364:99-109.

BEAVER, H. H., R. O. FAY, D. B. MACURDA, JR., R. C. MOORE, G. UBAGHS, AND J. WANNER. 1968. Blastoids, p. S298-S445. *In* R. C. Moore (ed.), Treatise on Invertebrate Paleontology, Part S, Echinodermata 1 (Vol. 2). The Geological Society of America and University of Kansas, New York and Lawrence.

BEAVER, H. H., AND A. J. FABIAN. 1998. Color patterns in Mississippian (Chesterian) blastoids. Journal of Paleontology, 72:332-338.

BEAVER, H. H., A. J. FABIAN, AND M. PALATAS. 2000. Summit structures in Mississippian blastoids. Journal of Paleontology, 74:247-253.

BOOKSTEIN, F. L. 1991. Morphometric tools for landmark data: geometry and biology. Cambridge University Press, Cambridge, 1-435.

BUTTS, C. 1917. Descriptions and correlations of the Mississippian formations of western Kentucky. Kentucky Geological Survey, Frankfort, 7-119.

CIGNONI, P., M. CORSINI, AND G. RANZUGLIA. 2008. MeshLab: an open-source 3D mesh processing system. ERCIM News, 73:47-48.

DEXTER, T. A., C. D. SUMRALL, AND M. L. MCKINNEY. 2009. Allometric strategies for increasing respiratory surface area in the Mississippian blastoid *Pentremites*. Lethaia, 42:127-137.

DRYDEN, I. L. 2007. Shapes: Statistical Shape Analysis. R Package Version 1.1-1., http://www.maths.nott.ac.uk/~ild/shapes.

FAY, R. 1961. The type of *Pentremites* Say. Journal of Paleontology, 35:868-873.

FAY, R. O. 1964. An outline classification of the blastoidea. Oklahoma Geology Notes, 24:81-90.

FOOTE, M. 1991. Morphological and taxonomic diversity in a clade's history: The blastoid record and stochastic simulations. University of Michigan Museum of Paleontology, Contributions from the Museum of Paleontology, 28:101-140.

FRALEY, C., AND A. E. RAFTERY. 2002. Model-based clustering, discriminant analysis, and density estimation. Journal of the American Statistical Association, 97:611-631.

FROST, S. R., L. F. MARCUS, F. L. BOOKSTEIN, D. P. REDDY, AND E. DELSON. 2003. Cranial allometry, phylogeography, and systematics of large-bodied papionins (primates: Cercopithecinae) inferred from geometric morphometric analysis of landmark data. The Anatomical Record Part A: Discoveries in Molecular, Cellular, and Evolutionary Biology, 275A:1048-1072.

GALLOWAY, J. J., AND H. V. KASKA. 1957. Genus *Pentremites* and its species. The Geological Society of America Memoir, 69:1-104.

HAMBACH, G. 1903. A revision of the blastoidea, with a proposed new classification and description of new species. St. Louis Academy of Science, Transactions, 13:1-67.

HOLLANDER, J., D. C. ADAMS, AND K. JOHANNESSON. 2006. Evolution of adaptation through allometric shifts in a marine snail. Evolution, 60:2490-2497.

KATZ, S. G., AND J. SPRINKLE. 1976. Fossilized eggs in a Pennsylvanian blastoid. Science, 192:1137-1139.

MACURDA, D. B., JR. 1980. Abnormalities of the carboniferous blastoid *Pentremites*. Journal of Paleontology, 54:1155-1162.

MITTEROECKER, P., AND P. GUNZ. 2009. Advances in geometric morphometrics. Evolutionary Biology, 36:235-247.

NELSON, W. J., L. B. S SMITH AND J. D. TREWORGY. 2002. Sequence stratigraphy of the lower Chesterian (Mississippian) strata of the Illinois basin. Illinois State Geological Survey circular, 107:1-70.

ORBIGNY, A. D. 1852. Cours elémentaire de paléontologie et de géologie stratigraphiques. Mason, Paris, 1-841.

SAY, T. 1820. Observations on some species of zoöphytes, shells principally fossil. American Journal of Science, 2:34-45.

SAY, T. 1825. On two genera and several species of crinoidea. Journal of the Academy of Natural Science Philadelphia, 1st Series, 4:289-296.

SLICE, D. E. 2007. Geometric morphometrics. Annual Review of Anthropology, 36:261-281.

WATERS, J. A., A. S. HOROWITZ, AND D. B. MACURDA. 1985. Ontogeny and phylogeny of the Carboniferous blastoid *Pentremites*. Journal of Paleontology, 59:701-712.

WEBBER, A. J., AND B. R. HUNDA. 2007. Quantitatively comparing morphological trends to environment in the fossil record (Cincinnatian Series; Upper Ordovician). Evolution, 61:1455-1465.

ZELDITCH, M. L., AND A. C. CARMICHAEL. 1989. Ontogenetic variation in patterns of developmental and functional-integration in skulls of *Sigmodon fulviventer*. Evolution, 43:814-824.

APPENDIX I

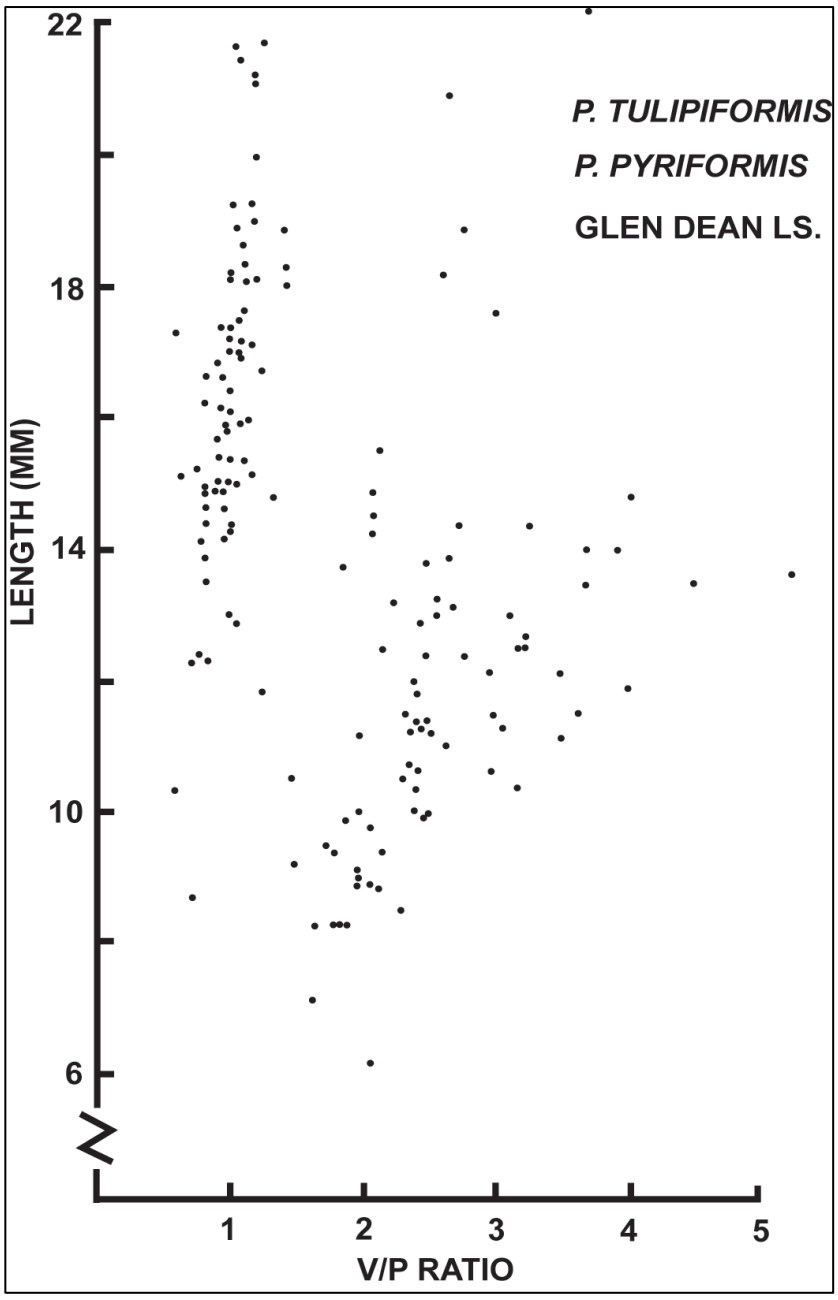

FIGURE II-1—Scatter plot of the vault-to-pelvis ratio versus thecal length in mm for *Pentremites* blastoids from the Pennyrile Parkway, Kentucky locality of the Upper Mississipian (Chesterian) Glen Dean Fm. Using this plot, Waters et al. (1985) determined the community included a pyriform species, *P. pyriformis* and a godoniform species, *P. tulipaformis* using traditional morphometrics (modified from Waters et al. 1985 dataset).

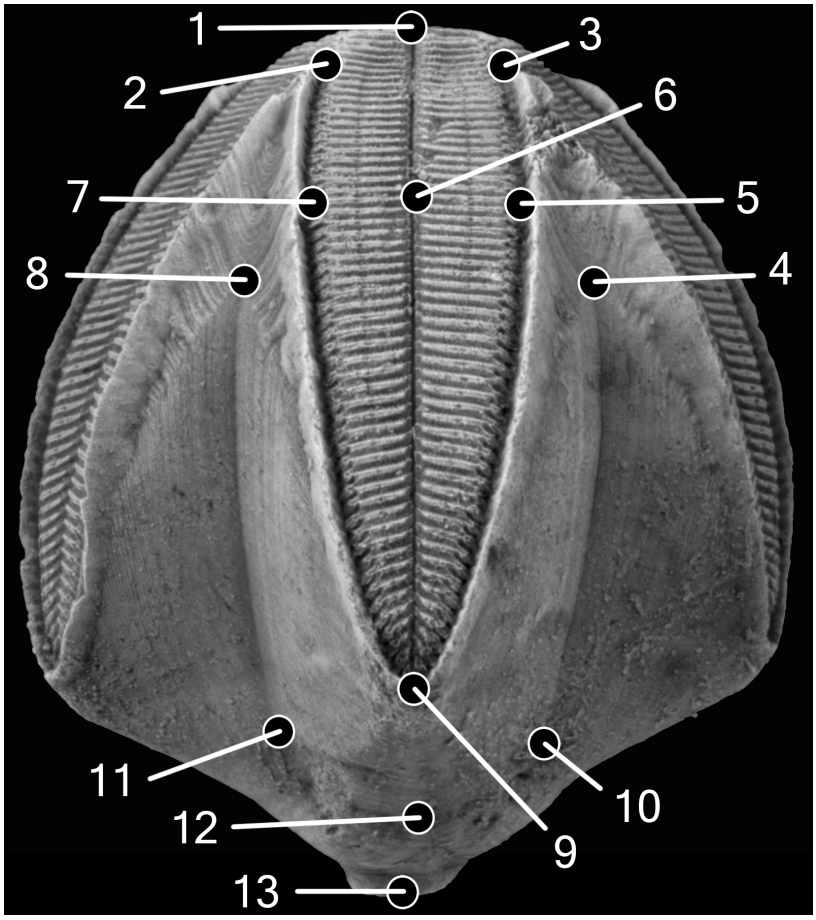

FIGURE II-2—Holotype CMC IP6479 of *Pentremites fredricki* n. sp. showing the positions of landmarks used to measure 3D shape in A ambulacral view; *1*, lancet/deltoid/deltoid triple plate junction in A ray; *2*, 3, AB and AE deltoid/side plate/side plate triple plate junction; *4, 8*, AE and AB deltoid/radial/radial triple plate junction respectively; *5, 7*, AE and EA deltoid/radial/side plate triple plate junction respectively; *6*, center line of lancet located by following lateral food groove from landmark 5 to main food groove; *9*, radial/side plate/side triple plate junction at ambulacral tip; *10*, radial/radial/zygous basal triple plate junction; *11*, radial/radial/azygous basal triple plate junction; *12*, A radial/azygous basal/zygous basal triple junction; *13*, center of the stem facet (lumen).

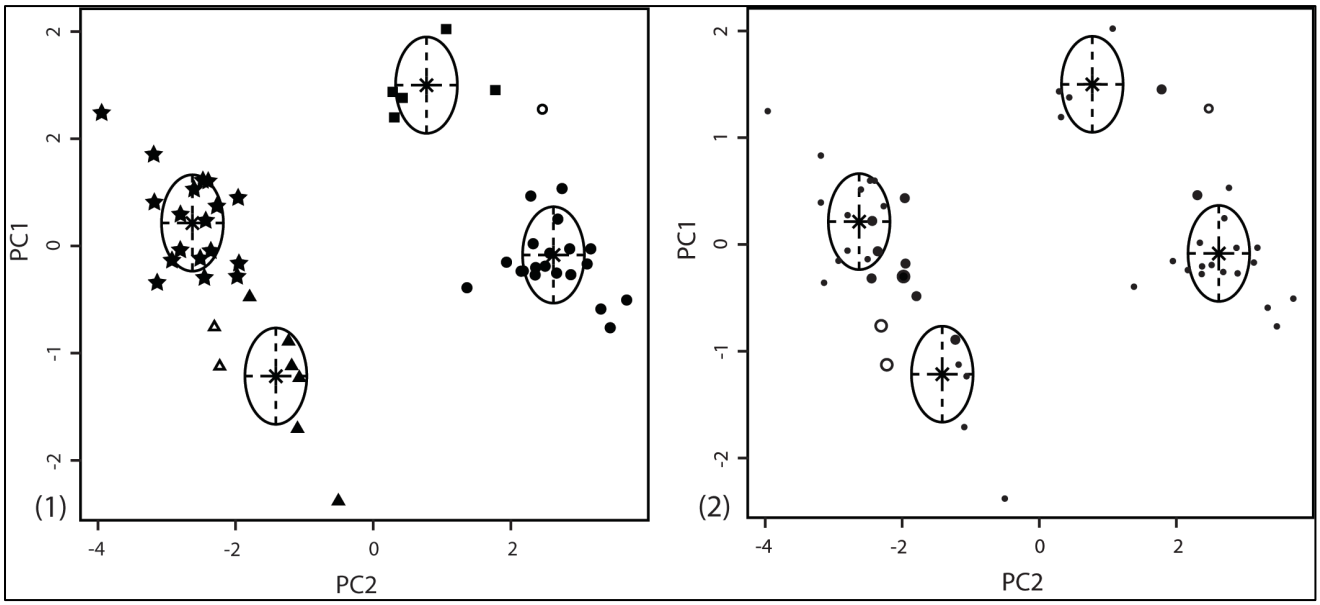

FIGURE II-3— Morphological groupings of individual *Pentremites* specimens based on thecal shape plotted along the first two principal components (PC) calculated from each data set; PC1 represents 74.8 percent variation and PC2 represents 8.41 percent variation explained by each component respectively. Ellipses represent the 95 percent confidence interval around the geometric mean. Classification of specimens by species based on apomorphy are: Stars = *P. tulipaformis*; Squares = *P. meganae*; Triangles = *P. fredericki* ; Circles = *P. pyriformis*. Filled shapes indicate correctly classified specimen whereas open shaped represent misclassified specimens. 2, Degree of uncertainty represented by the size of the points. Note that the open circles representing misclassified specimens also generally have the highest uncertainty.

FIGURE II-4—Photographs of specimens of *Pentremites meganae*, n. sp., whitened, x2 unless otherwise noted; *1*, *2*, *5*, *6*, paratype CMC IP53374, B ambulacral, summit, basal, CD interray views respectively, note the pathological irregularities on tips of A, B, and E ambulacra, the slightly shortened D ambulacrum, and compare with figure 5; *3*, *4*, *7*, *8*, holotype CMC IP53373, B ambulacral, summit, basal, AE interray views respectively; *9*, *10*, *14*, *15*, paratype CMC IP53375, A ambulacral, summit, basal, BC interray views respectively; *11*, *13*, *16*, *17*, immature paratype CMC IP53376, CD interray, D ambulacral, summit, basal views respectively, note relatively longer pelvis and shorter wider ambulacra; *12*, paratype CMC IP53374, detail of summit showing deltoid lips and spiracles x4, compare to Fig. 4.2; *18*, holotype CMC IP53373, detail of summit, x4.

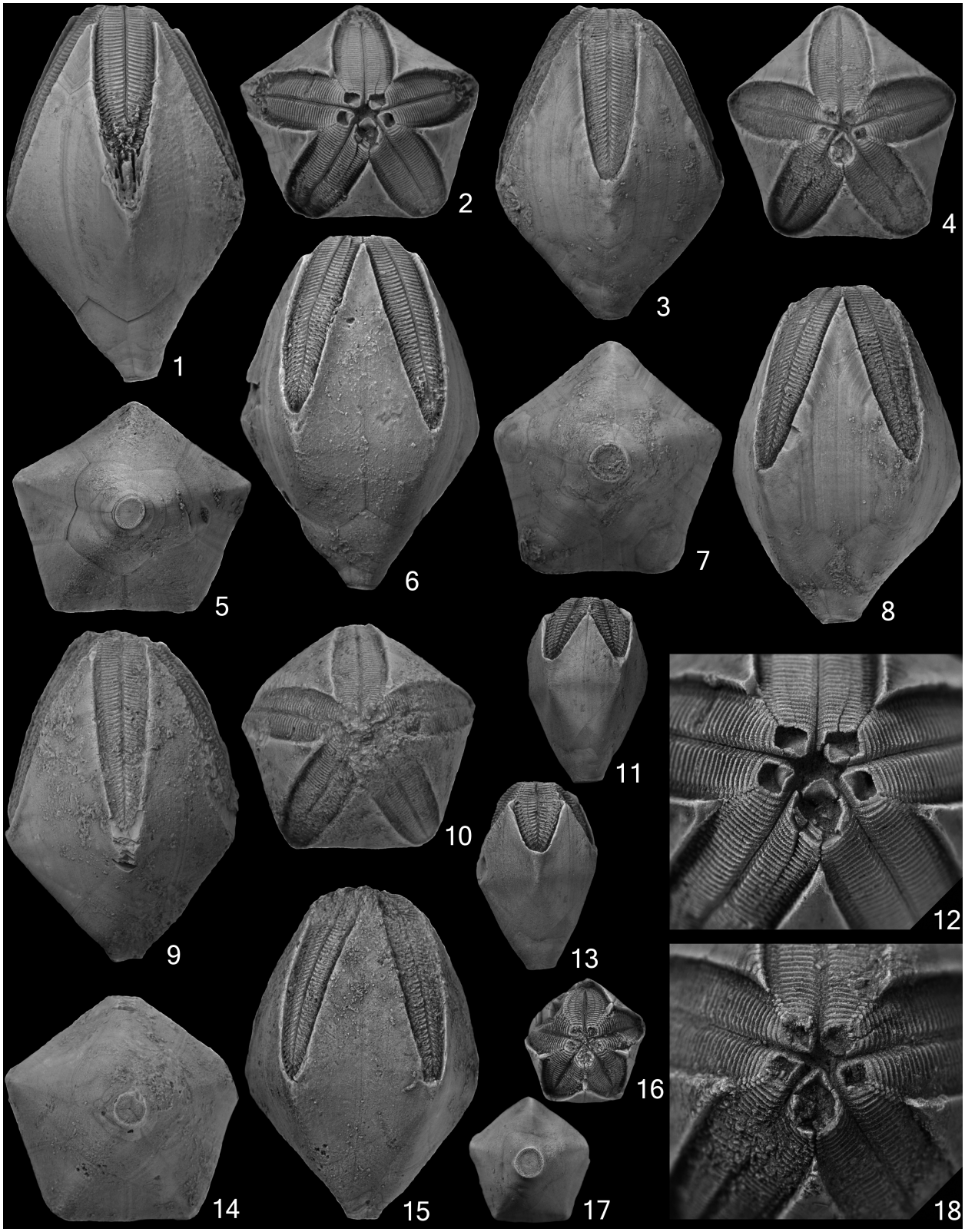

Figure II-4. Continued

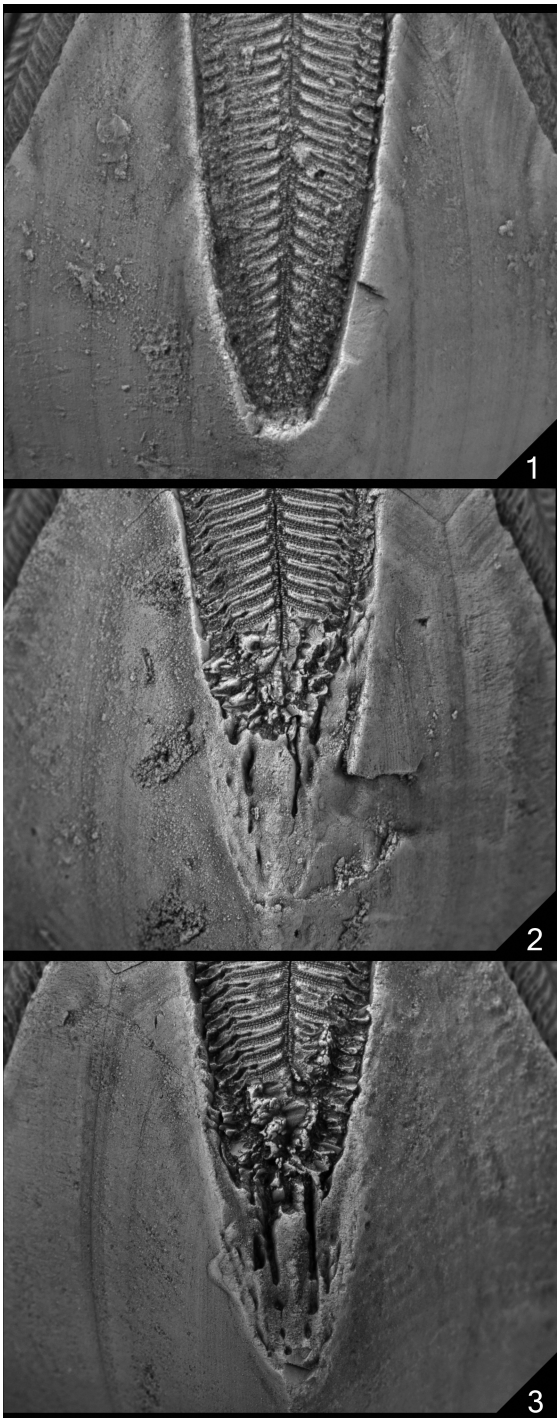

FIGURE II-5—Abnormal development in the ambulacral tips of *Pentremites meganae* n. sp., whitened, X6.5; *1*, holotype CMC IP53373, detail of A ambulacrum showing normal arrangement; *2*, *3*, paratype CMC IP53374 detail of E and B ambulacra respectively, note the pathological irregularities.

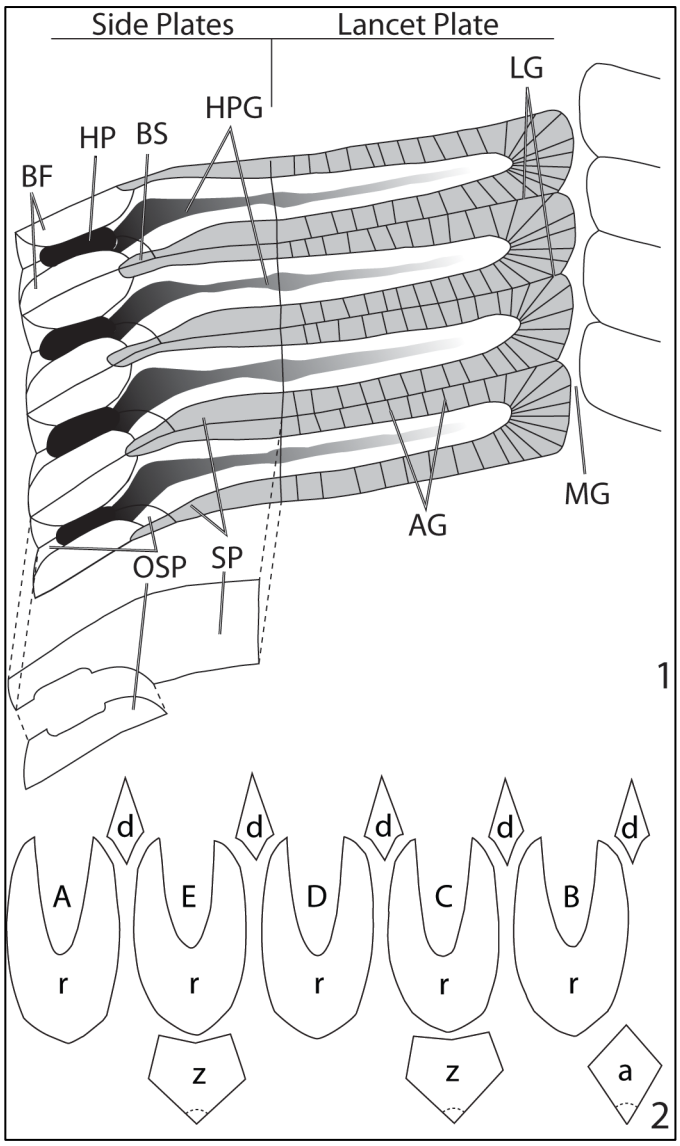

FIGURE II-*6*—Camera lucida drawing of *Pentremites meganae* n. sp. based on holotype CMC IP53373; *1*, View of the left side of ambulacrum. Articulation groove (AG), brachiole facet (BF), brachiole socket (BS), hydrospire pore (HP), hydrospire pore groove (HPG), lateral groove (LG), median groove (MG), side plate (SP), outer side plate (OSP), x24.6; *2*, plate diagram, ambulacra (A-E), azygous basal (a), zygous basal (z), radial (r), deltoid (d), x1.1.

FIGURE II-7—Photographs of specimens of *Pentremites fredericki*, n. sp., whitened, x2 unless otherwise noted; *1*, *2*, *5*, *6*, holotype CMC IP64791, summit, BC interray, A ambulacral, basal views respectively, note shortened C ambulacrum; *3*, *4*, *7*, *8*, paratype CMC IP64792, CD interray, basal, B ambulacral, summit views respectively, x2.5; *9*, *10*, *14*, *25*, paratype CMC IP64793, summit, C ambulacral, basal, AB interray views respectively, x3; *11*, *12*, *17*, *18*, immature paratype CMC IP64796, basal, A ambulacral, summit, DE interray views respectively, x3, note relatively longer pelvis and shorter wider ambulacra; *13*, *19*, *24*, *28*, *29*, paratype CMC IP64797, B ambulacral, summit, E oblique ambulacral, AE interray, basal views respectively, note that the deltoid septa are visible in the broken DE and AE spiracles; *15*, *16*, *20*, *26*, paratype CMC IP64794, AE interray, summit, D ambulacral, basal views respectively, note the pathological irregularities on tip of D ambulacral; *21*, *22*, *23*, *27*, immature paratype CMC IP64795, BC interray, basal, E ambulacral, summit views respectively, x3, note relatively longer pelvis and shorter wider ambulacra.

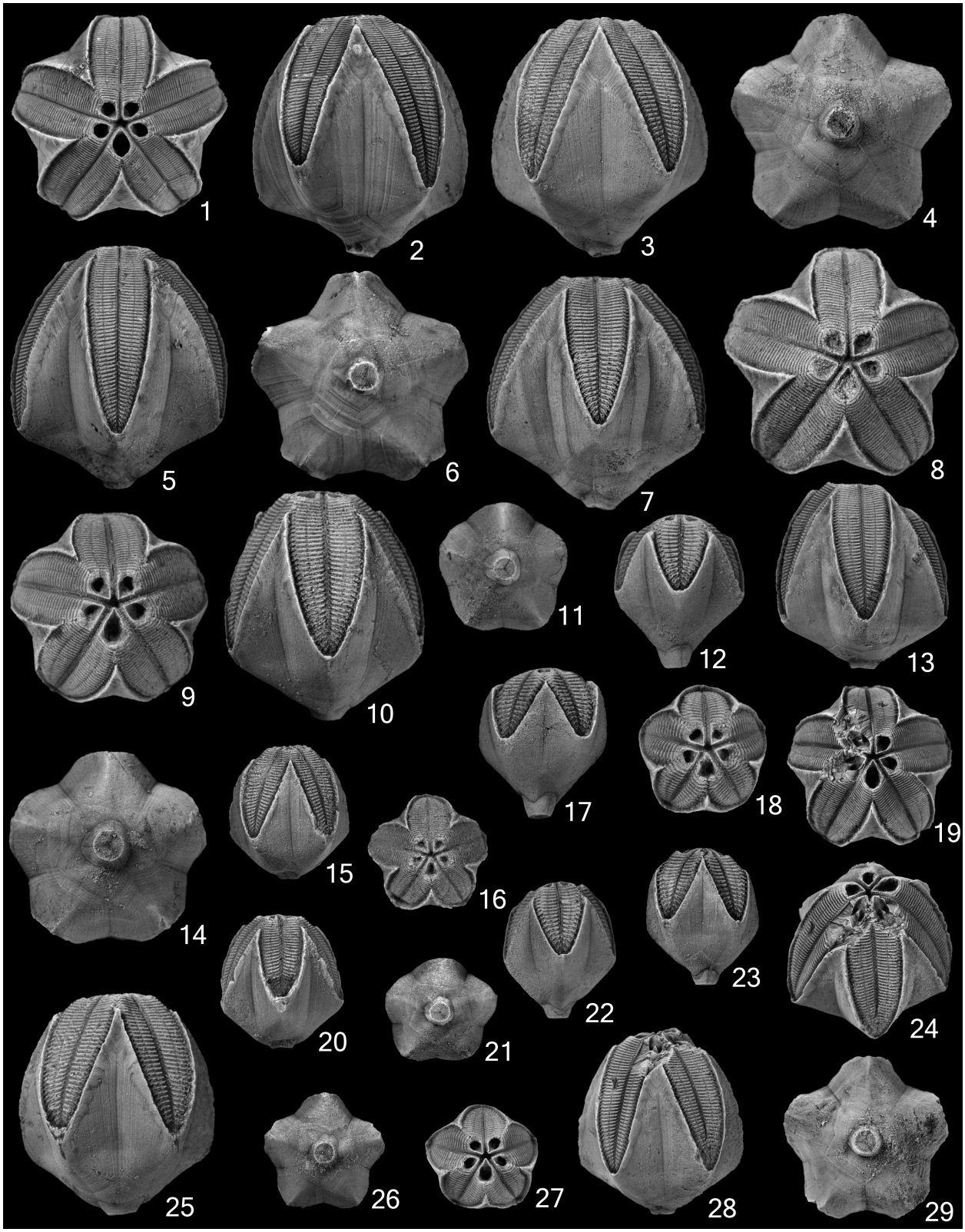

Figure II-7. Continued

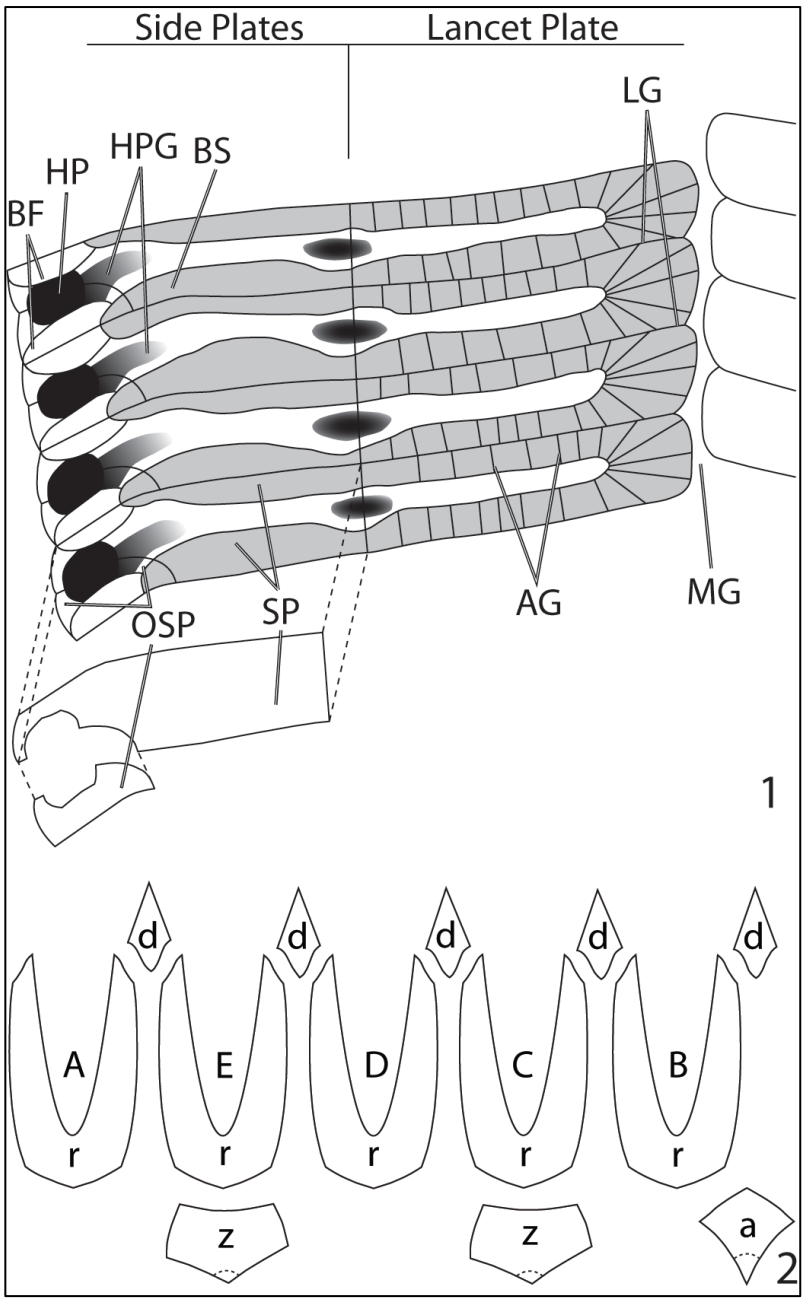

FIGURE II-8—Camera lucida drawing of *Pentremites fredericki* n. sp. based on paratype CMC IP64792; *1*, View of the left side of ambulacrum. Articulation groove (AG), brachiole facet (BF), brachiole socket (BS), hydrospire pore (HP), hydrospire pore groove (HPG), lateral groove (LG), median groove (MG), side plate (SP), outer side plate (OSP), x38; *2*, plate diagram, ambulacra (A-E), azygous basal (a), zygous basal (z), radial (r), deltoid (d), x1.8.

FIGURE II-9—Photographs of *Pentremites* species previously described. *1-12 Pentremites pyriformis* Say, whitened, x2.5; *1*, *2*, *6*, *7*, CMC IP66821, E ambulacral, basal, AB interray, summit views respectively; *3-5*, *8*, CMC IP66822, basal, summit, BC interray, D ambulacral views respectively; *9-12*, CMC IP66823, E ambulacral, basal, summit, BC interray views respectively; *13-24 Pentremites tulipaformis* Hambach, whitened, x3.5; *13*, *15*, *16*, *18*, CMC IP66824, E ambulacral, basal, summit, AB interray views respectively; *14*, *17*, *21*, *22*, CMC IP66825, summit, basal, AB interray, E ambulacral views respectively; *19*, *20*, *23*, *24*, CMC IP66826, DE interray, summit, A ambulacral, basal views respectively.

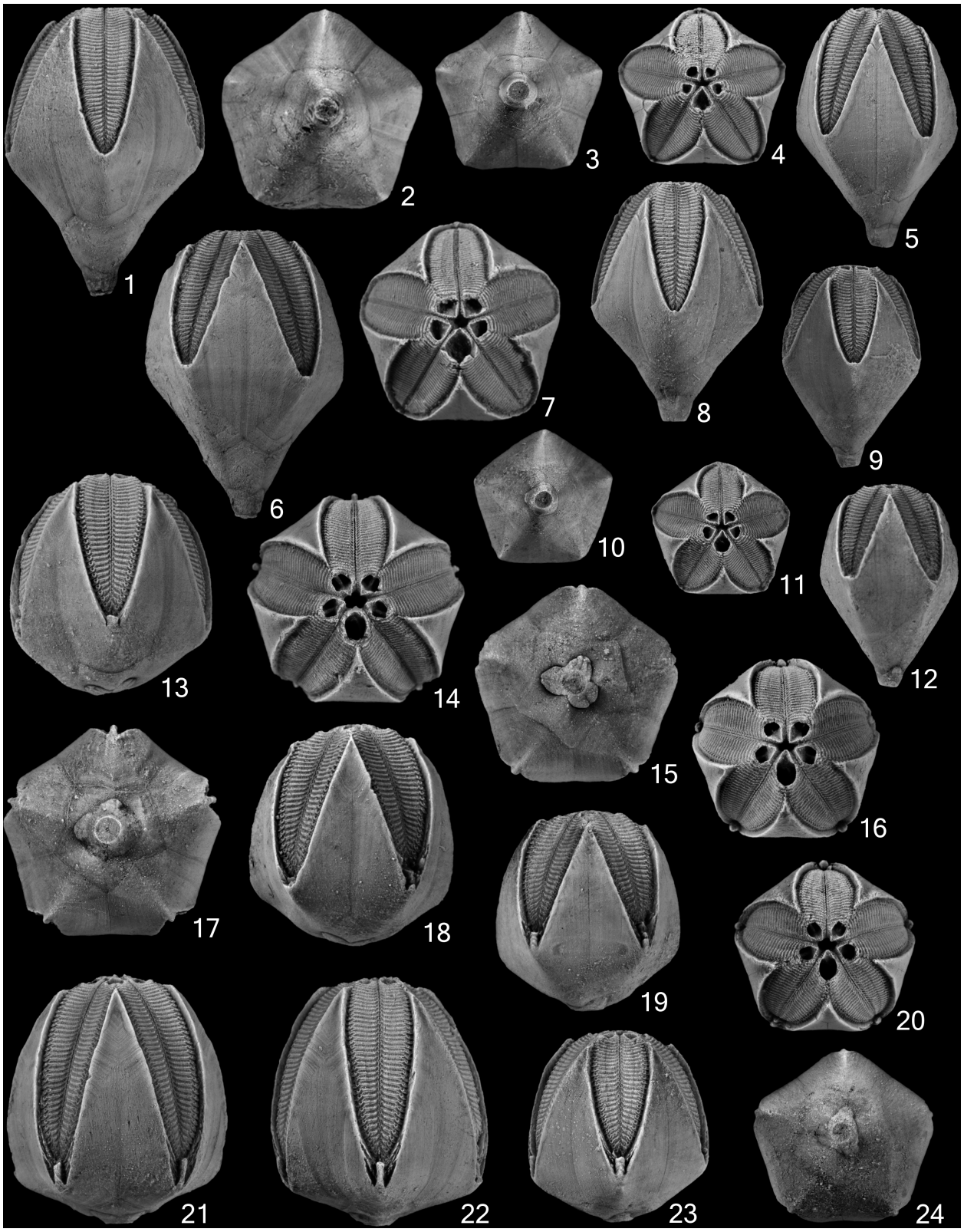

Figure II-9. Continued

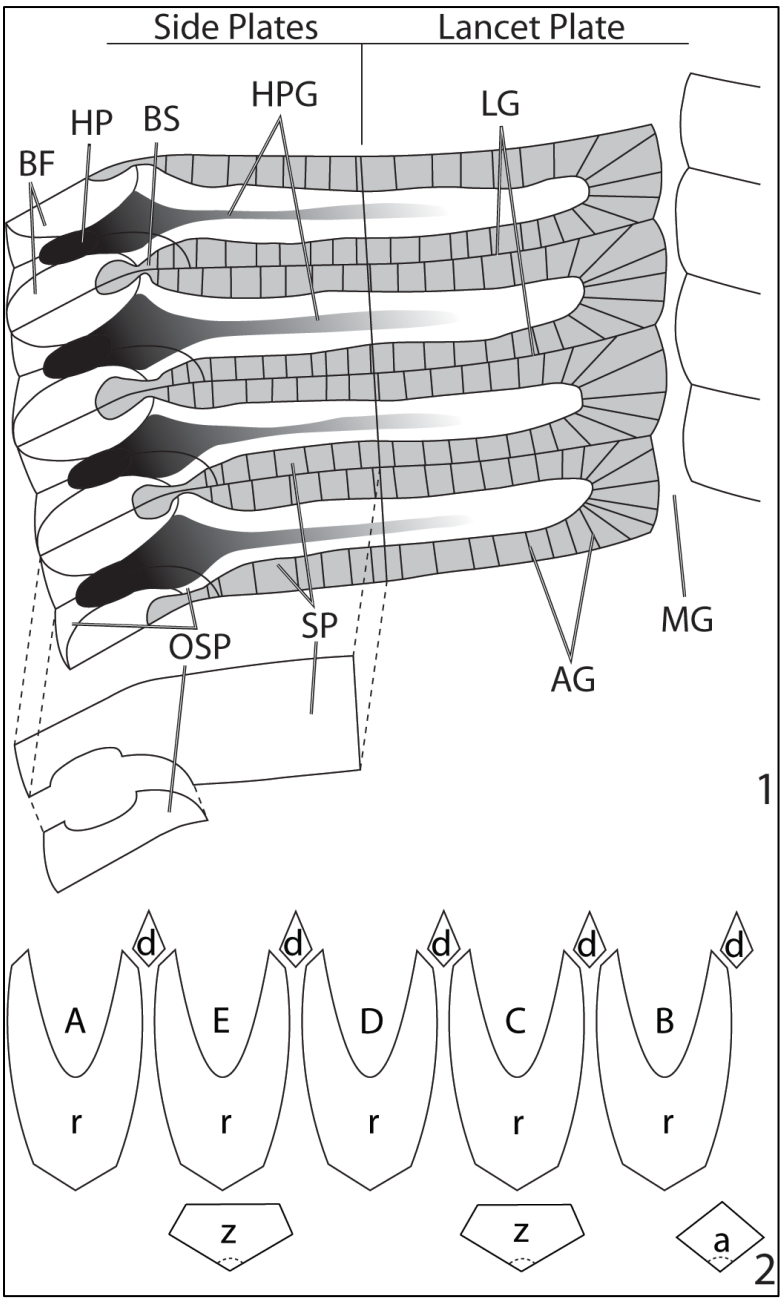

FIGURE II-10—Camera lucida drawing of *Pentremites pyriformis* Say based on specimen CMC IP66822 ambulacral section; *1*, left side of ambulacral. Articulation groove (AG), brachiole facet (BF), brachiole socket (BS), hydrospire pore (HP), hydrospire pore groove (HPG), lateral groove (LG), median groove (MG), side plate (SP), outer side plate (OSP), x37.5; *2*, plate diagram, ambulacra (A-E), azygous basal (a), zygous basal (z), radial (r), deltoid (d), x4.

FIGURE II-11—Photographs of *Pentremites* specimens preserving summit structures *1-8*, *10*, *Pentremites tulipaformis* Hambach, whitened; *1*, *2*, *4*, *5, 8,* CMC IP66827, CD interray, oblique, summit views respectively, note the small cover plates covering the ambulacra and a lack of differentiation of the cover plates along the main food grooves, x5.8; *5*, detail of summit showing cover plates over oral surface and spiracles, note the anal pyramid over the anispiracle in the CD position, x15.7; *8*, ESEM image showing detail of AB spiracle cover plates, x29; *3*, *6*, CMC IP66829, C ambulacral, summit views respectively, x11.7; *7*, *10*, CMC IP66828, A ambulacral and summit views respectively, x6; *9*, *11*, *12 Pentremites pyriformis* Say, whitened; *9*, *12*, CMC IP66830, C ambulacral, summit views respectively, note the very high cover plates covering the main food grooves and the spine like spiracle cover plates, x8.5; *11*, ESEM image showing detail of BC spiracle cover plates, x35.8.

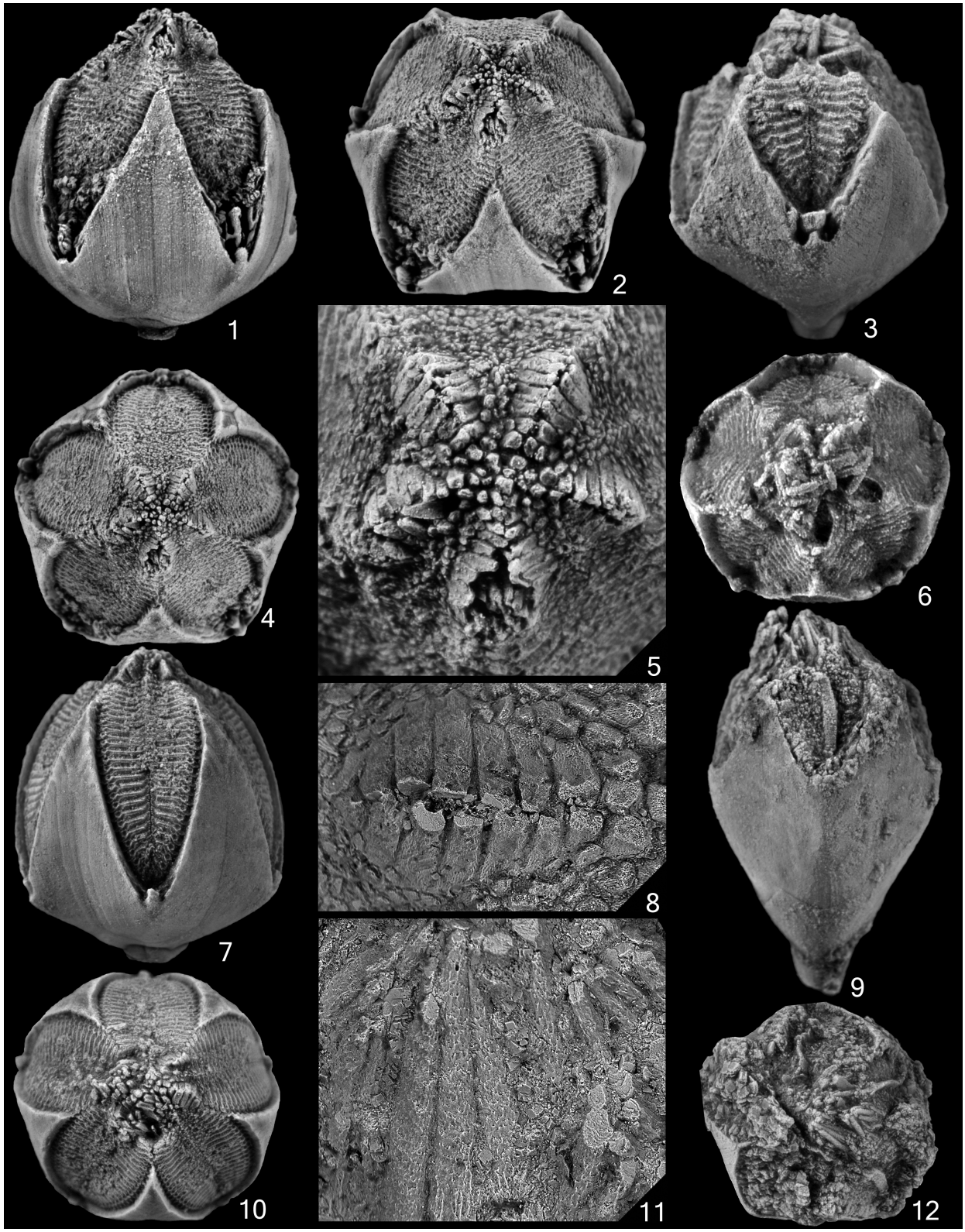

Figure II-11. Continued

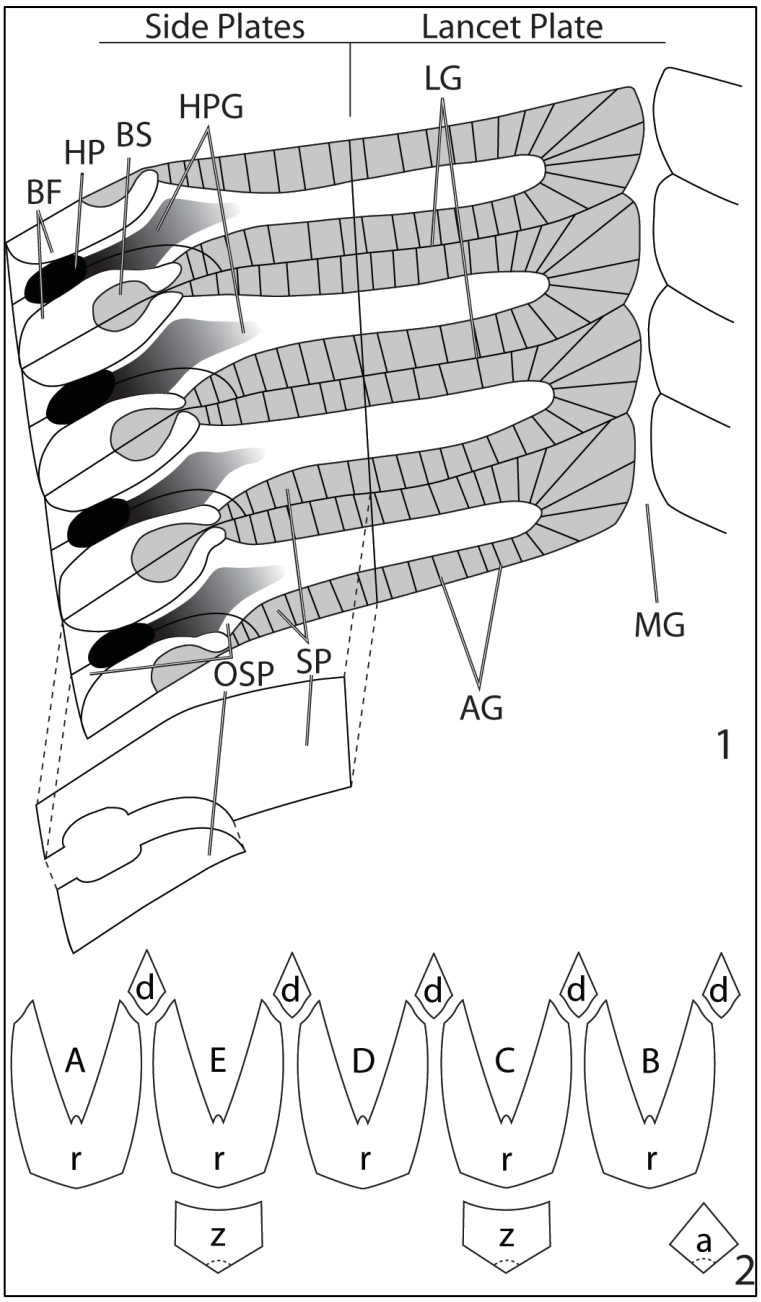

FIGURE II-12—Camera lucida drawing of *Pentremites tulipaformis* Hambach based on specimen CMC IP66824; *1*, left side of ambulacrum. Articulation groove (AG), brachiole facet (BF), brachiole socket (BS), hydrospire pore (HP), hydrospire pore groove (HPG), lateral groove (LG), median groove (MG), side plate (SP), outer side plate (OSP), x37.5; *2*, plate diagram, ambulacra (A-E), azygous basal (a), zygous basal (z), radial I, deltoid (d), x2.5.

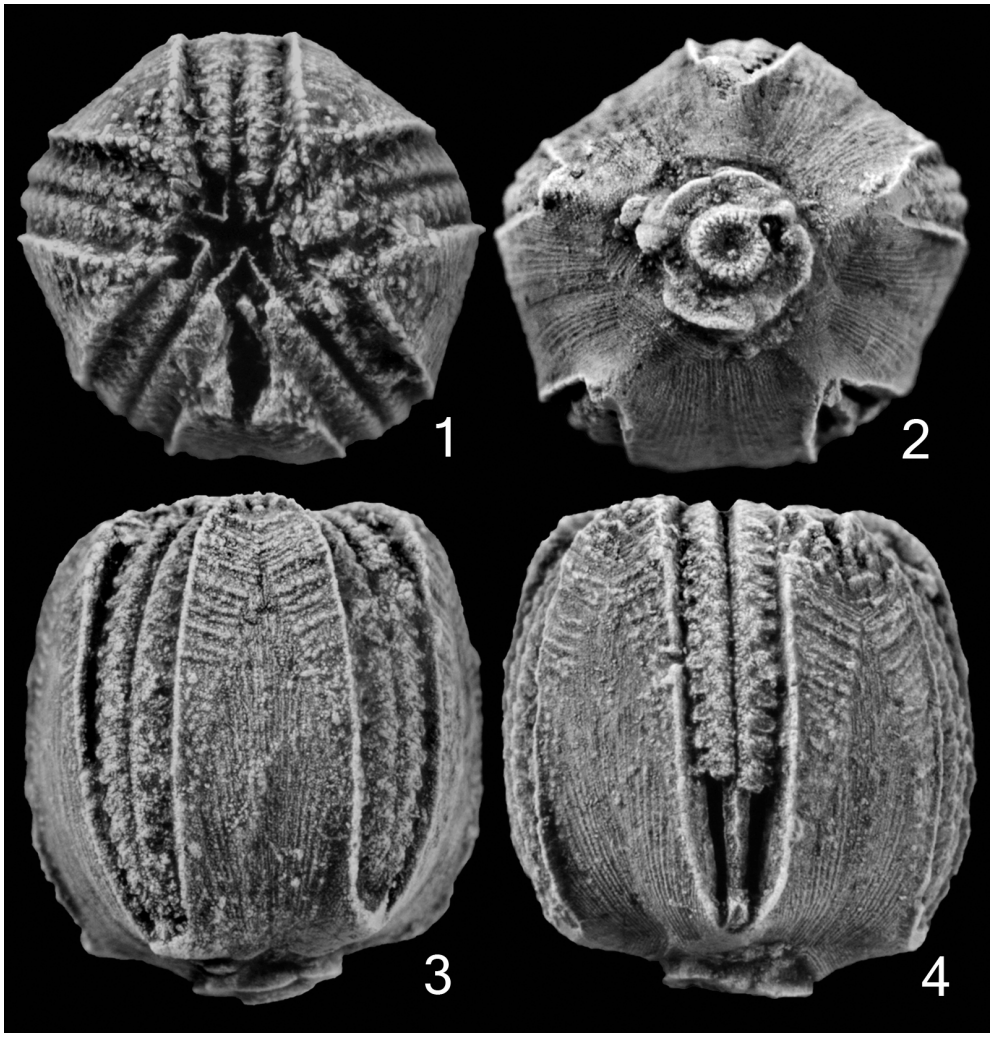

FIGURE II-13—Photographs of holotype CMC IP66831 of *Diploblastus fadigai* n. sp., whitened, x10.3; *1-4*, summit, basal, D ambulacral, AB interray views respectively, note the missing side plates on the D ambulacral exposing the lancet plate.

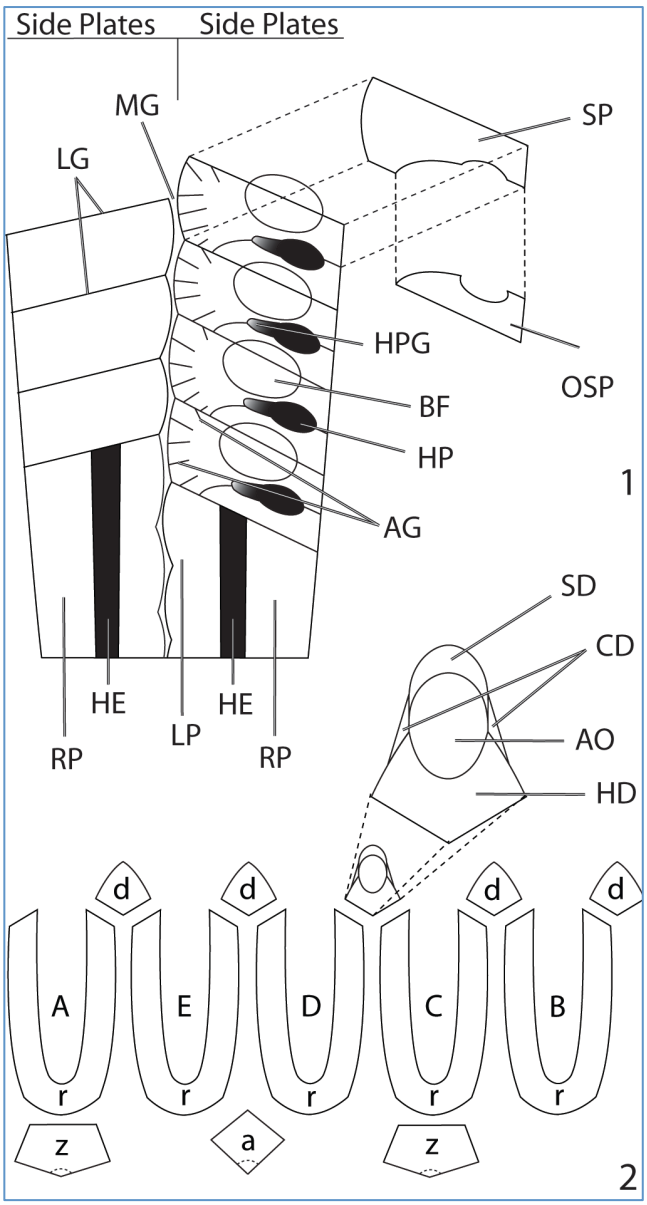

FIGURE II-14—Camera lucida drawing of *Pentremites fadigai* n. sp. based on holotype CMC IP66831; *1*, Left side of ambulacrum. Articulation groove (AG), brachiole facet (BF), hydrospire pore (HP), hydrospire pore groove (HPG), lateral groove (LG), median groove (MG), side plate (SP), outer side plate (OSP), radial plate (RP), lancet plate (LP), hydrospiralium entrance (HE), x46; *2*, plate diagram, ambulacra (A-E), azygous basal (a), zygous basal (Z), radial I, deltoid (d), superdeltoid (SD), cryptodeltoid (CD), hypodeltoid (HD), anal opening (AO), note azygous deltoid is in the DE position, x7.8.

TABLE II-1— Abbreviated BIC results from MCLUST for the five most optimal models with parameterizations and up to six components for the *Pentremites* dataset. As seen here, the model parameterizations utilized by MCLUST to search for morphological clusters are the distribution, volume, and shape of the data. Different combinations of the parameterizations were assigned BIC scores to find the appropriate model and number of components (i.e. species in the population).

	EII	**VII**	**EEI**	**VEI**	**EVI**
Distribution	Spherical	Spherical	Diagonal	Diagonal	Diagonal
Volume	Equal	Variable	Equal	Variable	Equal
Shape	Equal	Equal	Equal	Equal	Variable
1 Component	-858.0458	-858.0458	-619.9617	-619.9617	-619.9617
2 Component	-628.9748	-632.441	-601.3494	-605.0453	-616.2117
3 Component	-616.1298	-586.136	-593.2873	-569.1819	-597.4454
4 Component	**-545.8177**	-549.7836	-548.9095	-551.3041	-579.0886
5 Component	-559.4034	-558.9537	-563.1435	-561.9023	-606.1072
6 Component	-567.2003	-565.0652	-570.5371	-574.495	-620.4285

III. COMPARISON OF THE ONTOGENY OF CHESTERIAN PENTREMITID BLASTOIDS

This chapter is a reformatted version of a paper, by the same name, to be submitted to the journal Lethaia by James W. Atwood, Troy Fadiga, and Colin D. Sumrall.

ABSTRACT— This study utilizes geometric morphometrics to examine the ontogeny of the blastoid genus *Pentremites*. Specimens of *Pentremites fredericki*, *P. godoni*, *P. pyriformis*, *P. spicatus, P. symmetricus*, and *P. tulipaformis* were collected from four Upper Mississippian localities in Kentucky, Indiana, Tennessee, and Illinois, USA. Three-dimensional images were acquired for randomly selected specimens across the ontogeny of each species and coordinates were collected for a series of homologous landmarks that fully describe blastoid morphology through ontogeny. The data show that all species in this study share a common ontogenetic pathway and shape varies significantly with both size and by species. This result suggests that the initial shape of the theca just post metamorphosis has a strong influence on the mature thecal shape.

INTRODUCTION

It has been shown that our knowledge of blastoid paleobiology can be greatly expanded through the use of three-dimensional (3D) modeling and geometric morphometrics (Foote 1991; Atwood and Sumrall 2012). These studies showed the utility of 3D geometric morphometric methods for understanding shape disparity and species discrimination respectively. This paper extends these investigations to the study of the ontogeny of the blastoid *Pentremites* discern commonality and differences in the growth trajectories of closely related blastoids species.

This study utilizes laser imaging to collect landmark data and geometric morphometrics to analyze data. This approach provides a better understanding of blastoid ontogeny than classic linear measurements with calipers (Macurda 1975; Waters 1977; Waters et al. 1985). Three-dimensional geometric morphometrics preserves shape information recorded by three-dimensional preserved thecae, which is typically lost in using classic linear measurements. Consequently, it is better able to describe shape by analyzing data while retaining the spatial relationships among homologous landmarks.

Pentremites is the most abundant blastoid in North American Mississippian faunas, at times being the dominant echinoderm. In many localities, specimens of *Pentremites* can be collected by the hundreds providing large collections from which study specimens can be drawn (Waters et al. 1985; Dexter et al. 2009; Atwood and Sumrall 2012). Often these specimens are exquisitely preserved allowing their morphologies to be studied in great detail. Blastoids collected for this study range from 100μm to 4cm in thecal height (Fig. 1). While many blastoids collected from these localities were taphonomically damaged by crushing, breakage or compaction, a sufficient number of fully three dimensional and undistorted specimens were recovered for each species to allow ontogenetic study.

Most organisms exhibit large morphologic change during growth. Whether the change is metamorphosis, allometric scaling, or heterochronic changes, the ontogenetic transformation can be remarkable. Furthermore, environmental pressures can change the timing of ontogenetic events and how an organism grows drastically changing morphology between closely related species or within a single species (Zelditch, 1989). Since determining ages of individuals is often problematic, care has to be taken to not confuse systematic differences (genera/species) with ontogenetic variation.

PREVIOUS INVESTIGATIONS AND STRATIGRAPHY

Most significant work on pentremitid blastoid ontogeny was conducted from 1940 to 2009 (Moore 1940; Galloway and Kaska 1957; Waters 1977; Waters et al. 1985; Sevastopulo 2005; Dexter 2009). Recent work has preliminarily quantified blastoid ontogeny though caliper measurements of linear dimensions to quantify allometric change, the examination of immature blastoid forms (*Passalocrinus*) with speculations about the developmental sequence and the possible role heterochrony plays in blastoid evolution (Moore 1940; Galloway & Kaska 1957; Waters 1977; Waters et al. 1985; Sevastopulo 2005).

Beaver et al. (1967) identified four stages in blastoid ontogeny: larval stage (*Passalocrinus*), juvenile stage, adult stage, and gerontic stage (most mature form). The stages were poorly defined and there was much ambiguity in defining life stages and forms. In 2005, Sevastopulo argued that larval stage blastoids were free swimming (none have been recognized) and that *Passalocrinus* is the earliest post metamorphosis juvenile stage. Sevastopulo also argues that the greatest difference delineating juvenile from adult are the plating on the summit of *Passalocrinus* which are not possessed by the adult forms. That leaves only size to delineate adult and gerontic blastoids as defined by Beaver et al. (1967).

Most recently, Sumrall and Waters (2012) argue that the "oral" plates of *Passalocrinus* that cover the peristome are homologous with the primary peristomial cover plates. At this developmental stage, the oral plates (deltoids) are either not developed, small, or not exposed externally. The loss of the primary peristomial cover plates is a taphonomic artifact of the poor suturing of the theca as the ambulacra begin to develop. The oral plates express later when the peristomial border is evident and they bear the most

proximal ambulacra on their sutures (Sumrall and Waters 2012). It appears that no new plate circlets added post larval stage but the vault lengthens while the pelvis shortens respectively. Lastly, deltoid bodies become proportionately larger while the ambulacra add plates during growth by terminal addition (distally).

Although these changes can be captured by caliper measurements, they have not been analyzed using geometric morphometrics. By utilizing geometric morphometrics, individual plate growth patterns can be reassessed and growth patterns can be differentiated among species and by thecal region. Furthermore, the relative geometric changes between homologous landmarks can be determined.

SPECIES SELECTION AND STRATIGRAPHY

The Upper Mississippian (Chesterian) formations of the North American mid-continent yield large numbers of extraordinarily well-preserved marine fossils (Butts 1917; Nelson et al. 2002). This study focuses on blastoid collections derived from four sections of Chesterian strata preserved at different localities that yield large collections of six species of the blastoid genus *Pentremites*. Although there are nine recognized species of Chesterian *Pentremites,* only six were used in this study (Fig. 1). Species included in the study were selected based on the availability of fossil localities that could produce large numbers of specimens that were well preserved and undeformed. Specimens were collected from four different localities including: Pennyrile Parkway, KY, USA; Floraville, IL, USA; Sparta TN, USA; and Sulphur, IN, USA. All of these localities contained multiple species of *Pentremites* except for the Sparta, TN locality. In all cases species were easily separated by visual inspection or linear measurements.

Pennyrile Parkway, *Christian Co. Kentucky, USA*—This locality exposes strata of the Lower Chesterian Glen Dean Formation in a road cut along the Pennyrile Parkway in Christian County, southwestern Kentucky. The lowermost 1-2m of the exposed section contains highly weathered, fissile, fossiliferous, shale with minor limestone interbeds. The limestone is grayish brown on fresh faces and weathers light gray. The shale is light olive gray on fresh faces and weathers dark gray. The blastoid fauna includes four species of *Pentremites* including: *P. fredericki* (Fig. 1-16-1.20), *P. meganae*, *P. pyriformis* (Fig. 1.11-1.15), and *P. 69ulipaformis* (Fig. 1.6-1.10). Specimens of *P. meganae* were rare and did not preserve a complete enough ontogenetic sequence to be used in the study. The other three *Pentremites* species were present with sufficient numbers of well preserved specimens to be used in the study and were easily separated utilizing morphological criteria (Atwood and Sumrall 2012). Few other echinoderms were collected during this study but include cladid crinoids, discocystinid edrioasteroids, and single specimen of the blastoid *Diploblastus fadigai* (Atwood and Sumrall 2012).

Floraville, St. Clair Co. Illinois, USA —This locality exposes natural outcrops of the Lower Chesterian, Ridenhower Formation of the Paint Creek Group along the banks of a streambed located along either side of the Prairie Du Long Creek about 1.6 km north of Floraville, IL. The outcrops were composed of weathered, fissile, fossiliferous, light green shale with minor limestone interbeds. Blastoids found at this locality were primarily *P. godoni* (Fig. 1.1-1.5) with fewer *P. pyriformis*. For this study, only specimens of *P. godoni* were included from this locality because of the limited number of specimens of *P. pyriformis* that were collected. The two species are easily distinguished by simple vault pelvis ratio measurements (Waters et al., 1985). The Floraville, IL locality has a rich and

diverse echinoderm fauna including crinoids, blastoids, asteroids, and edrioasteroids (Sumrall 1996).

Sulphur, Crawford Co. IN, USA—The Sulphur Indiana locality of the Indian Springs Shale Member of the Big Clifty Formation of the Stephensport Group at Sulpur, Indiana is exposed along road cuts around the intersection of Interstate 64 and Indiana Highway 37. The outcrops are composed of fossiliferous grey shale interbedded with limestone. Specimens of *P. symmetricus* (Fig. 1.21-1.25) and *P. godoni* were present at the locality, but only *P. symmetricus* (called *P. pyriformis* by Dexter et al. (2009)) were present in sufficient numbers to be used in the study. The two species are easily separated using vault pelvis ratios. In addition to blastoids, the locality has a diverse crinoid and asteroid fauna (Horowitz 1965; Blake and Elliott 2003).

Sparta, White Co. TN, USA—The Sparta, Tennessee locality exposes the Upper Chesterian Pennington Formation. The locality was approximately 1.6 km off the Mill Creek road on a little used hiking trail. The locality preserves poorly exposed outcrops of highly weathered fossiliferous shale and no fresh strata are visible. The shale weathers light tan to gray in color. Collections were made primarily from float material derived from fossiliferous weathered shale in areas where blastoids were excavated in previous decades. This locality only had one blastoid species *P. spicatus* (Fig. 1.26-1.30). Few other echinoderms were noted except for tegmal wing plates of two species of *Pterotocrinus*.

METHODOLOGY

Collection.—For this study, it was important to minimize variance that resulted from causes other than allometric changes during ontogeny. Microevolutionary change was minimized

by limiting the collections to small stratigraphic intervals within each locality typically a single bed. This limited the affects of large-scale temporal and geographic mixing of heterogeneous populations. Because specimens from each locality were collected from a single bed, there is likely only very limited ecophenotypic variation. Phenotypic variation is always present, but its influence was minimized by robust sampling of each species. External sexual dimorphism has not been documented in blastoids, but again the robust sampling would have mitigated this factor. Thus the signal that was left in the dataset was largely a function of allometry and phenotypic variation.

Museum collections were not used in this study because they are often biased samples of well-preserved and large specimens with few or no small size blastoids (juveniles). Often they are culled of specimens perceived to be unusual. There is also no guarantee that all specimens in a sample lot are from the same bed at the same locality. Consequently, new collections of all species were assembled to assure that temporal and environmental mixing, paleoenvironment, and shape could be controlled and sampled randomly.

The focus during collection of material was to assure that we did not impose bias on the distribution of shape within the species populations. Size frequency data, however, was not preserved by the sampling techniques. At all localities, all blastoid specimens (typically larger specimens) were surface collected and additional (typically smaller specimens) were collected in bulk samples of weathered shale. This bulk material was dry sieved into five 20 L buckets to remove any larger rock fragments and larger modern plant material and roots from the samples.

Typically three to five buckets of bulk material were collected at each locality with the exception of the Pennyrile Parkway locality, where approximately 30 – 40 buckets of bulk material were collected for use in a previous study (Atwood and Sumrall 2012).

Bulk samples were washed in warm water followed by three percent hydrogen peroxide to break down the shale matrix and organic material releasing fossil residue from the shale. Blastoids were then retrieved from these residues via handpicking. This method generated large sample population collections of blastoids that included individuals from all sizes present at each locality. All localities except for the Sparta, TN produced at least one blastoid species present in too small of sample size to use in this study. However, with heavier collecting the underrepresented species could be utilized. By using this method, our samples were biased according to size frequency, but not biased according to shape. Similar methods were used to collect blastoids ontogenies for other studies (Dexter et al., 2009; Atwood and Sumrall, 2012).

For each sample locality, individual blastoids were sorted by species and screened for taphonomic deformation. Specimens were visually inspected by looking for deviation from the regular pentameral cross section and other obvious signs of deformation. If a blastoid showed nearly perfect radial symmetry, it was considered to be usable. Teratological specimens were removed, including specimens with four ambulacra, or ambulacra that were developmentally truncated with respect to other ambulacra on the same specimen. Rejecting specimens in this method left only phenotypic variation, sexual dimorphism and ontogenetic variation as the primary sources of variance within the six populations. Although external sexual dimorphism is not known in *Pentremites*, it has been

documented internally in the CD side hydrospires of *Pentremites rusticus* (Katz and Sprinkle 1976).

From the set of usable specimens, a study sample was selected. Specimens of each species were sorted by height into several size categories from which specimens were selected to assure that the full ontogeny was captured by specimen data. From each size category specimens were selected using a random number generator that was set to the population size of the group. Selected specimens were inspected under a binocular microscope to insure that all of the landmarks could be identified. Occasionally a specimen needed additional hand preparation to remove matrix covering the landmarks. If a specimen was damaged so that a landmark was unusable, it was replaced by another specimen using the random number generator. This method assured a full range of sizes were used in the study and specimens were not preferentially selected for shape. Because of the limits of the laser scanner, specimens 4mm and smaller in height were not included in the sample populations. Although a full range of heights were available for five species, *Pentremites spicatus* was limited in specimens of small size. However, the large mature height of this species allowed a comparable ranges in size with respect to the other species used in the study.

A total of 120 specimens were analyzed in this study (20 from each species), but because of scanning errors, some of the specimens were not used. These problematic scans were removed a-priori and were the result of alignment errors between the multiple scans of individual specimens. The analyses that follows, utilized 112 of the 120 scans (20 of *P. symmetricus* and *P. tulipaformis,* 19 *P. godoni,* 18 *P. spicatus* and *P. pyriformis,* and 17 *P. fredericki*).

Analysis.—To aid in the recording of data, landmarks were marked with a micro pen on specimens under high magnification prior to scanning to allow landmark positions to be recorded on the 3D specimen images. A 3D image of each specimen was attained using the Nextengine 3D Laser Scanner at the University of Tennessee. Specimens were scanned at the highest possible resolution, of 0.127mm in an A-ray orientation. Each image was composed of three scans that were 60 degrees apart rotated about an axis that was perpendicular to both the polar and A/CD axes of the specimens to insure total coverage of the A-ray. The A-ray was selected as it contains the juncture between one of the zygous basals and azygous basal. This provided a 3D image that included landmarks located along the peristomial border and stem facet (Fig. 2).

From these 3D images X, Y, Z coordinates of landmarks (modified from Foote, 1991) were recorded. These landmarks are morphologically common to all known species of blastoids, and fully describe the morphology of the specimens in 3D (Fig. 2). All landmarks were type I (sensu stricto Bookstein 1991), being positioned at three plate junctions of thecal plates except landmark 6 which was type 2 landmark. This landmark was positioned along the midline of the A ambulacrum where it intersects with the side food groove that intersects landmark seven along the edge of the ambulacrum.

Landmark data were collected from the models using the imaging program MESHLAB (Cignoni et al. 2008) and analyzed using R (language and environment for statistical computing and graphics). Landmarks were aligned and analyzed using the R package GEOMORPH (Adams and Otarola-Castillo 2013; R Core Team 2013). Landmarks were aligned using a generalized Procrustes superimposition (Bookstein 1991; Zelditch et al. 2004; Dryden 2007) that removed differences in location, scale, and orientation such

that differences between specimens reflect only shape. The residuals were then projected into a tangent Euclidean space, and these projected coordinates were used as shape variables. Ontogenetic allometry and group differences were assessed with a permutational Procrustes analysis of variance (ANOVA) (Goodall 1991) using 9,999 replicates. This analysis differs from traditional ANOVA by using Procrustes distances to assess goodness-of-fit instead of the sum of squares and by using permutations to approximate a null distribution instead of using a parametric F-distribution.

Multivariate allometry was visually inspected by plotting regression scores against the log of the centroid sizes (Drake and Klingenberg 2008). The regression scores indicate the amount of variation predicted by a regression plus the residual variation along the same direction as the regression. The regression coefficients used were taken from a regression model that included centroid size as a covariate and species identifier as a factor.

RESULTS AND DISCUSSION

The ANOVA results (Table 1) indicate that *Pentremites* shape varies significantly with size and by species, but there is not a significant interaction term between these two variables. It appears that all six of the *Pentremites* species share a statistically indistinguishable ontogeny over the size span sampled in this analysis. Figure 3 shows the regression scores plotted against the log centroid size, visually demonstrating that these *Pentremites* species have a shared, significant relationship to size. Even though they cannot be significantly separated as multiple ontogenies it appears visually that the pyriform group taxa (*P. pyriformis* and *P. symmetricus*) and godoniform group taxa (*P. fredericki, P. godoni, P. spicatus,* and *P. 75ulipaformis*) have different y-intercepts. This suggests that pyriforms

(long pelvis) and godoniforms (wide with short pelvis) most likely have different starting shapes. Interestingly, collections from the Glen Dean Formation where both pyriform group species (*P. meganae* and *P. pyriformis*) and godoniform group species (*P. fredericki* and *P. tulipaformis*) include *Passalocrinus specimens* with two different morphotypes. The first form (Fig. 4.1) resembles a pyriform group species while the second form (Fig. 4.2) resembles a godoniform suggesting that the early diversification of adult morphotype results from morphological changes seen just post metamorphosis.

From the six *Pentremites* ontogenies an average ontogenetic series of landmark means was calculated (Fig 5). Landmarks five, six, and seven show that ontogenetically the ambulacra become narrower with the respect to the total blastoid width while landmark nine shows that the tip of the ambulacra extends throughout ontogeny (Fig 5.2). The pelvis proportionately shortens ontogenetically as the stem facet shortens with respect to the pelvis (Fig 5.3). The distance between the mouth (landmark 1) and the deltoid tips (landmarks 2 and 3) proportionately decreases (Fig. 5.1). While the position of the deltoid body remains roughly constant through ontogeny, their lengths (the distances between landmarks 2, and 8, 3 and 4) increase with thecal size (Fig 5.2). Lastly, the radial plates appear to grow much more proximally than distally (Fig. 5.2, 3).

Even though this study was ultimately limited by the resolution of the laser scanner, we have demonstrated that six different species of *Pentremites* from four different localities have a common growth pattern that may be divided into the two morphotypes. It is our contention that these preliminary findings are accurate but to test this hypothesis, we will need to add more species, collect higher numbers of specimens, and have ability to image the smallest of specimens. There is also no rigorous hypothesis of *Pentremites* phylogeny

upon which to test ideas concerning the evolution of *Pentremites* via heterochrony.

CONCLUSIONS

With the use of 3-D geometric morphometrics we were able to discern that despite varied morphology all species of *Pentremites* in this study grow along the same morphological trajectory. Even though all taxa have different y-intercepts, godoniform taxa and pyriform taxa, as morphological groups, seem to have somewhat different trajectories with respect to each other. These two groups could possible be statistically separated given more data. Shape change during ontogeny largely consists of changing aspects of the pelvis, lengthening the ambulacra, shrinking the size of the summit, and enlargement the deltoid bodies.

ACKNOWLEDGEMENTS

We thank Daniel Frederick and Larry Knox for introducing us to two of the localities and aiding in sample collection. We also thank Tim Paton for spending many hours scanning blastoids. Assistance in the field was provided by B. Ford, R. Shroat-Lewis, G. Gilleaudeau, M. Schnuck, and E. Hogan. Assistance with museum collections was provided by Brenda Hunda, Cincinnati Museum Center. Two reviewers ____ and ____ provided valuable reviews that greatly improved the manuscript. The laser scanner was acquired in part through NSF grant EAR-0745918. Financial assistance for this study was provided by the NSF – Assembling the Echinoderm Tree of Life Grant, DEB-1036260.

REFERENCES

ADAMS, D., AND A. NISTRI. 2010. Ontogenetic convergence and evolution of foot morphology in European cave salamanders (Family: Plethodontidae). Bmc Evolutionary Biology, 10(1):1-10.

ADAMS, D. C., AND E. OTÁROLA-CASTILLO. 2013. Geomorph: an r package for the collection and analysis of geometric morphometric shape data. Methods in Ecology and Evolution, 4(4):393-399.

ATWOOD, J. W., AND C. D. SUMRALL. 2012. Morphometric Investigation of the Pentremites Fauna from the Glen Dean Formation, Kentucky. Journal of Paleontology, 86(5):813-828.

BEAVER, H. H., K. E. CASTER, D. J. W., R. O. FAY, H. B. FELL, R. V. KESLING, D. B. MACURDA, R. C. MOORE, G. UBAGHS, AND J. WANNER. 1967. Blastoids. P. S-297-455, *in* (R. C. Moore (ed.) Treatise on Invertebrate Paleontology (S)Echinodermata(1). The University of Kansas and The Geological Society of America, Boulder, 2.

BEAVER, H. H., AND A. J. FABIAN. 1998. Color Patterns in Mississippian (Chesterian) Blastoids. Journal of Paleontology, 72(2):332-338.

BEAVER, H. H., A. J. FABIAN, AND M. PALATAS. 2000. Summit structures in Mississippian blastoids. Journal of Paleontology, 74(2):247-253.

BLAKE, D. B., AND D. R. ELLIOTT. 2003. OSSICULAR HOMOLOGIES, SYSTEMATICS, AND PHYLOGENETIC IMPLICATIONS OF CERTAIN NORTH AMERICAN CARBONIFEROUS ASTEROIDS (ECHINODERMATA). Journal of Paleontology, 77(3):476-489.

BOOKSTEIN, F. L. 1991. Morphometric tools for landmark data: geometry and biology. Cambridge University Press, Cambridge, New York etc, i-xvii, 1-435 p.

BUTTS, C., S. KENTUCKY GEOLOGICAL, AND S. GEOLOGICAL. 1917. Mississippian formations of western Kentucky. State Journal Co., Frankfort.

CIGNONI, P., M. CORSINI, AND G. RANZUGLIA. 2008. MeshLab: an open-source 3D mesh processing system. ERCIM News, 73:47-48.

DEXTER, T. A., C. D. SUMRALL, AND M. L. MCKINNEY. 2009. Allometric strategies for increasing respiratory surface area in the Mississippian blastoid Pentremites. Lethaia, 42(2):127-137.

DRAKE, A. G., AND C. P. KLINGENBERG. 2008. The pace of morphological change: historical transformation of skull shape in St Bernard dogs. Proceedings of the Royal Society B: Biological Sciences, 275(1630):71-76.

DRYDEN, I. L. 2007. Shapes: Statistical Shape Analysis. R Package Version 1.1-1., http://www.maths.nott.ac.uk/~ild/shapes.

FOOTE, M. 1991. Morphological and Taxonomic Diversity in a Clade's History: The Blastoid Record and Stochastic Simulations. Contributions from the Museum of Paleontology, 28(6):101-140.

GALLOWAY, J. J., AND H. V. KASKA. 1957. Genus *Pentremites* and its Species. The Geological Society of America Memoir, 69:1-104.

GOODALL, C. 1991. PROCRUSTES METHODS IN THE STATISTICAL-ANALYSIS OF SHAPE. Journal of the Royal Statistical Society Series B-Methodological, 53(2):285-339.

HOROWITZ, A. S. 1965. Crinoids from the Glen Dean Limestone (Middle Chester) of Southern Indiana and Kentucky. Indiana Geological Survey Bulletin 34:52.

KATZ, S. G., AND J. SPRINKLE. 1976. Fossilized Eggs in a Pennsylvanian Blastoid. Science, 192(4244):1137-1139.

MACURDA, D. B. 1975. *Pentremites* (Blastoidea) of Burlington Limestone (Mississippian). Journal of Paleontology, 49(2):346-373.

MCKINNEY, M. L., AND K. J. MACNAMARA. 1991. Heterochrony : the evolution of ontogeny. Plenum, New York [etc.].

MOORE, R. C. 1940. Early Growth Stages of Carboniferous Microcrinoids and Blastoids. Journal of Paleontology, 14(6).

NELSON, W. J., AND S. ILLINOIS STATE GEOLOGICAL. 2002. Sequence stratigraphy of the lower Chesterian (Mississippian) strata of the Illinois Basin. Illinois State Geological Survey, Champaign, IL.

SEVASTOPULO, G. D. 2005. The early ontogeny of blastoids. Geological Journal, 40(3):351-362.

SUMRALL, C. D. 1996. Late Paleozoic edrioasteroids (Echinodermata) from the North American Midcontinent. Journal of Paleontology, 70(6):969-985.

SUMRALL, C. D., AND J. A. WATERS. 2012. Universal Elemental Homology in Glyptocystitoids, Hemicosmitoids, Coronoids and Blastoids: Steps Toward Echinoderm Phylogenetic Reconstruction in Derived Blastozoa. Journal of Paleontology, 86(6):956-972.

TEAM, R. C. 2013. R: A language and environment for statistical computing. R Foundation for Statistical Computing, http://www.R-project.org/, Vienna, Austria.

WATERS, J. A. 1977. Quantification of shape by use of Fourier analysis; the Mississippian blastoid genus *Pentremites*. Paleobiology, 3(3):288-299.

WATERS, J. A., A. S. HOROWITZ, AND D. B. MACURDA. 1985. Ontogeny and Phylogeny of the Carboniferous Blastoid *Pentremites*. Journal of Paleontology, 59(3):701-712.

ZELDITCH, M. L., AND A. C. CARMICHAEL. 1989. Ontogenetic Variation in Patterns of Developmental and Functional-Integration in Skulls of Sigmodon-Fulviventer. Evolution, 43(4):814-824.

ZELDITCH, M. L., AND W. L. FINK. 1996. Heterochrony and heterotopy: Stability and innovation in the evolution of form. Paleobiology, 22(2):241-254.

ZELDITCH, M. L., D. L. SWIDERSKI, D. H. SHEETS, AND W. L. FINK. 2004. Geometric Morphometrics for Biologists. Elsevier Academic Press (USA), San Diego.

APPENDIX II

Figure III-1—Generalized ontogeny of *Pentremites* species used in this study. Note the relative lengthening of the ambulacra while the pelvis shortens. All specimens have been whitened. 1-5, *Pentremites godoni*, 1, CMC IP70944; 2, CMC IP70943; 3, CMC IP70949; 4, CMC IP70960; 5, CMC IP70953; x1.8; 6-10, *Pentremites tulipaformis*, 6, CMC IP71023; 7, CMC IP71026; 8, CMC IP71030; 9, CMC IP71036; 10CMC IP66821; x2.1; 11-15, *Pentremites pyriformis*, 11, CMC IP66821; 12, CMC IP70964; 13, CMC IP70967; 14, CMC IP70972; 15, CMC IP70981; x1; 16-20, *Pentremites fredericki*, 16, CMC IP64791; 17, CMC IP64793; 18, CMC IP64796; 19, CMC IP65797; 20, CMC IP64794; x1.6; 21-25, *Pentremites symmetricus*, 21, CMC IP71004; 22, CMC IP71005; 23, CMC IP71009; 24, CMC IP71008; 25, CMC IP71011; x1.3; 26-30, *Pentremites spicatus*, 26, CMC IP70985; 27, CMC IP70990; 28, CMC IP70995; 29, CMC IP70999; 30, CMC IP71001; x0.8.

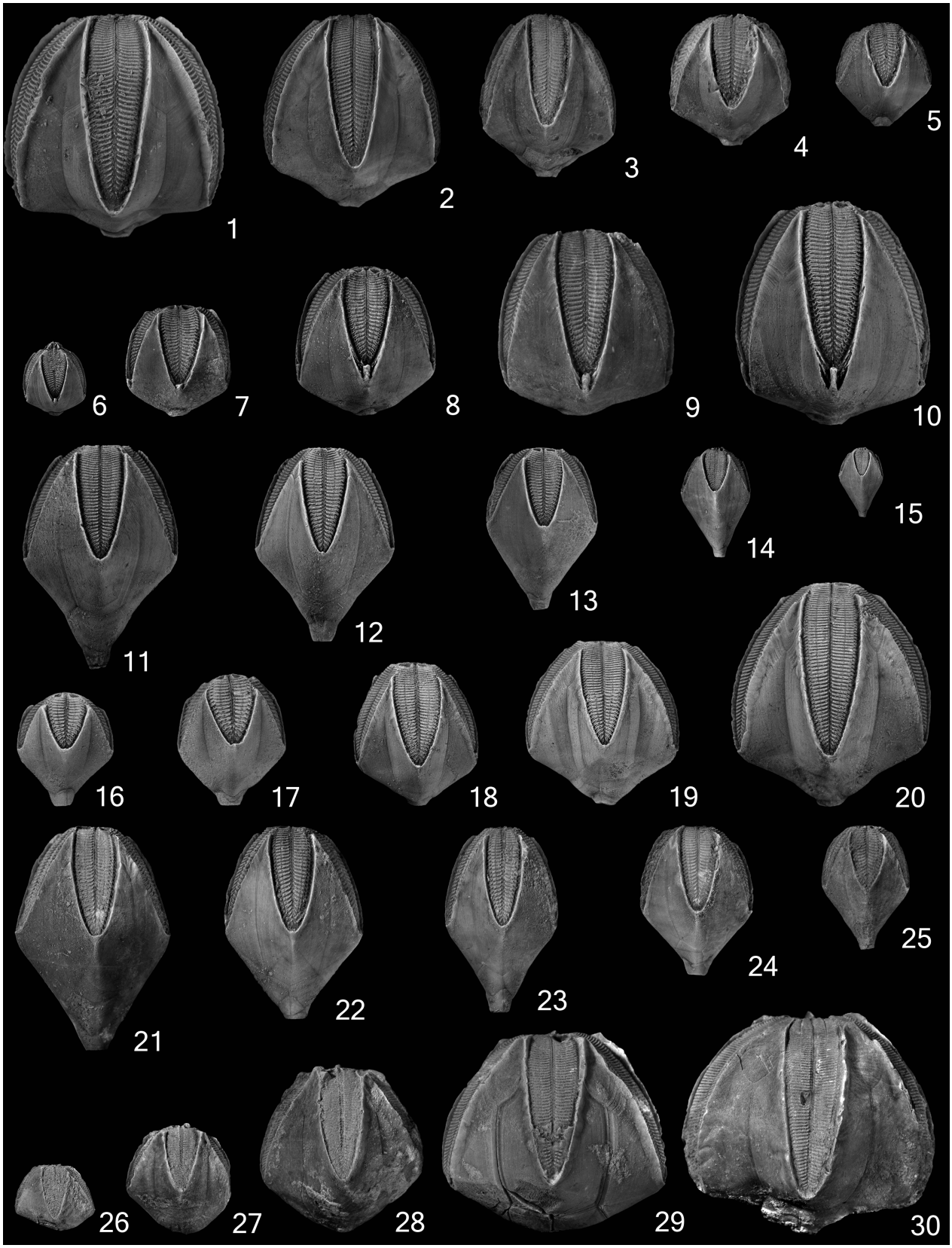

Figure III-1. Continued

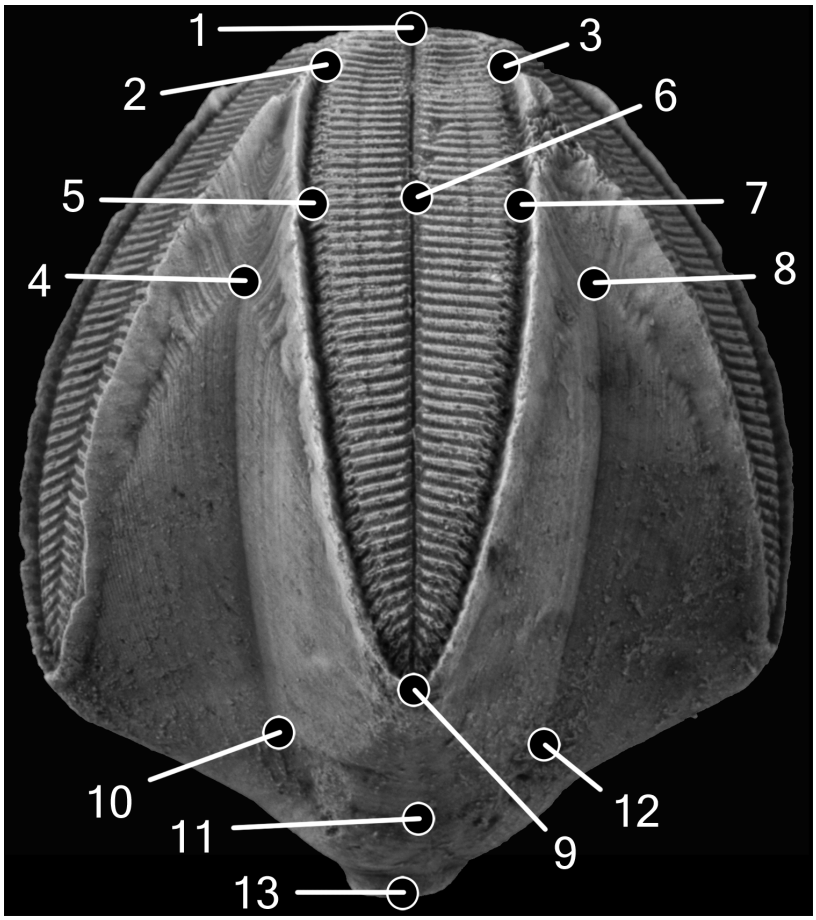

FIGURE III-2—*Pentremites fredricki* (CMC IP6479) showing the positions of landmarks used to measure 3D shape in A ambulacral view; *1*, lancet/deltoid/deltoid triple plate junction in A ray; *2*, *3*, AB and AE deltoid/side plate/side plate triple plate junction; *4, 8*, AE and AB deltoid/radial/radial triple plate junction respectively; *5, 7*, AE and EA deltoid/radial/side plate triple plate junction respectively; *6*, center line of lancet located by following lateral food groove from landmark 5 to main food groove; *9*, radial/side plate/side triple plate junction at ambulacral tip; *10*, A radial/azygous basal/zygous basal triple junction; *11*, radial/radial/azygous basal triple plate junction; *12*, radial/radial/zygous basal triple plate junction; *13*, center of the stem facet (modified after Atwood and Sumrall 2012).

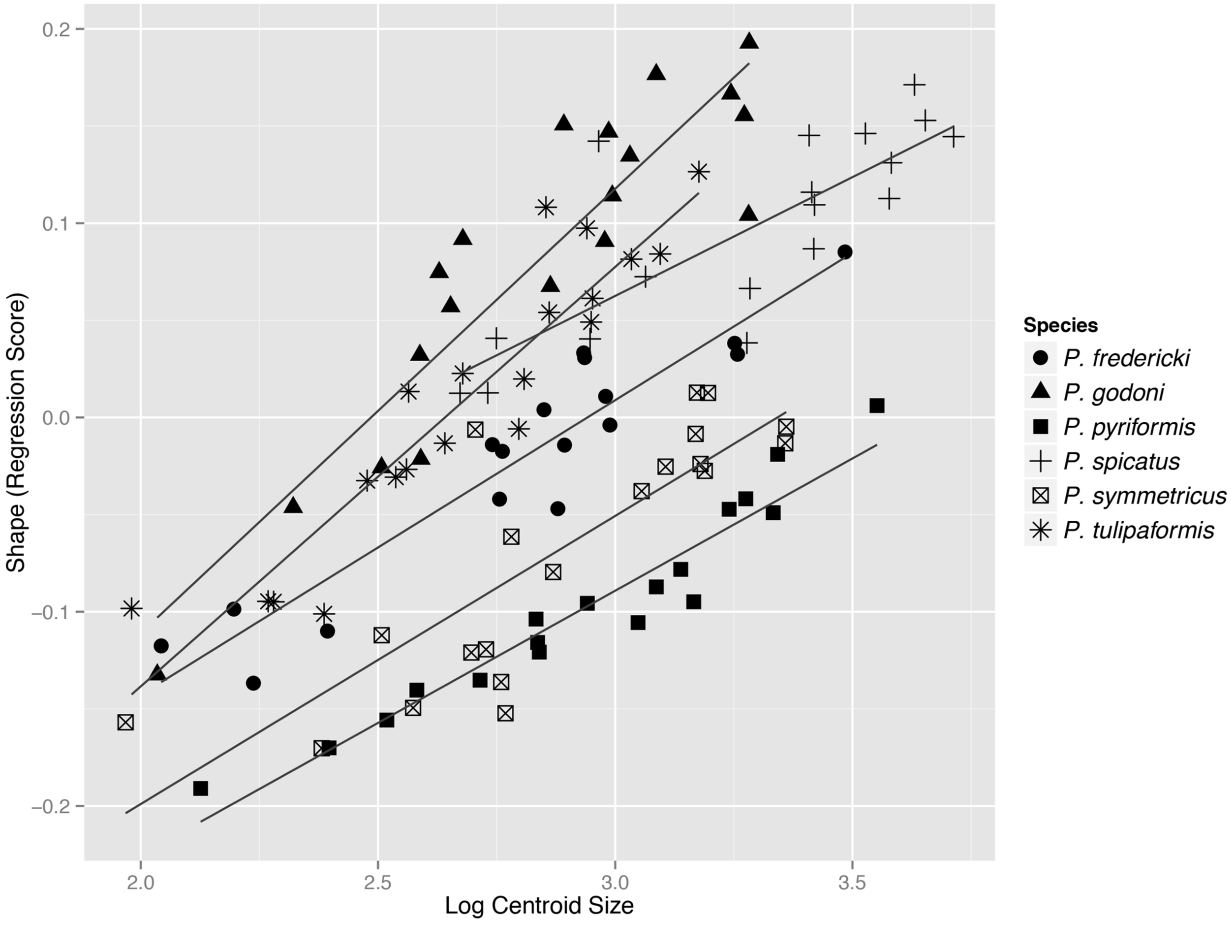

FIGURE III-3—Plot showing shape (regression score) vs. Log centroid size (geometric mean). Best-fit lines for each species are what specifically. Even though we cannot statistically show that there are multiple discernable growth patterns it appears that there are multiple starting points. Also note that the pyriform group species *Pentremites pyriformis* and *P. symmetricus* plot at the bottom of the graph whereas godoniform species plot near the top.

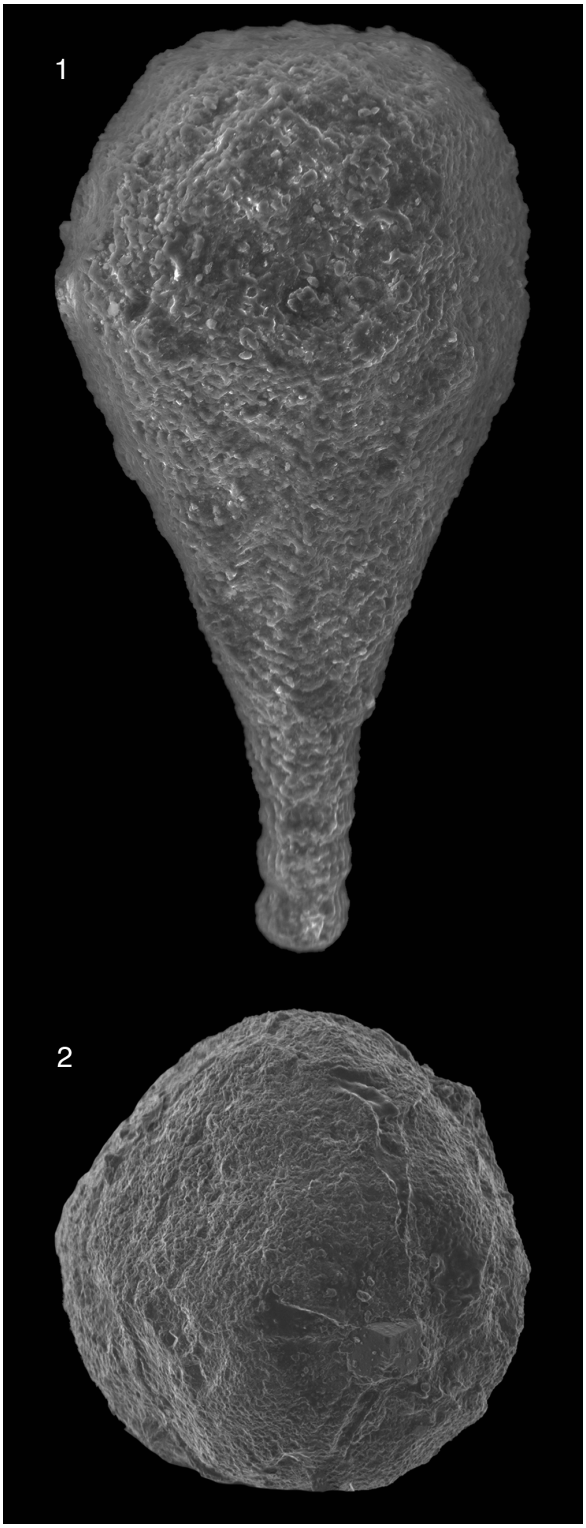

FIGURE III-4—Photographs of *Pentremites* juvenile stage termed *Passalocrinus;* 1, pyriform *Passalocrinus* (CMC IP67723) x272; 1, godoniform *Passalocrinus* (CMC IP71043) x272.

FIGURE III-5— Screenshot plots of the average ontogenetic series where small size (juvenile) is represented by black and large is represented by grey (adult); 1, slightly dipping summit view; 2, A ambulacral view; 3, orthogonal to A ambulacral view. Note that the deltoid tips (landmarks 2, 3) migrate towards the peristome (landmark 1), the ambulacral tup(landmark 9) migrates distally and the stem facet (landmark 13) migrates towards the peristome.

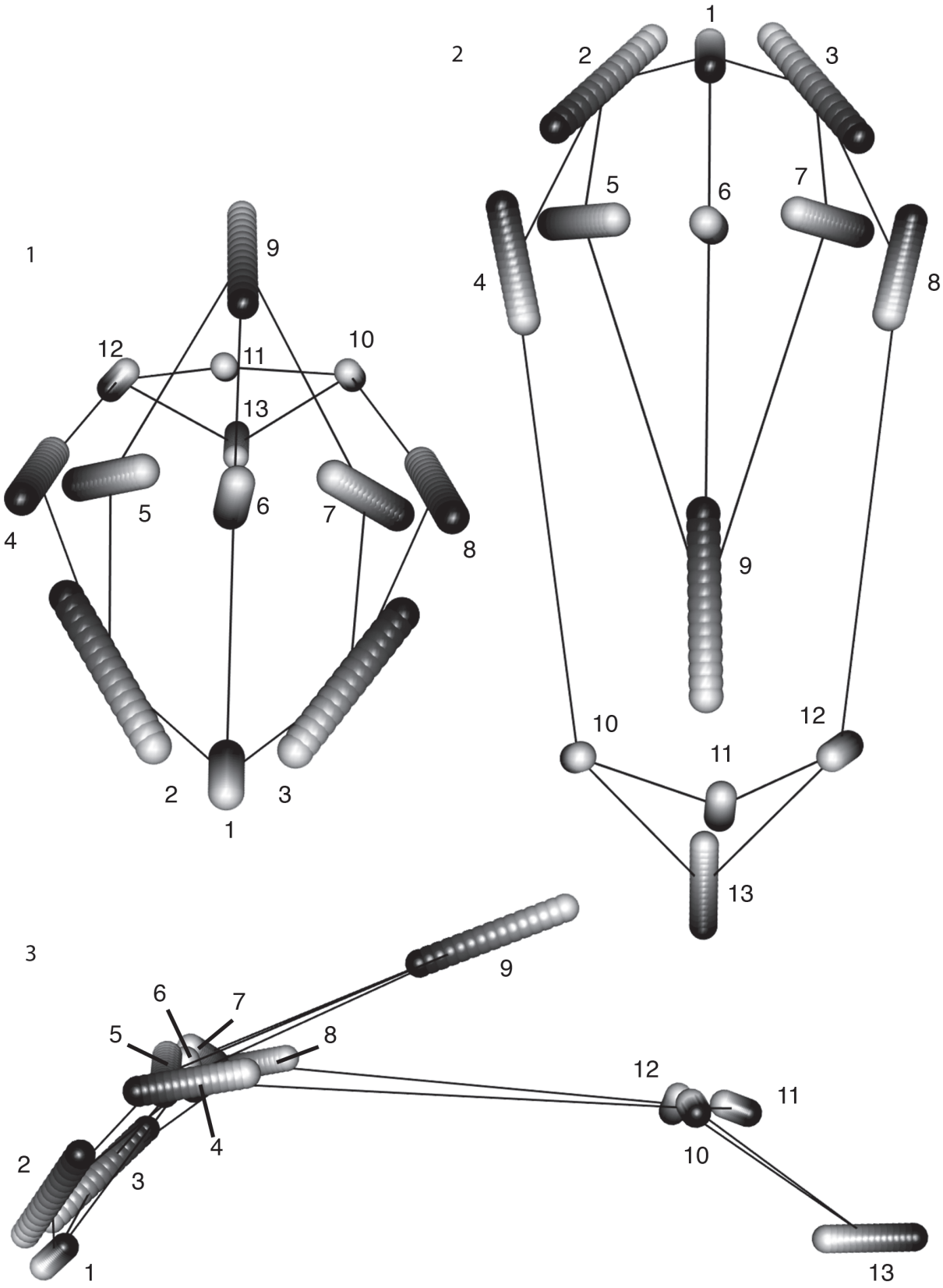

Figure III-5. Continued

TABLE III-1— The permutational procrustes ANOVA (9999 replicates). The ANOVA results (Table X) indicate that *Pentremites* shape varies significantly with size and by species, but there is not a significant interaction term between these two variables.

	df	SS.obs	MS	P.val
Csize	1	0.43168575	0.43168575	0.0001
Species	5	1.17110296	0.23422059	0.0001
Csize:Species	5	0.09258521	0.01851704	0.4779
Total	11	2.16099984	NA	NA

IV. BLASTOIDEA: ASSEMBLING THE ECHINODERM TREE OF LIFE

This chapter is a reformatted version of a paper, by the same name, to be submitted in the Journal of Systematic Palaeontology by Atwood, JamesW. Atwood, Johnny A. Waters, and Colin D. Sumrall.

ABSTRACT

A phylogenetic study of Blastoidea was conducted utilizing conventional morphologic characters and rigorous methodologies to provide a robust baseline phylogenetic hypothesis for the clade. This parsimony analysis included 21 terminal taxa with three outgroup taxa coded for 49 characters and 139 character states. Taxa were coded using exemplar species that cover most of the proposed lineages. All characters were unordered and equally weighted. A branch and bound search algorithm retrieved two equally most parsimonious trees (MPT) of 107 steps, with a consistency index 0.53, and retention index 0.73. *Macurdablastus* is inferred to be a fissiculate blastoid based on the structures of respiratory system and lack of spiracles. Because *Macurdablastus* is a sister taxon to Troosticrinidae, spiraculates are polyphyletic having been derived twice on the MPT from a paraphyletic Fissiculata. Non-troosticrinid spiraculates form a clade. Nucleocrinids, schizoblastids and the granatocrinid *Mesoblastus* form a clade that is a sister taxon to the clade containing the granatocrinid *Granatoblastus* nested within a paraphyletic Orbitremitidae, Diploblastidae and Hyperoblastidae. These two clades form a monophyletic group that is a sister taxon to the clade containing Ambolastomatidae and Pentremitidae. Non-*Macurdablastus* fissiculates form a clade. The Astrocrinidae and Neoschismitidae form a clade that is a sister taxon to the clade containing Codasteridae nested within a paraphyletic Orophocrinidae. These relationships suggest that the ordinal and familial classifications of Blastoidea are in need of revision.

INTRODUCTION

Blastoids are the longest-lived and most diverse group of the Blastozoa. Blastoids originated by the Middle Ordovician, reached their peak diversity by the Mississippian and went extinct during the End Permian extinction event (Broadhead 1984; Wanner 1940). Among extinct echinoderms, blastoids are ideal model organisms with which to study evolutionary processes because nearly all of the skeletal elements are universally shared among taxa thereby eliminating errors resulting from inaccurate assessment of homology (Fig. IV-1). Because of this deep-seated homology, changes in theca shape can be easily quantified using geometric morphometrics (Foote 1992; Atwood & Sumrall 2012). Thecal morphology has a strong influence on the number and arrangement of the feeding brachioles that arise from the ambulacral system suggesting that functional groups relate to thecal shape. These gross morphological classes group together phylogenetically, suggesting a genetic underpinning to thecal shape. Initial studies focused on homology, especially on the plating and construction of the oral surface of fossil echinoderms (Sumrall 2010; Sumrall and Waters, 2012) demonstrate that external morphology and homology can be reconciled across clades and used to score characters for phylogenetic inference. However, the potential of blastoids to be a model clade is seriously hampered by the lack of a modern phylogeny and classification.

Previous studies have examined blastoid phylogeny (Breimer & Macurda 1972; Waters & Horowitz 1993; Bodenbender 1995; Bodenbender & Fisher 2001; Sumrall & Brochu 2003; Sumrall & Waters 2012), but have left numerous questions unanswered. In this paper, we present a new phylogenetic analysis for Blastoidea based on a maximum parsimony analysis of 21 ingroup taxa with 139 informative character states. This study

integrates data from previous analyses, reinterpretation of taxa and morphology, and new characters gleaned from detailed observation of specimens. We compare our results to previous studies, evaluating both tree congruence and tree conflict. Our results provide a solid phylogenetic framework for the Blastoidea that can be utilized in the larger Assembling the Echinoderm Tree of life project (AEToL) for deciphering the evolution of the Blastozoa and the pelmatozoan echinoderms.

INSTITUTIONAL ABBREVIATIONS

USNM: National Museum of Natural History, Smithsonian Institution, Washington, D.C., USA; **CMC-IP**: Cincinnati Museum Center, Cincinnati, Ohio, USA; **NMNL:** Naturalis Center for Biodiversity, Leiden, Netherlands.

PREVIOUS INVESTIGATIONS

Since the recognition of Blastoidea (Say 1825), paleontologists have proposed many classification schemes with varying levels of inclusiveness. Roemer (1851) conducted the first morphologic study of Blastoidea, discovering the ambulacral pores and associated internal respiratory folds (hydrospires). Roemer divided the Blastoidea into four groups based on external thecal morphology including Floreales (conical theca and petaloid ambulacra); Elliptici (globular theca); Truncati (theca with a flat summit); and Clavati (conical theca and linear ambulacra) (Roemer 1851). Etheridge & Carpenter (1886) divided the Blastoidea into two orders, Regulares and Irregulares. Regulares was conceptualized as bearing five “normal” ambulacra and was subdivided into five families (Pentremitidae, Troostoblastidae, Nucleoblastidae, Granatoblastidae, and Codasteridae).

Irregulares was diagnosed as bearing four "normal" ambulacra and one "short" ambulacrum and included one family (Astrocrinidae) to receive the anomalous *Astrocrinus*. Bather (1899) and Jaekel (1918) argued that blastoids were derived from diploporan cystoids based on plate arrangement and similarities in the ambulacral system and included paracrinoids within Blastoidea. Jaekel (1918) differentiated the orders Fissiculata and Spiraculata based primarily on the presence of spiracles in the summit.

Wanner (1940) produced a new classification of blastoids, in which parablastoids, protoblastoids, as defined by Bassler (1938), and coronates were removed from Blastoidea leaving only the orders Fissiculata and Spiraculata. Wanner's classification forms the basis of the Treatise on Invertebrate Paleontology classification (Beaver *et al*. 1967). Waters and Horowitz (1993) revised the ordinal level classification of blastoids by dividing the Spiraculata into five orders based on their interpretation of iterative evolution of fissiculates into spiraculates. This inference was based largely on morphological features but the study did not rigorous test the phylogenetic hypotheses.

Breimer & Macurda (1972) comprehensively revised the taxonomy of the fissiculate blastoids. This monograph presents a phylogenetic hypothesis of the fissiculate blastoids, but it predates rigorous methodologies. Because spiraculate taxa were not included, the monophyly of fissiculates could not be tested (Sprinkle 1974).

Donovan & Paul (1985) conducted a study of coronates that included blastoids and the unusual blastozoan *Lysocystites*, while omitting parablastoids. Their results were essentially the same as Jaekel (1918). This hypothesis was later refuted by Sumrall & Waters (2012).

Bodenbender (1995) and Bodenbender & Fisher (2001) utilized stratocladistics, crystallographic axis orientation, and conventional morphological characters to analyze the phylogeny of Blastoidea. The relationships they inferred were incongruent with the classification of Beaver *et al*. (1967). Sumrall & Brochu (2003) concluded that the relationships inferred by Bodenbender and Fisher phylogeny were strongly influenced by the inclusion of stratigraphy in the analysis. Stratigraphic patterns are not direct results of phylogeny and may confound the results when used out of context. Sumrall & Brochu (2003) reanalyzed the Bodenbender and Fisher matrix using a maximum parsimony algorithm and recovered relationships that, although unusual in some respects, were more congruent with the classification of Beaver *et al*. (1967).

The Bodenbender & Fisher (2001) analysis also employed differentially weighted and ordered characters, practices that have problematic underpinnings. Differential weighting assigns a different evolutionary cost for certain character transformations over others. This requires an a-priori understanding of the relative importance of certain character transformation types over others (Smith 1994; Felsenstein 2004). Because there is no reasonable way to determine relative importance a-priori most phylogenetic studies assign an equal weight to all character transformations.

Ordering characters assigns differential cost for changing from one character state to another in an a-priori assignment of a transformation series. This practice is incompatible with phylogenetic studies because it requires a pre-knowledge of the evolutionary relationships to generate the character transformation series, which in turn is used to infer the phylogeny. As a result most phylogenetic studies do order character states and determine the polarity of character transformations a-posteriori.

BLASTOID MORPHOLOGY

The blastoid body plan consists of a theca, numerous biserial brachioles for feeding, and a stem and root system for attachment to the seafloor. A few taxa lived directly on the seafloor and were stemless as adults. Blastoids had more than 200,000 calcite plates, mostly in the brachioles and various cover plate systems in a complete individual (Sumrall & Waters 2005). The vast majority of specimens preserved in the fossil record have lost the brachioles and cover plates. Therefore classification schemes and inferences of phylogy typically only thecal plate morphologies (Fig. IV-1).

THECA

The theca of a blastoid is conservative in that it is composed of 13 to 18 major body plates (Fig. IV-1). These plates include five orals (deltoids), five radials, three basals, and five lancets (not exposed externally in many taxa). Blastoids exhibit a wide rage of thecal morphologies within the fundamentally conservative body plan (Fig. IV-1).

Primary peristomial cover plates. These five cover plates are the embryological plates over the peristome (Sumrall and Waters 2012). In a few taxa such as *Elaeacrinus* primary peristomial cover plates are large and fixed.

Orals. Oral plates (Deltoids) form the border of the peristome and are located interradially at the intersection of two adjacent ambulacra. A single oral plate located on every side except the CD interray. In troosticrinids the oral plates are confined to the oral surface around the peristome whereas in most other blastoids the oral plate extends outward forming a major portion of the thecal wall called a deltoid body (Figs. IV-1.6, 1.10).

Anus. Elements in CD interray of the blastoid theca are historically termed anal deltoids, because they are associated in various ways with the anal opening. The anus may

or may not be confluent with spiracles, in families that posses them. The anus is bordered by two to six plates that have conventionally been classified as deltoids (orals) (Fig. IV-2). In fissiculate blastoids the anus is positioned by itself (Fig. IV-1.7) where as in spiraculates it is commonly combined with a spiracle (anispiracle) (Fig. IV-1.5). In some spiraculates families the anus is separate but is still bordered by "anal deltoids".

Radials. The five radial plates are typically elongate U or V-shaped skeletal elements, which often form the majority of the theca as expressed externally. Radials surround the distal ambulacra and are bordered by oral plates, basal plates, and side plates in the ambulacral area. In fissiculates they bear hydropore clefts along the sides of the ambulacra (Fig. IV-1.13) whereas in spiraculates the floor plates (side plates) suture to them (Fig. IV-1.1).

Basals. Three basal plates adjoin the most distal portion of radial plates. A smaller azygous (positioned in the BC interradius) and two larger zygous basals meet at the distal pole to form the stem facet where the stem (in species who possess them) attaches (Fig. IV-1.8). In some taxa the stem facet is protuberant (Fig. IV-1.8) whereas it is sunken into a basal cavity in others (Fig. IV-1.10).

Floor plates. Floor plates, commonly termed side plates and outer side plates, form a double biseries where brachiole facets are shared between primary and secondary floor plates. The primary food groove lies along the suture between right and left floor plates. If the lancet is exposed (Fig. IV-1.10), floor plates abut the lancet and the primary food lies along the lancet midline.

Lancet. A narrow linear radially positioned thecal element in the median of each ambulacrum is the lancet. In fissiculates the floor plates articulate exclusively to the lancet.

In many blastoids, floor plates cover the lancet, but in a few genera, such as *Pentremites*, they are completely or partially exposed.

Hydrospires. All blastoids possess thin-walled endothecal respiratory structures called hydrospires. Fissiculates have exposed hydrospire along the deltoids and radials parallel to the ambulacra, and spiraculates have hydrospire pores along the sides of the ambulacra opening into hydrospires (Waters & Horowitz 1993).

The basis of the blastoid ordinal classification [in the Treatise] is based on if the hydrospires are exposed (Fig. IV-1.13) (Fissiculata) or not (Fig. IV-1.10) (Spiraculata). Hydrospire fields are the areas on or in the theca where hydrospires occur.

Spiracles. Spiracles are excurrent structures of the water vascular system on the summit of the blastoid. Incurrent structures of the water vascular system are hydrospire pores when the hydrospires are covered by side plates (Figs. IV-1.11,1.16). They can vary between five and ten in number. Fissiculate blastoids do not have spiracles.

BRACHIOLES

Brachioles are thin biserial feeding appendages, which articulate with each brachiole facet along the ambulacra. Brachioles are approximately 1-2 times thecal length and are rarely preserved (Beaver et al. 1967).

STEM

The stem is typically short (<10 cm), homeomorphic, and composed of flat circular columnals. Each columnal is pierced by a medial lumen that traverses the length of the stem. Although the majority of blastoids have a functional stem as adults, a few specialized genera are stemless (Beaver et al. 1967). The stem of blastoids is rarely preserved attached to the theca.

MATERIALS AND METHODS

Ingroup selection. For this project, exemplar species were selected to cover the major groups of blastoids. Generally, two to three species from different genera were coded per blastoid "family". This methodology served two purposes. First, it sampled a wide range of distinct morphologies, which allowed for a larger character data set. Secondly, it allowed a preliminary test for the monophyly of each family included in the analyses.

Individual species for the analysis were selected based on preservation of thecal morphology to minimize missing data in the phylogenetic matrix. Species with preserved stem and brachioles were given special preference. All species were coded primarily from observation of specimens, although codings were supplemented from descriptions in the primary literature.

The phylogenetic matrix included 21 ingroup taxa of which 8 were fissiculates and 13 were spiraculates (Table 1). In this study, we interpreted *Macurdablastus* as a member of Fissiculata, based primarily on the absence of spiracles on the blastoid summit. All known spiraculate blastoids exhibit 5 to ten spiracles near the peristome on the summit of the theca. Moreover, the treatise (Beaver *et al*. 1968) defines a fissiculate blastoid to be a blastoid whose hydrospires are exposed. *Macurdablastus* appears to have sideplates, positioned so that the hydrospires would be left exposed similar to other fissiculates.

Outgroup selection. Most recent studies on stem echinoderm phylogeny have inferred close relationships between blastoids, coronoids and *Lysocystites* (Paul & Smith 1984; Smith 1984; Sumrall 1997). Most recent studies have, therefore, selected outgroups drawn from these taxa (Donovan & Paul 1985; Bodenbender 1995; Bodenbender & Fisher 2001; Sumrall & Brochu 2003; Sumrall & Waters 2012). For this study the coronoids

Cupulocorona gemmiformis, Stephanocrinus angulatus, and *Lysocystites sculptus* were used because they are represented by very well preserved specimens that are readily accessible.

Characters. Character data for each species came from a variety of sources. All of the taxa used were studied from reposited specimens housed in public institutions (Table 1). Some information such as internal features of the hydrospires were not directly observed in all cases, and such observations were mined from previous studies. Each species was photographed from several views to document morphologies.

Characters were in part derived from previous studies including Bodenbender (1995), Bodenbender & Fisher (2001), and Sumrall & Waters (2012). In many cases the characters were reinterpreted to better describe the underlying morphologies. In other cases new characters and character states were developed. The complete list of characters is contained in Appendix 1.

Character reinterpretations stem primarily from viewing blastoids through the Universal Elemental Homology model (UEH) of Sumrall *et al.* (2010). This model separates plate types into homologous elements using development, location, function, and symmetry. By refining and defining terms commonly used in the blastoid literature in the UEH model, blastoid morphology can be reconciled within the clade and linkages between blastoids and related taxa can be more easily determined.

The blastoid thecal plates historically called deltoids are homologous with oral plates when utilizing UEH. Each oral plate is assigned an alphanumeric designation following Sumrall & Waters (2012), and anal ray oral plate arrangements as defined by Beaver *et al*. (1967) have been revised. The primary differences are the designations of the hypodeltoid and the epideltoid that are found bordering the anus in spiraculate blastoids.

These oral plates are now referred to as O7 and O1 respectfully according to the UEH. Designations were not assigned to the remainder of the anal side oral plates because homology could not be unambiguously established. Anal side designations as outlined by Beaver et al. (1967), were refined by omitting Group 1, which included blastoids with only one anal side deltoid and superdeltoids, because such taxa do not exist.

The blastoid peristome is covered by a series of cover plates termed primary peristomial cover plates (Sumrall *et al*. 2010; Sumrall & Waters 2012). These plates are the first cover plates to develop as seen by their presence in *Passalocrinus*, cover the peristome and are positioned interradially at the bifurcation points of the ambulacra. They vary among taxa as being small and undifferentiated over the peristome as in *Pentremites* or large and differentiated as *Nucleocrinus*.

Ambulacral floor plates in blastoids are commonly referred to as side plates. Pairs of adjacent side plates share a secondary food groove, brachiole facet and in spiraculate taxa hydrospire pores. Side plates can completely conceal the lancet plates or be separated along the ambulacral midline by the lancet plate. Side plates can be sutured only to the lancet plate as in taxa bearing a hydrospire cleft or sutured both the lancet plate and adjacent deltoid/radial in taxa lacking the hydrospire cleft.

The respiratory structures of blastoids are the hydrospires. These internal endothecal respiratory structures are thin-walled canals through which seawater flows for gas exchange. The way in which water enters and exits these structures is variously interpreted and forms the core difference between fissiculate and spiraculate blastoids. Here we refine some of the terminology to more accurately code the differences in hydrospire construction. Respiratory fields refer to the number of areas on a single theca

that posses one or more hydrospire fold. A hydrospire pore is an individual opening between each side plate and outer side

plate pair, which leads to underlying respiratory structures (hydrospire folds) in the shallow interior of the theca. A hydrospire cleft is a single valley-like opening between the abradial ends of the side plates and the radial/deltoid plates that traverses the length of the ambulacrum. This cleft provides access to the underlying respiratory slit-like hydrospire slits that provide access to the hydrospire folds.

PHYLOGENETIC ANALYSES

A character matrix consisting of the exemplar 21 ingroup taxa (Table 1) was scored for 49 discrete characters with 139 informative character states (Appendix 1). The data matrix was constructed using MorphoBank 3.0: web application for morphological phylogenetics and taxonomy (O'Leary & Kaufman 2012). All character states were unordered and equally weighted. Characters were drawn form an unpublished dataset compiled by Waters, Horowitz, and Macurda, and the published analyses of Bodenbender (1995), Bodenbender & Fisher (2001), and Sumrall & Waters (2012). Several new characters were also included in the analysis. Characters were checked for redundancy and reduced to the set of informative characters. Characters were drawn from all morphological features of the blastoid, but certain features such as internal anatomy, brachioles, stem, and holdfast features were lacking in nearly every case.

The matrix was polarized using *Lysocystites sculptus* (S3163), *Cupulocorona gemmiformis* (SUI 97615), and *Stepahnocrinus angulatus* (SUI 49743) as outgroup taxa. Several analyses inferred these taxa to be sister taxa to Blastoidea but in different

branching order (Paul & Smith 1984; Smith 1984, 1990; Paul 1988; Sumrall 1997; Sumrall & Waters 2012). Consequently, outgroup taxa were placed as a polytomy with respect to the ingroup taxa.

Phylogenetic analyses were conducted using PAUP 4.0a123 (Swofford 2003). A branch-and-bound search algorithm was implemented to ensure retrieval the complete set of most parsimonious trees (MPTs). Tree robustness was assessed with a bootstrap analysis of 10,000 pseudoreplicate matrices using a branch-and-bound search algorithm. The results were presented as a majority rule consensus tree. Bremer support was calculated for each of the nodes as the number of additional evolutionary steps required before the nodes collapsed in a broader strict consensus tree.

To test the veracity of alternate phylogenetic hypotheses presented in Bodenbender & Fisher (2001) and Sumrall & Brochu (2003) separate topologically constrained analyses were run. Taxa were pruned from the trees inferred by these previous studies such that they included only the taxa used in the present study. Ambiguous relationships were collapsed into polytomies. The data matrix was then analyzed using the same protocols as above except constrained to save only those trees congruent with the tree from each of the previous studies.

RESULTS

The analysis recovered two equal most parsimonious trees (MPT) that differed only in *Lophoblastus* and *Mesoblastus,* having their positions interchanged. This resulted in a polytomy in the strict consensus tree (Fig. IV-4.1). These MPTs have lengths of 107 steps,

with a consistency index 0.53, and retention index 0.73. This suggests that the matrix is noisy despite resulting in relatively few MPTs.

Macurdablastus is inferred to be the sister taxon to Troosticrinidae which contains the sister genera *Troosticrinus* and *Metablastus* (Fig. IV-4.1). This clade has low bootstrap and Bremer support likely resulting from the large number of missing data associated with the poorly preserved *Macurdablastus*. However, this clade is supported by several characters including ambulacral length (Fig. IV-3.12.1), ambulacral shape (Fig. IV-3.12.1), and the absence of a deltoid body (Fig. IV-3.8.1). As argued above on morphological grounds, *Macurdablastus* is a fissiculate. Importantly, this would imply that spiraculates are polyphyletic being derived twice on the tree from a paraphyletic Fissiculata. The MPTs also inferred that non-Troosticrinid spiraculates form a clade that is sister taxon to the non-*Macurdablastus* fissiculates.

Non-troosticrinid spiraculates form a clade, which circumscribes three smaller spiraculate clades (Fig. IV-4.1). The larger clade is united by a globular thecal shape and the presence of hydrospire pores. The nucleocrinids *Elaeacrinus* and *Nucleocrinus*, are sister genera, and united by presence of large flat primary peristomial cover plates (Fig. IV-3.41), and the presence of very large deltoids. The anal deltoids lack an exposed epideltoid (Fig. IV-3.3.1) and are comprised of a hypodeltoid and cryptodeltoids that traverse a large portion of the total thecal length (Fig. IV-3.3.1). This relationship is very robust having an extremely high bootstrap proportion and high Bremer support (Fig. IV-4.1).

The granatocrinid *Mesoblastus,* the schizoblastid *Lophoblastus*, and the nucleocrinids form a clade that is supported with a high to moderate bootstrap proportions and Bremer support (Fig. IV-4.1). The presence of parallel, non-heteromorphic ambulacral

outline shape (Fig. IV-3.2.1) and the ambulacra elevated above the surrounding thecal plates unite this clade (Fig. IV-3.1.1).

The nucleocrinid, *Mesoblastus*, *Lophoblastus* clade is a sister taxon to a second non-troosticrinid spiraculate clade circumscribing the granatocrinid *Granatocrinus* nested within a paraphyletic Orbitremitidae. This orbitremitid group includes: *Globoblastus*, *Orbitremites*, the diploblastid *Diplobastus,* and the hyperoblastid *Eleuthrocrinus* (Fig. IV-4.1). *Orbitremites* and *Granatocrinus* are sister taxa united by having a single respiratory structure (hydrospire fold) per field and oral plates that border a larger proportion of the ambulacra than the radial plates. This is a robust relationship having a high bootstrap proportion and high Bremer support (Fig. IV-4.1). *Orbitremites* and *Granatocrinus* are sister taxa to *Globoblastsus.* This clade is supported by moderate to low bootstrap proportion and moderate Bremer support. It is united by ambulacra that project below the basal plates (Fig. IV-3.11.1) and deltoid nodal ornamentation (Fig. IV-3.10.1). *Orbitremites*, *Granatocrinus*, and *Globoblastus* are sister taxa to *Diploblastus* forming a clade that is sister taxa to *Eleuthrocrinus* (Fig. IV-4.1). These last two nodes were not preserved by the bootstrap analysis where they were recovered in the 50 percent consensus tree and are, therefore, represented as a polytomy.

The *Diploblastus-Eleuthrocrinus* clade and *Elaeacrinus-Mesoblastus* clade form a monophyletic group that is a sister taxon to the third non-troosticrinid spiraculate clade that contains the pentremitids *Ambolostoma* and *Pentremites* (Fig. IV-4.1). The pentremitids are united by side plates that abut the lancet rather than overlap (Fig. IV-3.9.1) and abaxial convex shape of the ambulacra (Fig. IV-3.5.1). The pentremitids have high bootstrap proportion with low Bremer support.

Non-*Macurdablastus* fissiculates also form a clade, which circumscribes two smaller clades (Fig. IV-4.1). The astrocrinid *Astrocrinus* and neoschismitid *Timoroblastus* are sister taxa and have moderate bootstrap and Bremer support. These taxa are united by the presence of a hydrospire cleft (Fig. IV-3.6.2) and ambulacra depressed below the surrounding plates (Fig. IV-3.6.1). *Astrocrinus* and *Timoroblastus* are sister taxa to the neoschismitid *Hadroblastus.* This relationship is robust having a moderate bootstrap proportion and Bremer support (Fig. IV-4.1). This clade is united having deltoids that surround more of the ambulacra than do the radials (Fig. IV-3.6.3) and deltoids that are projected above the summit (Fig. IV-3.7.1).

The astrocrinids, neoschismitid clade is sister taxon to the second smaller non-*Macurdablastus* fissiculate clade. It contains the codasterids *Pterotoblastus* and *Codaster* nested within a paraphyletic Orophocrinidae that circumscribes *Orophocrinus* and *Brachyschisma* (Fig. IV-4.1). The codasterids are sister taxa that are united by having only eight respiratory fields (Fig. IV-3.14.1) and an approximately equal ratio of deltoid and radials surrounding the ambulacra (Fig. IV-3.13.1). This relationship is robust having a moderate to high bootstrap proportion and moderate Bremer support. The codasterids are sister taxa to *Brachyschisma* forming a clade that is sister to *Orophocrinus* (Fig. IV-4.1) This relationship has a low bootstrap proportion and moderate Bremer support. This clade is united by concave interambulacral shape (Fig. IV-3.16.1) and recessed aboral radial-radial sutures (Fig. IV-3.15.1).

DISCUSSION

Although of a more limited scope, the present study is not congruent with the Breimer & Macurda (1972) tree, which predates the widespread use of phylogenetic analysis. Instead the inferred relationships were based on a few key characters. Secondly, there were very few over-lapping taxa making a direct comparison of these two studies difficult. Lastly, Breimer & Macurda (1972) only investigated fissiculates, which has been interpreted to not be monophyletic in other studies (Sprinkle 1974; Bodenbender & Fisher 2001; Sumrall & Brochu 2003). It is possible that if spiraculates were added to their study or more fissiculates to our study they may in fact share more evolutionary relationships.

To test the support for the Bodenbender & Fisher (2001) and Sumrall & Brochu (2003) trees on our matrix, topologically constrained analyses were run for two other studies (see above). Both of the constrained analyses, from previous studies, recovered trees that were significantly less parsimonious than the present analysis.

The Bodenbender & Fisher (2001) tree yielded 153 steps with consistency index of 0.38, and retention index of 0.50 when ran with our matrix. The tree length is 46 steps longer or 143 percent the length of our MPT. This tree shows paraphyletic fissiculata with respect to polyphyletic spiraculata. The collapse of several families, which were inferred by our analysis, suggests that the relationships inferred by the Bodenbender and Fisher analysis are spurious. First, the pentremitids with *Eleuthrocrinus* form a clade that is sister to a clade containing codasterids with *Timoroblastus.* This relationship raises concern because we found that these genera have few shared characters and should not have this relationship. We also find that *Diploblastus* is sister to *Metablastus* and together they are sister to *Troosticrinus*. This relationship is troubling for two reasons. *Diploblastus* is not

similar to either genus to the other genera in terms of shared characters. Last, *Metablastus* and *Troosticrinus* being so very similar it is hard to fathom that a parsimony analysis, that is supposedly based on homologous characters, would not place these two genera as sister taxa.

The Sumrall and Brochu tree yielded 139 steps, with consistency index of 0.42 and retention index of 0.57. The resulting tree length is 32 steps longer or 130 percent tree length of our MPTs. This study was simply a reanalysis of the BBF matrix in the absence of stratigraphic data, and did not evaluate the characters or character states presented by the Bodenbender and Fisher study. Consequently, it eliminated the two problematic relationships discussed above, while, yielding a paraphyletic Fissiculata with respect to a monophyletic Spiraculata. Regardless, when compared to the present study, the stratocladistic analysis of the Bodenbender and Fisher matrix is less congruent than the maximum parsimony analysis.

CONCLUSIONS AND FUTURE DIRECTIONS

This study provides a character based phylogenetic hypothesis for blastoid evolution. Relationships inferred by this study suggest that the treatise classification for Blastoidea – dividing them into spiraculates and fissiculates inadequately reflects the true evolutionary history of the group. Instead, it was found that Fissiculata is paraphyletic with respect to polyphyletic Spiraculata. This study confirms the Waters & Horowitz (1993) hypothesis that spiraculates are polyphyletic but fails to define the number of originations. A more detailed study is needed to test the hypothesis of iterative evolution of spiraculates from fissiculates.

This study also infers two large blastoids clades. One circumscribes all non-*Macurdablastus* fissiculates and one that circumscribes all non-Troosticrinid spiraculates. Indeed, in the absence of *Macurdablastus* and Troosticrinids, the two clades approximate the Treatise blastoids orders. Although additional independent origins of Spiraculata may be uncovered in future studies as suggested, by Waters & Horowitz (1993) this does not invalidate this two-clade system. Many more taxa need to be included to resolve this issue.

Although the Bodenbender & Fisher (2001) and Sumrall & Brochu (2003) analyses failed to recover many of the traditionally defined families, our analysis our new analysis is more congruent with traditional classifications. This is not surprising given tendency for earlier systematists to remove taxa from families that evolved key innovations and erect new families to receive them.

We believe that stratocladistics and differential character weighting/ordering have led to the erroneous hypothesis presented in earlier studies. Because ordering and differentially weighting characters gives certain character state transformations more or less importance, these techniques can greatly influence the outcomes. By doing so, researchers are implying a-priori knowledge about character importance or phylogeny, which results in circularity to phylogenetic inference. Because the removal of stratocladistics by Sumrall & Brochu (2003) generated a more parsimonious tree on our matrix than the one using stratocladistics and ordered and differentially weighted characters we feel confident that our results more accurately reflect the true phylogeny. At least they are formed in an explicit and repeatable framework.

In the future, we feel that the paraphyletic and polyphyletic families that were identified can be clarified with the addition of more genera and internal character data that

is being developed from existing collections. Also, we would like to incorporate all families that were not represented in this study as well as add taxa outlined in Waters & Horowitz (1993) to test the hypothesis of iterative origination of the spiraculates. We believe that we have constructed a viable and robust hypothesis with which can now be confidently incorporated into the AEToL project as well as expanded upon in future studies.

ACKNOWLEDGEMENTS

We thank B. Hunda Cincinnati Museum Center, M. Florence/D. Leven US National museum, S. Donovan, Naturalis, Center for Biodiversity and P. Mikkelsen Paleontological Research Institution for providing access to specimens used in this study. Assistance with character development and analysis was provided by T. Fadiga. For assistance collecting specimens T. Fadiga, L. Knox, and D. Frederick are greatly thanked. Two reviewers ____ and ___ provided useful comments that greatly improved the manuscript. This research was supported by NSF DEB-1036260 to CDS as part of the Assembling the Echinoderm Tree of Life Project. Waters was supported by a Temminck Fellowship from NCB Naturalis and from Research Opportunity Awards from the AEToL project.

REFERENCES

ATWOOD, J. W., AND C. D. SUMRALL. 2012. Morphometric Investigation of the Pentremites Fauna from the Glen Dean Formation, Kentucky. Journal of Paleontology, 86(5):813-828.

BASSLER, R. S. 1938. Pelmatozoa palaeozoica (generum et genotyporum index et bibliographia). Fossilium Catalogus, I: Animalia:194.

BATHER, F. A. 1899. A phylogenetic Classification of the Pelmatozoa. Report British Association, 1898:pp. 916-923.

BEAVER, H. H., K. E. CASTER, D. J. W., R. O. FAY, H. B. FELL, R. V. KESLING, D. B. MACURDA, R. C. MOORE, G. UBAGHS, AND J. WANNER. 1967. Treatise on Invertebrate Paleontology (S)Echinodermata(1). The University of Kansas and The Geological Society of America, Boulder, 2.

BODENBENDER, B. 1995. Morphological, crystallographic, and stratigraphic data in cladistic analyses of blastoid phylogeny, Contributions from the Museum of Paleontology. University of Michigan, 201-257.

BODENBENDER, B. E., AND D. C. FISHER. 2001. Stratocladistic analysis of blastoid phylogeny. Journal of Paleontology, 75(2):351-369.

BREIMER, A., AND B. MACURDA. 1972. The Phylogeny of Fissiculate Blastoids. Verhangelingen der Koninklijke Nederlandsche Akademie van Wetenschappen, Afdeeling Natuurkunde Eerste Reeks, Deel 26 (3):1-390.

BROADHEAD, T. W. 1984. Macurdablastus a Middle Ordovician blastoid from the southern Appalachians. University of Kansas Paleontological Contributions Paper:1-10.

DONOVAN, S. K., AND C. R. C. PAUL. 1985. Coronate Echinoderms from the Lower Paleozoic of Britain. Palaeontology, 28(Aug):527-543.

ETHERIDGE, R. J., AND P. H. CARPENTER. 1886. Catalogue of the Blastoidea. British Museum of Natural History, 1:322.

FELSENSTEIN, J., AND J. FELENSTEIN. 2004. Inferring phylogenies. Sinauer Associates Sunderland, 2.

FOOTE, M. 1991. Morphological and Taxonomic Diversity in a Clade's History: The Blastoid Record and Stochastic Simulations. Contributions from the Museum of Paleontology, 28(6):101-140.

JAEKEL, O. 1918. Phylogenie und System der Pelmatozoen. Palaeontologische Zeitschrift Berlin, 3:(1-128).

MOORE, R. C. 1954. Status of invertebrate paleontology. Bulletin of the Museum of Comparative Zoology, 112:125-149.

O'LEARY, M. A., AND S. G. KAUFMAN. 2012. MorphoBank 3.0: Web application for morphological phylogenetics and taxonomy., http://www.morphobank.org.

PAUL, C. R. C. 1988. The phylogeny of the cystoids. Current Geological Concepts, 1:199-213.

PAUL, C. R. C., AND A. B. SMITH. 1984. The early radiation and phylogeny of echinoderms. Biological Reviews of the Cambridge Philosophical Society, 59(4):443-481.

ROEMER, F. 1851. Monographie der Fossilen Crinoidenfamilie der Blastoideen, und der Gattung Pantatrematites in Besondern. Archiv fer Naturgeschichte, 1(3):323-397.

SAY, T. 1825. On two genera and several species of Crinoidea. Being reprint from J Ac Nat Sci Philad, ser. 1(iv):pp. 289-296.

SMITH, A. 1994. Systematics and the fossil record: documenting evolutionary patterns. Wiley. com.

SMITH, A. B. 1984. Classification of the Echinodermata. Palaeontology, 27(3):431-459.

SMITH, A. B. 1990. Evolutionary diversification of echinoderms during the early Palaeozoic. Systematics Association Special Volume, 42:265-286.

SPRINKLE, J. 1974. Review. Journal of Paleontology, 48(6):1295-1296.

SUMRALL, C., L. HARRIS, S. BÖTTGER, C. WALKER, AND M. LESSER. 2010. A model for elemental homology for the peristome and ambulacra in blastozoan echinoderms. Echinoderms: Durham, 12:269-276.

SUMRALL, C., J. A. WATERS, AND ANONYMOUS. 2005. How many ossicles do blastoids and other echinoderms actually have? Abstracts with Programs - Geological Society of America, 37(2):12.

SUMRALL, C. D. 1997. The role of fossils in the phylogenetic reconstruction of Echinodermata. The Paleontological Society Papers, 3:267-288.

SUMRALL, C. D., AND C. A. BROCHU. 2003. Resolution, sampling, higher taxa and assumptions in stratocladistic analysis. Journal of Paleontology, 77(1):189-194.

SUMRALL, C. D., AND J. A. WATERS. 2010. Universal Homology in Glyptocystitoid Hemicosmitoid, Coronoids and Blastoids: Steps Toward Echinoderm Phylogenetic Reconstruction in derived Blastozoa. Journal of Systematic Palaeontology.

SUMRALL, C. D., AND J. A. WATERS. 2012. Universal Elemental Homology in Glyptocystitoids, Hemicosmitoids, Coronoids and Blastoids: Steps Toward Echinoderm Phylogenetic Reconstruction in Derived Blastozoa. Journal of Paleontology, 86(6):956-972.

SWOFFORD, D. L. 2003. PAUP*: phylogenetic analysis using parsimony, version 4.0b10.

WANNER, J. 1940. Neue Blastoideen aus dem Perm von Timor (mit einem Beitrag zur Systematik der Blastoideen). Geological Expedition of the University of Amsterdam to the Lesser Sunda Islands in the south-eastern part of the Netherlands East Indies 1937, 1:pp. 215-277.

WATERS, J. A. 1990. The Palaeobiogeography of the Blatoidea (Echinodermata). Paleozoic Palaeogeography and Biogeography, 12:339-352.

WATERS, J. A., AND A. S. HOROWITZ. 1993. Ordinal-level evolution in the Blastoidea. Lethaia, 26(3):207-213.

Appendix III

Figure IV-1. 1, 2 *Eleutrocrinus cassedayi* (USNM S3476), x2.2. 1, lateral view showing side plates sutured to the ambulacral wall. 2, summit view. 3, 4, *Astrocrinus bennei* (USNM 37365), x3.9. 3, summit view showing rhombiform ambulacra. 4, basal view. 5, 6, *Ambolostoma baileyi* (USNM 111726), x1.3. 5, summit view exhibits anus confluent with spiracle in CD interray. 6, lateral view. 7, 8, *Pterotoblastus gracilis* (USNM 248340), x1.9. 7, summit view. 8, lateral view illustrating protruding stem facet. 9, 10, *Hadroblastus convexus.* (USNM S0765), x1.7. 9, lateral view. 10, summit view. 11, 12, *Orbitremites sp.* (CMC-IP 71044), x2.3. 11, summit view. 12, lateral view 13, 14, *Orophocrinus stelliformis* (USNM 41067), x1.2. 13, summit showing isolated anus in CD interray and hydrospire clefts leaving hydrospires exposed. 14, lateral view. 15, 16, *Elaeacrinus verneuili* (CMC-IP 35431), x1.3. 17, 18, *Macurdablastus uniplicatus* (USNM 359645), x7.2. 17, summit view. 18, basal view.

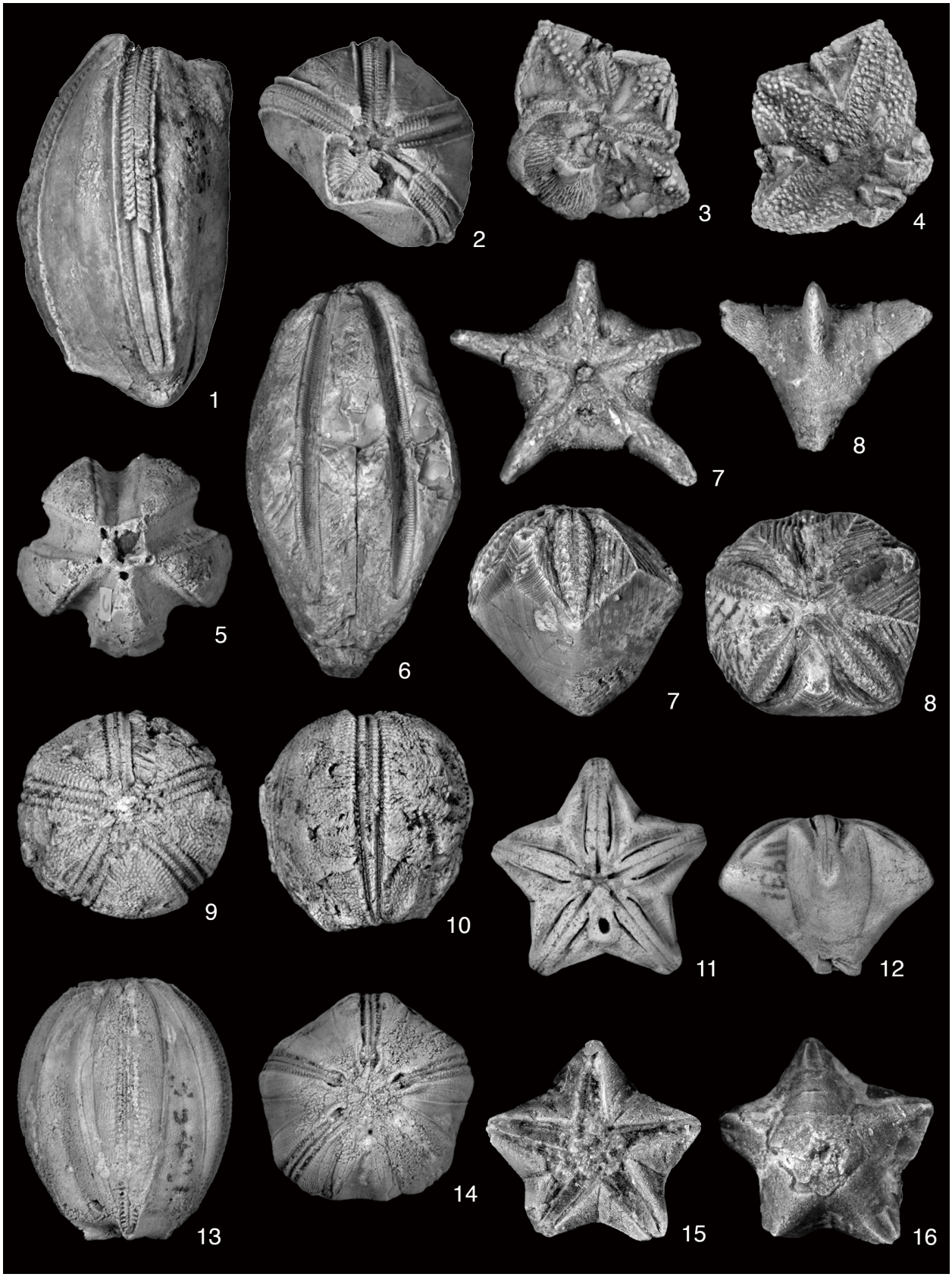

Figure IV-1. Continued

Figure IV-2. Revision of blastoid oral plate arrangements in the CD interray after Beaver et al. 1976. Major differences are the omission of the oral group including blastoids that have only one oral plate in the CD interray because none exist and O1 and O7 designations given to the epideltoids and hypodeltoids respectively according to Universal Elemental homology after (Sumrall and Waters 2012). 1, *Heteroschisma* type, hypodeltoid and epideltoid expressed, anus enclosed by hypodeltoid. 2, *Angioblastus* type, hypodeltoid and epideltoid expressed, anus enclosed by hypodeltoid and epideltoid approximately same amount. 3, *Nymphaeoblastus* type, hypodeltoid and epideltoid expressed, anus enclosed by hypodeltoid and epideltoid, mostly by hypodeltoid. 4, *Elaeacrinus* type, hypodeltoid, epideltoid, and cryptodeltoids expressed, anus enclosed by hypodeltoid, epideltoid, and cryptodeltoids, mostly by cryptodeltoids. 5, *Nucleocrinus* type, Hypodeltoid and cryptodeltoids expressed, anus enclosed by hypodeltoid and cryptodeltoids, mostly by cryptodeltoids. 6, *Polydeltoideus* type, hypodeltoid, epideltoid, paradeltoids, and cryptodeltoid, anus bordered approximately evenly by all deltoids. 7, *Cryptoblastus* type, hypodeltoid and epideltoid, anus bordered by hypodeltoid, epideltoid, and hidden cryptodeltoid evenly. 8, *Decaschisma* type, hypodeltoid, epideltoid, and subdeltoid, only hypodeltoid and epideltoid border anus. 9, *Phaenoschisma* type, hypodeltoid and epideltoid, anus bordered by hypodeltoid and epideltoid, mostly by epideltoid. 10, Pentremitidea type, hypodeltoid, epideltoid, and subdeltoid, anus bordered only by subdeltoid and hypodeltoid, mostly by hypodeltoid.

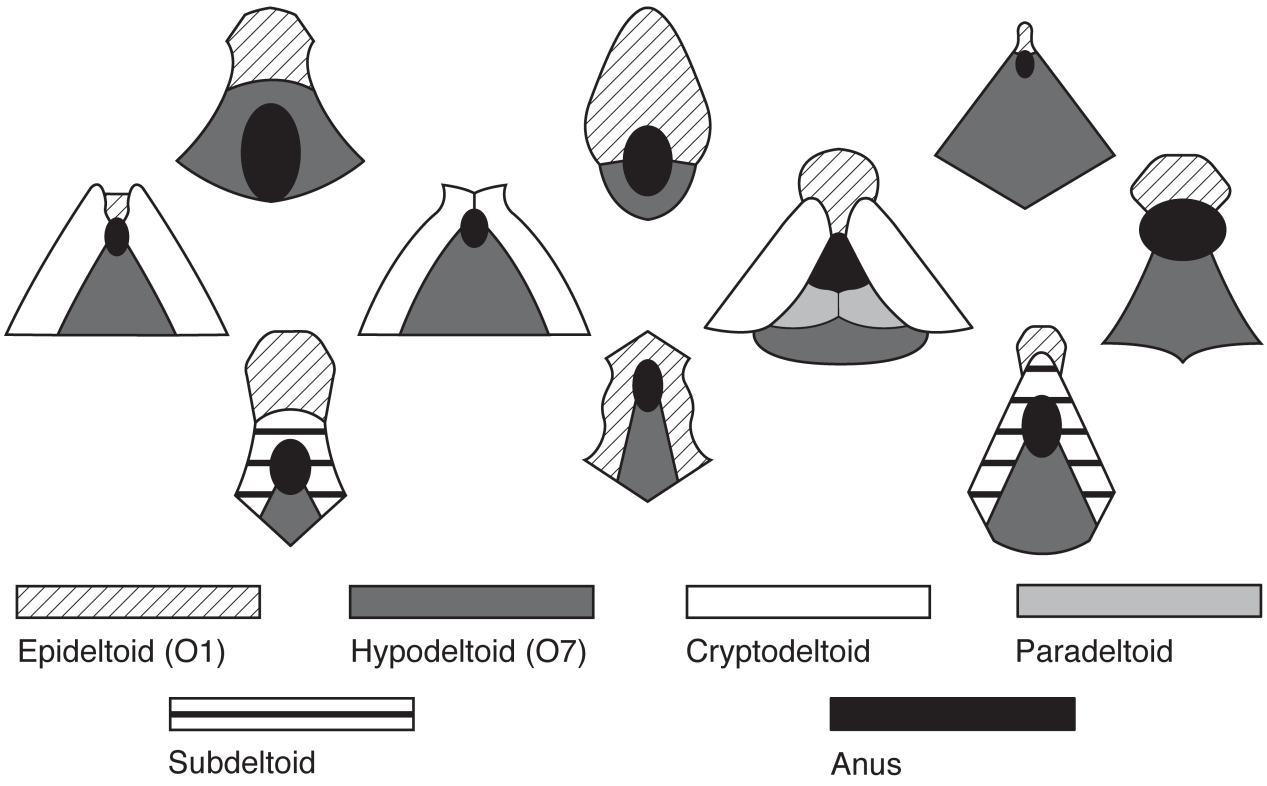

Figure IV-2. Continued

Figure IV-3. A, B, *Lophoblastus neglectus* (USNM S3726), x2. A, summit view 1, illustrates ambulacra elevated above the surrounding thecal plates. B, lateral view 1, illustrates parallel non-heteromorphic ambulacral shape. C, D, *Nucleocrinus sp.* (USNM 455893), x1.4. C, lateral view 1, illustrates the lack of an exposed epideltoid with large cryptodeltoids. D, summit view 1, illustrates large flat primary peristomial cover plates. E, I, *Pentremites fredericki* (CMC-IP 6479), x1.6. E, lateral view 1, illustrates abaxial convex ambulacral shape. I, summit view 1, illustrates side plates that abut the lancet plate. F, G, *Timoroblastus sp.* (USNM L8463), x1.3. F, summit view 1, illustrates ambulacra depressed below surrounding plates 2, illustrates hydrospire cleft 3, illustrates deltoids that surround more of the ambulacra than radials. G, lateral view 1, illustrates deltoids that project above the summit. H, L, *Troosticrinus reinwardti* (CMC-IP 67717), x2.3. Lateral view 1, illustrates the absence of a deltoid body. L, summit view. 1, exhibits flat ambulacral shape. J, K, *Globoblastus norwoodi* (USNM S6800), x1.3. J, summit view 1, illustrates deltoid nodal ornamentation. K, lateral view 1, illustrates ambulacra that extend below the basal plates. M, N, *Codaster robustus* (USNM S4573), x2.2. M, lateral view 1, illustrates ambulacra that are surrounded by equal parts radial and deltoid. N, summit view 1, illustrates only eight respiratory fields. O, P, *Brachyschisma corrugatum* (USNM 387783), x1.6. O, lateral view 1, illustrates recessed aboral radial-radial sutures. P, summit view 1, illustrates concave interambulacral shape.

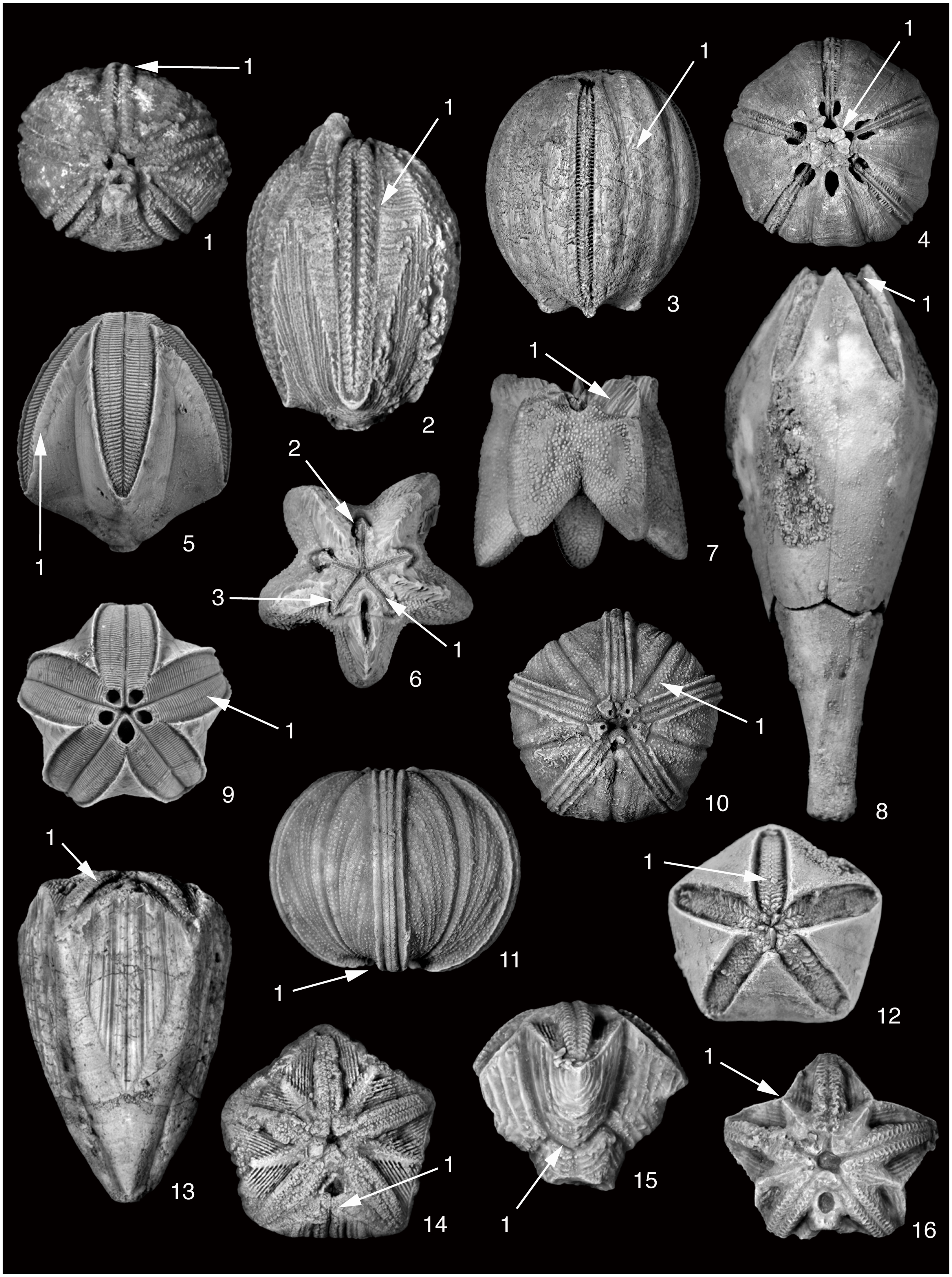

Figure IV-3. Continued

Figure IV-4. 1, A strict consensus of the two most parsimonious trees (107 steps, CI = 0.53, RI = 0.73) recovered by the current analysis. Numbers next to nodes are bootstrap percentages (10,000 replicates)/Bremer support values. 2, The strict consensus tree of the analysis of the current matrix constrained to the topology of (Bodenbender & Fischer 2001). No bootstrap percentages or Bremer support were available for comparisons.

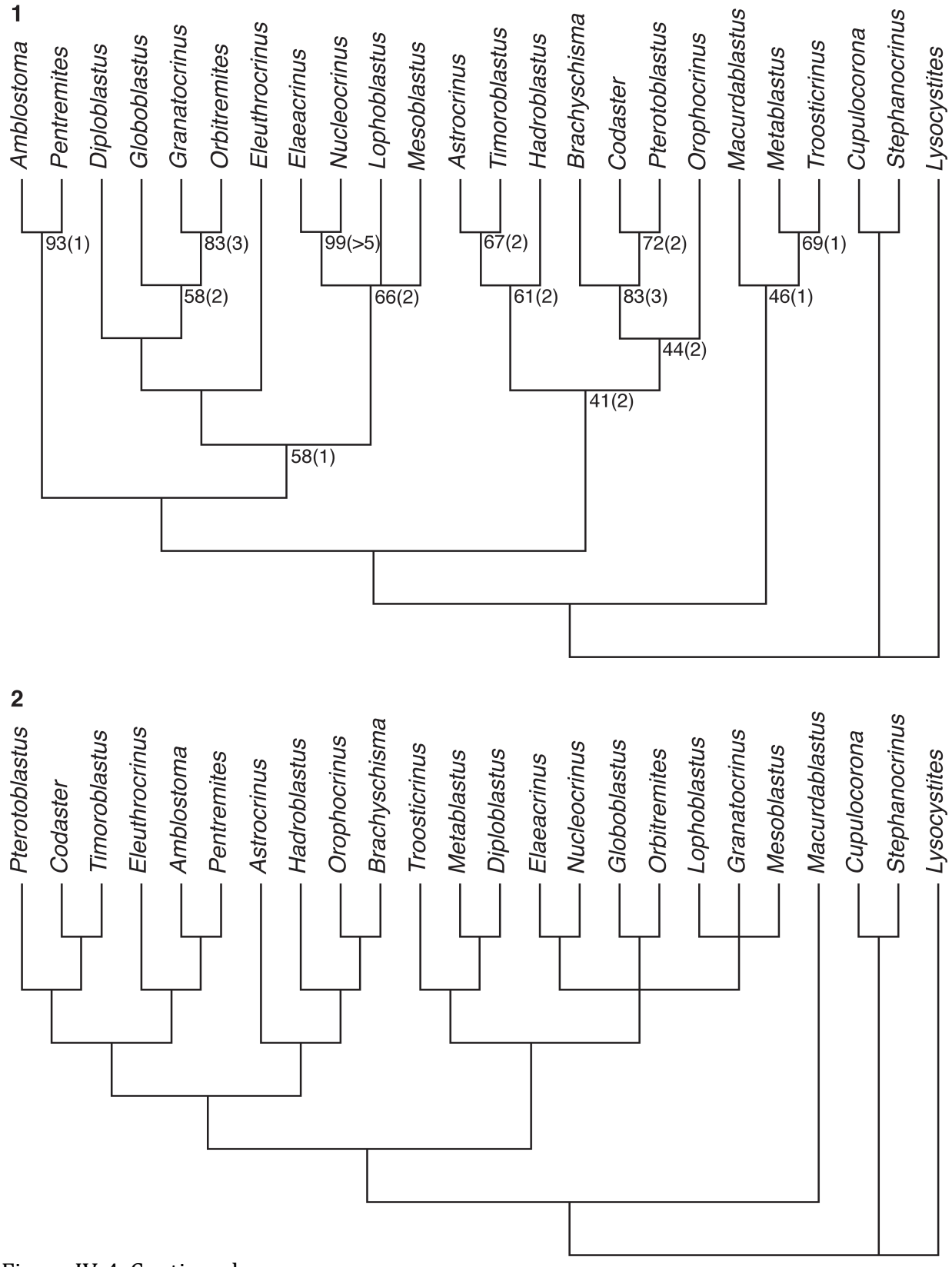

Figure IV-4. Continued

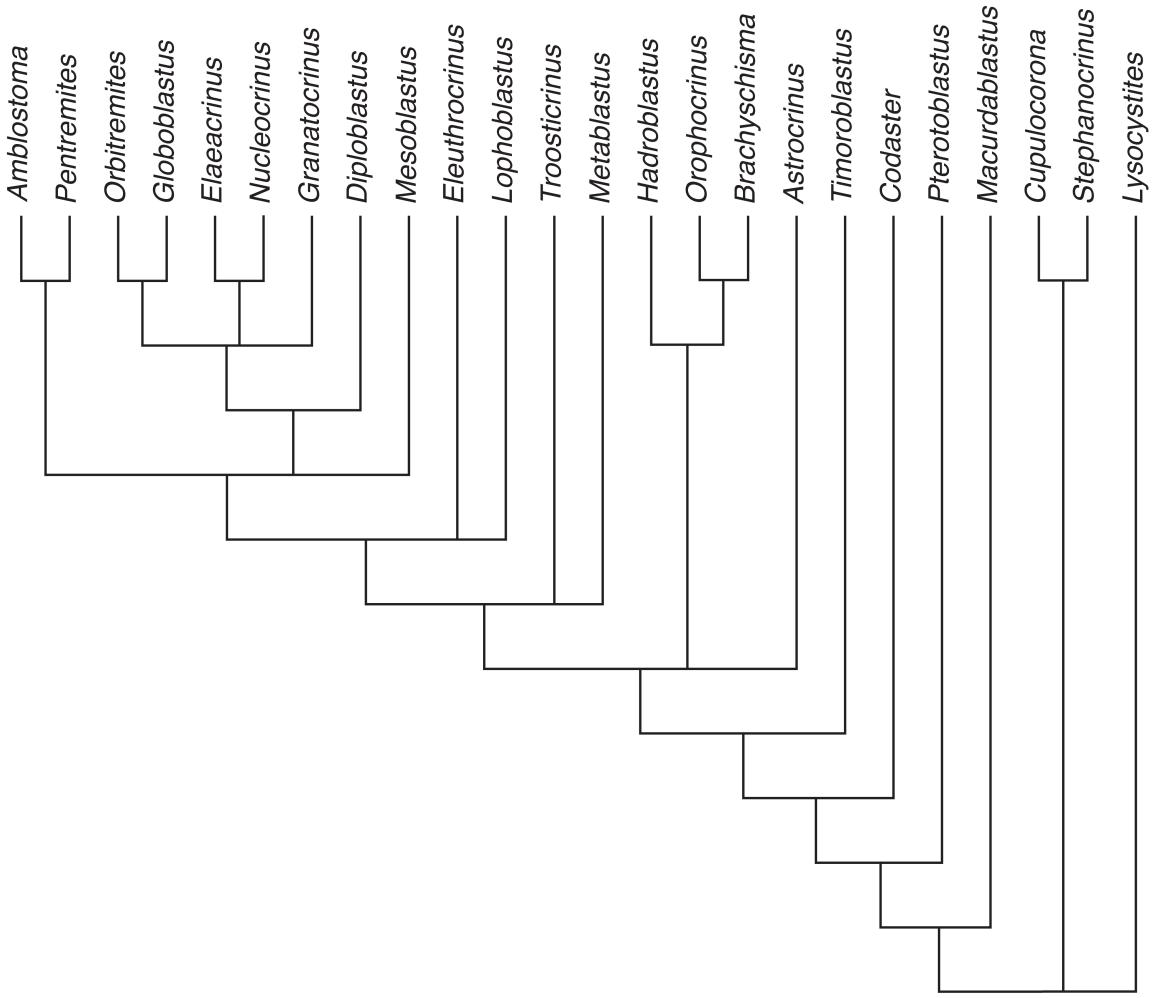

Figure IV-5. The strict consensus tree of the analysis of the current matrix constrained to the (Sumrall & Brochu 2003) topology. No bootstrap percentages or Bremer support were available for comparisons. The only difference in this tree and the previous tree (Bodenbender & Fischer 2001) is the absence of stratocladistics, differential character ordering and weighting by the Sumrall and Brochu (2003) analysis.

Table IV-1. This table shows the current order, family, genus, species, period, and repository for all blastoids utilized in this study.

Order	Family	Genus	Species	Period	Repository
Fissiculata	Neoschismatidae	*Timoroblastus*	*sp.*	Permian	NMNL
Fissiculata	Neoschismatidae	*Hadroblastus*	*convexus*	Carboniferous	USNM
Fissiculata	Orophocrinidae	*Orophocrinus*	*stelliformis*	Carboniferous	USNM
Fissiculata	Orophocrinidae	*Brachyschisma*	*corrugatum*	Devonian	USNM
Fissiculata	Astrocrinidae	*Astrocrinus*	*bennei*	Carboniferous	CMC-IP
Fissiculata	Codasteridae	*Codaster*	*robustus*	Devonian	USNM
Fissiculata	Codasteridae	*Pterotoblastus*	*gracilis*	Permian	USNM
Spiraculata	Troosticrinidae	*Metablastus*	*sp.*	Carboniferous	USNM
Spiraculata	Troosticrinidae	*Troosticrinus*	*reinwardti*	Silurian	UTK
Spiraculata	Hyperoblastidae	*Eleuthrocrinus*	*cassedayi*	Devonian	USNM
Spiraculata	Diploblastidae	*Diploblastus*	*fadigai*	Carboniferous	CMC-IP
Spiraculata	Nucleocrinidae	*Nucleocrinus*	*sp.*	Devonian	USNM
Spiraculata	Nucleocrinidae	*Elaeacrinus*	*verneuili*	Devonian	CMC-IP
Spiraculata	Orbitremitidae	*Orbitremites*	*derbiensis*	Carboniferous	Waters
Spiraculata	Orbitremitidae	*Globoblastus*	*norwoodi*	Carboniferous	USNM
Spiraculata	Granatocrinidae	*Mesoblastus*	*crenulatus*	Carboniferous	USNM
Spiraculata	Granatocrinidae	*Granatocrinus*	*granulatus*	Carboniferous	USNM
Spiraculata	Schizoblastidae	*Lophoblastus*	*neglectus*	Carboniferous	USNM
Spiraculata	Pentremitidae	*Pentremites*	*fredericki*	Carboniferous	CMC-IP
Spiraculata	Pentremitidae	*Ambolostoma*	*baileyi*	Carboniferous	USNM
Indeterminate	Indeterminate	*Macurdablastus*	*uniplicatus*	Ordovician	USNM

V. CONCLUSIONS

1. The geometric morphometry used during the first study demonstrated its usefulness in separating closely related species that have been difficult to assess using conventional apomorphies.
2. The model-based clustering algorithm of MCLUST chose a model with four components. The corresponding four-group classification matches the four empirically diagnosed species with 94.23 percent accuracy.
3. It is likely that the misclassifications in this study result from the small sample size of the two lesser-represented species.
4. These geometric morphometric methods can be used in any clade with a set of homologous points or as an exploratory experiment where the number of subpopulations is unknown.
5. The only shortcoming is that underrepresented organisms could fail to be identified or identified incorrectly.
6. With geometric morphometrics we were able to discern that despite varied morphology all species of *Pentremites* in this study grow along the same morphological trajectory.
7. Godoniform and pyriform taxa, as morphological groups, seem to have somewhat different trajectories with respect to each other even though we haven't been able to separate them statistically.
8. Shape change during ontogeny largely consists of changing aspects of the pelvis, lengthening the ambulacra, and enlargement the deltoid bodies.
9. This study has provided a robust character based phylogenetic hypothesis for blastoid evolution that can be incorporated into the AEToL project.

10. Relationships inferred by this study suggest that the treatise classification for Blastoidea – dividing them into spiraculates and fissiculates inadequately reflects the true evolutionary history of the group.
11. It was found that Fissiculata is paraphyletic with respect to polyphyletic Spiraculata.
12. This study has validated the Waters & Horowitz (1993) hypothesis that spiraculates are polyphyletic but fails to define the number of originations.
13. A more detailed study is needed to test the hypothesis of iterative evolution of spiraculates from fissiculates.
14. This study also infers two large blastoids clades. One demarcates all non- *Macurdablastus* fissiculates and one that demarcates all non-Troosticrinid spiraculates.
15. Although the Bodenbender & Fisher and Sumrall & Brochu analyses failed to recover many of the traditionally defined families, our analysis is more congruent with traditional classifications.
16. It is our contention that stratocladistics and differential character weighting/ordering have led to the flawed hypothesis presented in earlier studies.
17. Since the removal of stratocladistics by Sumrall & Brochu (2003) generated a more parsimonious tree on our matrix than the one utilizing stratocladistics and ordered/differentially weighted characters we feel confident that our results more accurately reflect the true phylogeny.
18. Paraphyletic and polyphyletic families that were identified can be clarified with the addition of more genera and internal character data that is being developed from existing collections.

Supplemental Material

APPENDIX IV

P. fredericki CMC IP64792
1 17.1740 -50.3921 17.0320
2 17.9458 -52.2910 19.2827
3 17.9533 -48.1713 18.6694
4 22.9560 -46.4997 20.2871
5 21.3418 -47.8302 21.0280
6 21.5143 -50.0829 20.9448
7 21.3407 -52.5057 21.5228
8 22.1623 -53.8673 21.1770
9 29.9910 -50.4267 22.6437
10 32.7950 -48.3303 17.1034
11 33.3296 -50.7009 17.3968
12 32.1571 -53.6838 17.9783
13 34.8405 -51.8361 13.6782

P. fredericki CMC IP64793
1 17.1894 -52.8549 16.9902
2 18.5013 -54.3275 19.0516
3 18.2043 -50.4791 18.2677
4 21.5874 -48.9567 19.0619
5 20.6787 -49.8814 19.6329
6 20.6902 -52.0916 19.8201
7 21.1431 -54.0873 20.5002
8 21.9275 -54.9668 20.3129
9 26.9501 -51.3056 20.9648
10 29.0565 -49.9259 16.6787
11 29.9360 -51.5651 16.8177
12 29.4584 -53.8994 17.7351
13 31.1305 -52.3442 14.6913

P. meganae CMC IP53374
1 3.7896 -45.8318 12.7808
2 4.6030 -48.0602 14.7401
3 5.5261 -43.2285 14.1406
4 12.3973 -41.5503 15.3945
5 11.5108 -43.4820 16.7186
6 10.4316 -45.9917 17.2118
7 10.6447 -48.5773 17.4752
8 11.1722 -50.7781 17.1606
9 20.8905 -46.7497 20.2101
10 28.8238 -44.9003 12.7027
11 30.8425 -48.8480 13.2425
12 28.1547 -52.7790 14.7931
13 35.9748 -50.8064 9.3493

P. fredericki CMC IP66832
1 15.2824 -51.0071 13.4420
2 15.7968 -52.6078 15.6275
3 16.1972 -48.3299 14.7343
4 20.0534 -46.6058 16.8148
5 19.1686 -47.6108 17.3344
6 19.1450 -50.2332 17.4056
7 18.7981 -52.6931 18.4698
8 19.4456 -53.9755 18.2929
9 27.8319 -50.4039 20.2563
10 30.8902 -48.9120 15.4608
11 31.7222 -51.0289 15.7771
12 30.3413 -54.0193 16.8178
13 33.4778 -52.5116 13.1397

P. fredericki CMC IP64791
1 11.6262 -48.4444 13.9774
2 12.2039 -50.5707 16.4865
3 12.8960 -46.1264 15.7782
4 19.1880 -44.2924 18.8951
5 17.2117 -45.7608 19.5084
6 16.7275 -48.6329 19.5722
7 16.4511 -51.2530 20.3244
8 17.8653 -53.1403 20.1502
9 28.5751 -49.9524 22.5734
10 31.5302 -47.8753 16.0144
11 32.4441 -50.5422 16.2883
12 31.0223 -53.5158 17.1254
13 34.1464 -51.9101 12.4316

P. meganae CMC IP53373
1 5.9306 -46.9085 10.4606
2 6.6533 -48.9011 12.2954
3 7.1069 -44.5781 11.4424
4 15.0280 -42.1108 13.9969
5 12.9254 -44.0833 15.0936
6 12.2293 -46.4143 15.6567
7 12.4907 -49.2215 15.9652
8 14.1960 -51.6411 15.7763
9 23.3463 -46.8146 18.8539
10 30.0260 -44.5210 11.8873
11 32.5496 -48.5680 12.2746
12 29.5350 -52.8208 13.7916
13 36.0911 -50.3635 7.4002

P. fredericki CMC IP66833
1 15.9977 -53.2884 15.3422
2 16.2233 -54.8274 17.2229
3 16.2520 -51.1610 16.6788
4 18.6468 -49.5362 18.4650
5 18.1608 -50.5869 18.7645
6 18.2765 -52.6674 18.8476
7 18.1983 -54.5784 19.3591
8 18.8313 -55.6566 19.7216
9 23.9736 -51.9146 21.9560
10 27.0899 -49.9087 18.0372
11 28.1418 -51.9441 18.4164
12 27.2013 -54.5940 19.2861
13 29.6292 -53.0263 15.8231

P. fredericki CMC IP64794
1 17.6472 -52.3444 17.1513
2 18.4953 -53.7925 18.8652
3 18.6785 -50.3457 18.2186
4 20.7535 -49.4865 19.1166
5 20.4299 -50.1748 19.4531
6 20.2805 -52.0897 19.6500
7 20.1517 -53.9624 20.0381
8 20.2234 -54.8648 20.1912
9 26.0006 -52.3887 20.9180
10 28.0206 -50.5464 17.2327
11 28.9892 -52.5162 17.1891
12 27.8128 -54.9035 18.4082
13 29.5794 -53.4422 14.8935

P. meganae CMC IP53375
1 3.9438 -46.9988 8.0845
2 4.6429 -49.0301 10.4837
3 4.9369 -44.4008 9.4337
4 11.8596 -41.7640 11.8263
5 11.1348 -44.3430 13.2001
6 10.6952 -46.4322 13.8476
7 11.0910 -48.6875 14.3835
8 11.4094 -51.3993 14.1300
9 22.5475 -46.3722 16.7837
10 28.2982 -43.9998 10.4529
11 30.8677 -47.7803 10.4469
12 28.3539 -52.0129 11.9463
13 34.7373 -49.5736 5.8774

P. meganae CMC IP66834
1 1.2039 -47.6378 7.1999
2 1.5681 -49.5821 8.9104
3 1.9210 -45.5227 7.8532
4 9.1190 -42.8472 10.8634
5 8.0855 -45.0179 11.9076
6 7.5329 -47.2777 12.1906
7 8.0753 -49.7368 12.9238
8 9.2747 -52.7265 12.8582
9 17.6893 -46.8241 16.0758
10 25.9771 -43.6695 9.5661
11 28.5727 -46.9203 10.2533
12 26.6781 -50.8375 11.2738
13 33.2837 -47.3116 6.3421

P. meganae CMC IP66835
1 6.2934 -48.4393 14.1524
2 7.5352 -50.2776 15.9469
3 7.9599 -45.8688 14.8811
4 14.9759 -44.3297 15.7859
5 14.3950 -45.7165 17.1594
6 13.8189 -48.1987 17.9973
7 13.9506 -50.8370 18.1825
8 14.3540 -52.9501 17.9347
9 24.7192 -48.4074 19.6859
10 29.6155 -46.8000 12.5280
11 31.4883 -49.9190 13.0883
12 29.0880 -53.6551 14.9634
13 34.8293 -52.0371 8.8390

P. meganae CMC IP66836
1 15.5738 -50.0127 16.4712
2 16.2735 -52.0659 17.5768
3 16.4055 -48.3392 18.5290
4 20.9666 -47.1994 20.0929
5 19.7145 -48.6227 20.4236
6 19.1609 -50.6153 19.9180
7 19.9393 -52.9633 19.6421
8 21.0725 -54.3557 18.8373
9 25.2286 -51.1427 21.7362
10 31.8742 -47.0007 17.8836
11 33.9586 -49.6332 17.5535
12 32.4349 -53.2712 17.2341
13 38.6412 -48.7760 14.0884

P. pyriformis CMC IP66837
1 4.3880 -63.8004 7.4997
2 4.9724 -65.3237 9.1506
3 5.2694 -61.8419 8.8588
4 8.0815 -60.6281 10.2812
5 7.6644 -61.5842 10.6137
6 7.4930 -63.5758 10.5206
7 7.4055 -65.6121 11.1194
8 7.2808 -66.4367 11.0709
9 14.0365 -63.6867 13.4551
10 18.8674 -62.3762 9.2806
11 20.1035 -64.8438 9.8353
12 18.5650 -67.0842 10.0744
13 24.4963 -65.5118 6.8128

P. pyriformis CMC IP66838
1 5.9015 -65.0199 6.6848
2 6.3206 -66.1375 8.3766
3 6.2913 -63.1686 7.5359
4 8.6553 -61.2850 8.9815
5 8.3580 -62.2373 9.3800
6 8.5105 -64.0628 9.4081
7 8.6334 -65.7794 10.4561
8 9.0173 -67.0215 10.5531
9 15.0987 -63.1861 12.1816
10 19.8926 -62.0998 7.7769
11 20.7697 -64.0254 8.8024
12 19.5034 -66.1312 9.2038
13 26.2408 -64.5947 6.5486

P. pyriformis CMC IP66839
1 3.7903 -64.7842 9.9046
2 4.3777 -66.3518 11.7653
3 4.1325 -62.6720 11.1822
4 6.4129 -61.0433 13.1703
5 6.4140 -62.1197 13.1952
6 6.4311 -64.0714 13.1582
7 6.6462 -66.1632 13.8663
8 6.7824 -67.3366 13.9426
9 12.7163 -63.4476 16.0972
10 18.8690 -62.0098 12.2364
11 19.7268 -63.4842 12.7506
12 18.7351 -65.6676 12.9378
13 24.2427 -64.2975 10.4753

P. pyriformis CMC IP66840
1 5.0963 -64.0485 8.7097
2 6.1238 -65.4668 10.5305
3 6.1199 -61.8833 9.7743
4 9.4672 -60.1544 10.8197
5 9.0941 -61.1451 11.3941
6 9.2382 -63.1819 11.5203
7 9.1769 -65.0780 12.3263
8 9.5643 -66.2621 12.3069
9 15.1307 -62.6376 13.1352
10 20.3147 -61.7572 8.3243
11 21.4660 -63.6839 8.9868
12 20.2820 -66.0636 9.6484
13 26.2480 -64.5889 5.7134

P. pyriformis CMC IP66841
1 6.7559 -61.7086 14.2634
2 7.9380 -63.8050 16.1373
3 8.4959 -59.9284 15.4334
4 12.3780 -59.1890 16.2819
5 11.6515 -60.2365 16.7892
6 11.3352 -62.2879 16.7585
7 11.0360 -64.3081 17.4611
8 10.8843 -65.5169 17.3664
9 19.3071 -63.7108 17.8296
10 23.1478 -62.7869 12.3119
11 23.9035 -64.9486 12.6287
12 22.7289 -67.0143 13.0457
13 27.1172 -66.1149 9.0620

P. pyriformis CMC IP66842
1 8.3778 -53.0931 12.9355
2 9.3184 -54.5325 14.6818
3 9.1471 -50.9606 14.1870
4 11.7220 -49.6441 15.2497
5 12.0897 -50.6872 15.7979
6 12.0779 -52.5266 15.4826
7 12.2416 -54.4251 16.1319
8 11.9557 -55.3457 16.0401
9 18.0450 -52.1464 16.9001
10 21.6162 -50.2550 11.8183
11 22.8792 -52.1324 12.3588
12 21.9155 -54.2828 12.6963
13 26.4505 -52.8231 8.9817

P. pyriformis CMC IP66843
1 6.6445 -52.8264 13.9672
2 7.7466 -54.4958 15.3853
3 7.7332 -50.9258 15.1461
4 10.7315 -49.4194 16.0694
5 10.3396 -50.7603 16.5440
6 10.2826 -52.6255 16.3059
7 10.3279 -54.4317 16.8021
8 10.7703 -55.5588 16.4772
9 16.9858 -52.4185 17.4635
10 21.0653 -50.3645 12.1917
11 22.2310 -52.1771 12.3199
12 21.3299 -54.4841 12.5462
13 26.1883 -52.5506 8.5717

P. pyriformis CMC IP66844
1 8.5600 -52.5759 12.9384
2 9.7159 -54.3568 14.4465
3 9.7114 -50.8132 14.1876
4 12.5683 -49.5563 15.0169
5 12.2325 -50.6280 15.5210
6 12.2600 -52.3388 15.3362
7 12.1790 -54.2558 15.7240
8 12.4682 -55.2807 15.5899
9 18.4607 -52.3636 16.9209
10 22.4589 -50.8301 12.1800
11 23.4615 -52.6683 12.4278
12 22.3449 -54.8507 12.7441
13 26.7937 -53.4068 9.0415

P. pyriformis CMC IP66845
1 7.5663 -52.5029 12.7994
2 8.5170 -54.0277 14.1813
3 8.5440 -50.6086 13.9399
4 11.4749 -49.0901 14.9001
5 11.2497 -50.3371 15.4476
6 11.4040 -52.1095 15.3407
7 11.3846 -54.0128 15.8607
8 11.1539 -54.9640 15.5331
9 17.1746 -51.8612 16.9793
10 21.3875 -50.1661 11.9991
11 22.5763 -52.3260 12.2621
12 21.5939 -54.5665 12.7050
13 26.0429 -52.9534 9.1399

P. pyriformis CMC IP66846
1 6.3490 -51.1685 12.1095
2 6.5901 -53.0619 13.5903
3 7.3783 -49.4403 13.9192
4 10.2860 -48.7611 15.7309
5 10.0062 -49.9376 16.2018
6 9.8052 -51.8232 15.4592
7 9.5411 -54.0011 15.9469
8 9.5264 -55.2453 15.4523
9 16.3201 -53.0654 17.8639
10 20.4263 -51.2375 13.4691
11 21.0024 -53.2962 13.5197
12 19.6927 -55.3330 13.3340
13 24.8356 -54.0459 10.5301

P. pyriformis CMC IP66847
1 8.8331 -53.4638 10.4617
2 9.7634 -55.1944 12.0181
3 9.6166 -51.4636 11.9958
4 11.5457 -50.2738 13.1249
5 11.6322 -51.3826 13.2592
6 11.8293 -53.2143 13.1818
7 11.7733 -55.1733 13.3111
8 11.6442 -56.0351 13.2007
9 17.1914 -53.2937 15.3204
10 22.0432 -51.3547 11.5695
11 23.3459 -53.4853 11.7339
12 21.7513 -55.7852 11.9279
13 27.4673 -54.2979 9.1968

P. pyriformis CMC IP66848
1 8.3506 -52.3298 9.6639
2 8.6224 -53.7612 11.2887
3 9.0726 -50.4581 10.9194
4 11.4650 -49.2071 12.1280
5 11.2357 -50.2002 12.6415
6 11.2934 -52.1690 12.6533
7 11.1705 -53.9176 13.2904
8 11.4312 -54.9977 13.1539
9 17.0894 -51.9512 14.7751
10 22.0517 -50.9428 10.1360
11 22.8247 -52.7652 10.4214
12 21.7666 -54.7261 10.7690
13 26.5686 -53.7349 8.0150

P. pyriformis CMC IP66849
1 9.0568 -53.2152 8.8520
2 10.2025 -55.0912 10.0570
3 9.8052 -51.4562 10.5881
4 13.0077 -50.1900 12.0940
5 12.5590 -51.2924 12.1588
6 12.4214 -53.2422 11.4994
7 12.9968 -55.2643 11.5695
8 13.3902 -56.1805 11.1873
9 19.3008 -52.9919 13.2053
10 22.9730 -50.2247 8.6687
11 24.1114 -51.9927 8.4180
12 23.1052 -54.1296 8.1864
13 27.7828 -51.5828 4.9658

P. pyriformis CMC IP66850
1 11.2874 -51.3853 9.6778
2 11.9495 -53.1314 11.0808
3 12.3800 -49.5853 10.9114
4 14.6846 -48.7607 12.2144
5 14.2007 -49.7214 12.2399
6 14.0889 -51.5716 11.9596
7 13.8631 -53.6099 12.5096
8 14.0587 -54.5212 12.5189
9 20.5188 -52.2672 14.2332
10 26.1302 -50.8034 9.4135
11 27.2242 -53.1310 9.4407
12 25.6274 -55.4974 9.6570
13 31.4251 -53.8734 5.6117

P. pyriformis CMC IP66851
1 8.5949 -53.0359 8.4209
2 9.3935 -54.4937 9.8654
3 9.3434 -51.0765 9.6496
4 12.3228 -49.5272 10.4559
5 11.7733 -50.7152 10.8673
6 11.8485 -52.6085 10.5324
7 12.0023 -54.4972 11.1502
8 12.6991 -55.5697 10.9886
9 18.1235 -52.2049 11.8667
10 21.8674 -51.0236 7.0858
11 22.7989 -52.5389 7.2872
12 21.7774 -54.6155 7.6018
13 26.6923 -53.0751 4.2108

P. pyriformis CMC IP66852
1 9.6349 -54.0402 6.9406
2 10.7038 -55.4920 8.6640
3 10.4668 -51.9412 8.3679
4 12.0766 -50.7154 9.2384
5 12.5346 -51.5321 9.5347
6 12.7412 -53.4049 9.5111
7 12.4908 -55.3604 9.8154
8 12.3874 -56.0451 9.7506
9 18.0062 -52.7931 11.2039
10 22.8351 -51.0840 6.7047
11 23.8810 -53.0162 7.2311
12 23.0250 -54.9711 7.3428
13 27.6083 -53.3456 4.1469

P. pyriformis CMC IP66821
1 7.3771 -50.7812 8.5630
2 8.3232 -52.8747 10.2639
3 8.6640 -48.6229 9.7593
4 12.7262 -47.5621 11.1892
5 11.5018 -48.6941 11.4646
6 11.3501 -50.8663 11.2082
7 11.0616 -53.0157 11.8316
8 11.7565 -54.4215 11.7926
9 18.8894 -51.7344 12.6841
10 23.1812 -50.8270 7.4279
11 23.9854 -53.0352 7.6246
12 22.5475 -55.1645 7.8687
13 28.0784 -54.1482 3.7252

P. tulipiformis CMC IP66857
1 10.3451 -63.4113 11.0875
2 10.3523 -65.2661 12.1685
3 10.7718 -61.9595 12.6269
4 15.8900 -59.9153 14.7656
5 14.7527 -61.9612 15.3130
6 14.6408 -63.7301 14.6679
7 14.4095 -65.8006 14.8159
8 15.1388 -67.8565 14.2632
9 21.9566 -64.2339 15.0530
10 24.2728 -61.2864 11.2894
11 24.7973 -63.9489 10.9438
12 24.0699 -66.4708 10.4466
13 24.6736 -64.0080 7.5416

P. pyriformis CMC IP66853
1 9.0290 -53.1425 7.1065
2 9.8547 -54.5531 8.4603
3 9.8661 -51.0744 7.9828
4 12.2461 -49.8836 8.8774
5 12.0152 -50.9356 9.2558
6 11.9816 -52.6993 9.1331
7 12.0410 -54.4527 9.8415
8 12.2828 -55.4024 9.8564
9 16.9427 -52.3610 10.8382
10 21.9010 -50.7820 6.4205
11 22.9864 -52.4321 6.7496
12 21.7814 -54.9609 7.4366
13 26.5992 -53.4991 3.5668

P. pyriformis CMC IP66855
1 10.6076 -53.4808 10.6443
2 11.6792 -54.9828 12.1610
3 11.5177 -51.8595 11.7606
4 14.7615 -50.5084 12.6738
5 14.4323 -51.3845 12.9636
6 14.4282 -53.1033 12.7223
7 14.6841 -54.7928 13.3671
8 15.1397 -55.8018 13.2739
9 21.2354 -52.9023 13.9808
10 25.2182 -51.6443 9.7609
11 26.2473 -53.3051 10.0122
12 25.1812 -55.2387 10.3916
13 29.4952 -54.0832 6.8290

P. tulipiformis CMC IP66858
1 5.4957 -63.3475 11.5313
2 5.3453 -64.7115 12.9375
3 5.2961 -61.6962 12.7318
4 9.1720 -58.9238 15.6098
5 8.2863 -60.7919 16.0987
6 8.4278 -62.7601 15.7388
7 8.5805 -64.5464 16.3795
8 9.6254 -66.4825 16.2906
9 14.8183 -62.2182 17.9446
10 18.2363 -60.0363 14.2821
11 18.9357 -62.1656 14.0352
12 18.2498 -64.8182 14.9257
13 19.6009 -62.6356 11.9019

P. pyriformis CMC IP66854
1 7.7406 -52.8617 8.7739
2 8.4403 -54.3271 9.9645
3 8.6501 -50.7934 9.7045
4 11.7780 -49.3136 10.6869
5 11.3614 -50.4174 11.0462
6 11.3532 -52.2486 10.9246
7 11.3342 -54.2576 11.5921
8 11.8726 -55.2582 11.5751
9 17.6015 -51.9537 12.3793
10 22.6860 -50.2838 7.4040
11 24.0334 -52.3472 7.6324
12 22.7466 -54.7254 8.2847
13 27.4336 -53.3275 4.0050

P. tulipiformis CMC IP66856
1 6.4118 -64.4053 4.2399
2 6.5418 -65.8106 6.0879
3 6.7253 -62.5794 5.6132
4 10.9128 -60.5221 7.4139
5 10.2527 -61.9982 7.9906
6 10.1694 -63.8554 7.7585
7 10.3590 -65.6983 8.7345
8 10.8293 -67.2186 8.5542
9 16.4001 -63.7634 9.4572
10 19.3580 -62.2915 5.2714
11 19.8654 -63.9287 5.2982
12 19.0149 -66.4554 6.0179
13 20.6762 -64.6679 2.9932

P. tulipiformis CMC IP66859
1 7.9580 -64.3954 8.5363
2 8.2967 -65.9117 9.9722
3 8.3919 -62.6716 9.7001
4 12.2621 -60.9633 11.8155
5 11.6477 -62.2234 12.3313
6 11.4784 -63.9926 12.0657
7 11.6234 -65.8346 12.6281
8 12.1450 -67.2289 12.5006
9 17.2857 -64.0044 13.3445
10 20.0988 -62.7370 9.9259
11 20.4344 -64.3205 9.9966
12 19.8060 -66.3342 10.6406
13 21.0278 -65.0417 8.0321

P. tulipiformis CMC IP66860
1 8.4360 -53.4519 10.9661
2 8.7914 -54.7137 12.6084
3 8.6386 -51.7304 12.1643
4 12.4860 -49.6157 13.8601
5 11.8434 -50.9971 14.5464
6 11.9512 -52.8406 14.4784
7 12.0897 -54.6388 15.0591
8 12.7456 -55.9071 14.7440
9 17.2665 -52.4037 15.3267
10 19.5528 -50.6861 11.5698
11 20.3475 -52.5356 11.3547
12 19.9115 -54.6431 12.1328
13 21.2221 -53.3073 9.2712

P. tulipiformis CMC IP66861
1 7.2266 -53.3142 15.2276
2 8.3896 -55.0012 16.9512
3 8.1348 -51.4171 16.7600
4 11.8863 -49.6895 17.7350
5 11.5513 -50.8889 18.2604
6 11.6427 -52.7795 18.0726
7 11.8146 -54.8593 18.5056
8 12.4625 -56.0224 18.2146
9 18.7477 -52.3745 17.8371
10 20.1754 -50.5939 14.3505
11 20.7995 -52.3782 14.3761
12 20.3294 -54.6029 15.2319
13 21.0662 -53.0101 11.9018

P. tulipiformis CMC IP66862
1 6.5137 -52.0267 10.9268
2 7.1463 -53.6790 12.6268
3 7.0822 -50.2104 12.4425
4 12.1849 -48.4834 14.3085
5 11.1857 -50.1381 14.9892
6 11.0967 -51.9916 14.4335
7 11.4101 -53.8414 14.8197
8 12.2931 -55.7355 14.1181
9 16.8029 -52.3329 15.1003
10 19.4341 -49.8188 10.8168
11 19.9522 -52.2368 10.3399
12 19.1429 -55.0751 11.0811
13 20.4590 -52.4495 7.8098

P. tulipiformis CMC IP66863
1 5.9601 -52.5726 12.3910
2 6.1577 -54.3161 13.5059
3 6.2009 -51.2192 13.6306
4 10.6655 -50.0867 16.4745
5 9.8279 -51.4075 16.8877
6 9.7143 -53.0155 16.2790
7 9.7481 -55.0810 16.4882
8 10.7679 -56.4219 15.8530
9 16.4036 -53.5014 17.8099
10 19.0543 -51.0082 14.7645
11 19.9331 -52.8310 14.4668
12 18.9266 -55.2896 14.4458
13 21.0627 -52.8635 11.8427

P. tulipiformis CMC IP66864
1 8.0380 -52.1761 12.6045
2 8.3299 -53.5193 13.9495
3 8.6225 -50.8200 13.7246
4 13.0750 -48.8557 15.7236
5 12.2926 -50.4997 16.3367
6 11.9373 -52.2790 15.8941
7 12.1336 -53.9557 16.6314
8 12.7749 -55.5675 16.1581
9 17.9007 -52.4870 17.0278
10 20.2595 -50.1079 12.9448
11 21.0153 -52.3803 12.4776
12 20.5090 -54.8252 13.1312
13 21.5571 -53.1239 10.0704

P. tulipiformis CMC IP66865
1 11.5037 -52.9085 9.4862
2 11.8952 -54.2954 10.9429
3 11.6799 -51.4462 10.7697
4 15.3691 -49.5028 12.4911
5 14.7675 -50.9497 12.8501
6 14.7853 -52.6291 12.4843
7 15.0126 -54.5610 13.1579
8 15.7868 -55.9388 12.8875
9 20.8172 -52.4141 13.5206
10 23.1298 -50.7542 9.9602
11 23.8479 -52.5325 9.7651
12 23.2324 -54.8336 10.4441
13 24.7036 -52.8944 7.5740

P. tulipiformis CMC IP66866
1 12.1985 -52.8867 8.3210
2 12.5752 -54.4125 9.5488
3 12.6998 -51.2414 9.3847
4 16.4090 -49.5436 11.0443
5 15.7492 -50.8808 11.5987
6 15.7315 -52.6324 11.4510
7 15.6920 -54.3016 11.8799
8 16.7677 -55.7009 11.7520
9 20.8724 -52.3222 13.0594
10 23.3891 -50.0994 9.7936
11 24.2573 -52.0185 9.6548
12 23.8467 -54.8851 10.3058
13 25.3430 -52.7052 7.1462

P. tulipiformis CMC IP66867
1 9.9853 -52.8259 9.9645
2 10.1075 -54.1998 11.2728
3 10.2447 -51.4413 10.9656
4 14.1556 -49.6138 13.2637
5 13.2855 -51.0313 13.8649
6 13.0931 -52.6587 13.5234
7 13.1560 -54.4188 14.1222
8 13.5793 -55.7988 13.7886
9 18.1594 -52.8082 15.4486
10 21.3463 -51.1062 12.1969
11 21.9520 -52.8849 12.1544
12 21.0392 -55.3391 12.7737
13 23.2424 -53.6670 9.9143

P. tulipiformis CMC IP66868
1 9.1609 -53.6554 6.3321
2 9.5693 -54.9514 7.6138
3 9.4354 -51.8238 7.2849
4 12.6124 -49.8920 9.3527
5 12.2100 -51.1812 9.9586
6 12.4801 -52.8514 9.6942
7 12.4287 -54.5559 10.3719
8 12.8315 -55.7895 10.2894
9 17.4387 -52.5140 11.2625
10 20.7082 -50.9199 7.9926
11 21.5414 -52.7330 8.0703
12 20.6784 -55.0475 8.8236
13 22.2780 -53.5284 5.7142

P. tulipiformis CMC IP66869
1 8.9399 -52.9791 8.2987
2 9.4421 -54.4306 9.8302
3 9.2942 -51.2217 9.2238
4 13.2118 -49.2858 10.7234
5 12.4961 -50.7695 11.3714
6 12.5104 -52.5430 11.1505
7 12.5667 -54.1765 11.8547
8 13.3797 -55.6698 11.7280
9 18.4898 -52.3878 12.4898
10 20.5488 -50.9881 8.7289
11 21.1079 -52.7479 8.6794
12 20.2740 -55.0745 9.5266
13 21.9845 -53.4480 6.5142

P. tulipiformis CMC IP66904
1 8.3867 -53.2979 6.0120
2 8.7140 -54.5911 7.1041
3 8.5820 -51.7590 6.9351
4 13.2999 -49.5006 8.9139
5 12.6625 -50.9766 9.6287
6 12.6105 -52.5952 9.6418
7 12.9280 -54.3073 9.9642
8 13.7816 -55.9485 9.4855
9 17.5471 -52.2434 10.0308
10 19.6538 -50.4367 6.7165
11 20.4211 -52.3889 6.3165
12 20.0586 -54.5386 7.0633
13 20.9900 -52.8310 4.2760

P. tulipiformis CMC IP66825
1 7.3191 -52.5899 6.0574
2 7.5595 -53.8564 7.2027
3 7.7359 -51.1743 6.8621
4 12.0032 -49.6002 8.2611
5 11.6268 -50.7570 9.1143
6 11.3583 -52.4215 8.9333
7 11.2673 -54.0577 9.5080
8 11.5416 -55.4142 9.1302
9 17.0427 -52.8326 9.6120
10 19.1766 -51.5476 6.1256
11 19.7212 -53.2742 5.9658
12 18.9784 -55.1943 6.7409
13 20.3633 -54.0574 3.8565

P. tulipiformis CMC IP66870
1 8.1994 -52.7101 6.2081
2 8.6593 -54.3082 8.2290
3 8.7983 -50.6212 7.8888
4 12.6159 -49.1755 9.4843
5 11.5848 -50.2663 9.8960
6 11.5255 -52.2935 9.7055
7 11.4777 -54.4518 10.2925
8 12.0798 -55.6374 9.9692
9 17.4489 -52.4978 11.1853
10 20.3397 -50.7562 7.8213
11 21.0280 -53.0359 7.4980
12 19.2934 -55.8544 8.4656
13 21.5151 -53.8170 4.8718

P. tulipiformis CMC IP66905
1 8.8107 -52.7273 5.2400
2 9.4204 -54.2330 6.5357
3 9.5437 -51.2152 6.3996
4 13.5482 -49.4775 7.8355
5 13.0264 -51.0093 8.2449
6 12.9276 -52.6226 8.0861
7 13.2182 -54.4001 8.8419
8 13.3780 -55.8222 8.5163
9 18.4473 -52.6756 9.1693
10 21.1822 -50.9305 5.8130
11 21.7629 -53.0213 5.6710
12 20.6547 -55.2944 6.5215
13 22.8644 -53.8822 3.3750

P. tulipiformis CMC IP66903
1 6.3520 -52.9639 7.4411
2 6.5682 -54.4284 8.8630
3 6.5763 -51.1925 8.5604
4 10.9477 -49.5045 10.5767
5 10.3676 -50.7747 11.1497
6 10.4490 -52.5176 10.8810
7 10.4490 -54.2676 11.4608
8 10.6906 -55.6997 10.9461
9 15.7011 -52.4616 11.9820
10 18.4704 -50.6395 8.2925
11 19.2924 -52.3420 7.8450
12 18.4366 -54.7390 8.9203
13 19.8876 -53.0071 6.0208

P. tulipiformis CMC IP66906
1 6.9811 -52.9672 5.9917
2 7.1141 -54.1939 7.2992
3 7.3355 -51.5936 6.8030
4 11.9149 -49.7862 8.4976
5 11.1978 -51.1552 9.3144
6 11.0461 -52.7179 9.1807
7 10.9516 -54.2876 9.7990
8 11.4502 -55.5753 9.6101
9 16.3536 -52.9749 9.9555
10 18.8303 -51.4865 6.2955
11 19.3311 -53.4284 6.1374
12 18.6362 -55.4744 7.2290
13 19.6046 -54.2033 4.2814

APPENDIX V

P. fredericki CMC 64792	P. fredericki CMC IP64793	P. fredericki CMC IP64795
25.5665-64.048920.7769	21.5604-61.484418.2177	12.0376-64.753219.7051
25.1222-62.13922.9128	20.6315-59.457319.8832	13.3916-66.188220.4703
25.2288-66.150622.8412	21.0567-63.327820.2789	12.8546-63.370920.3984
20.9482-60.361725.0625	17.3332-58.413921.4403	14.7166-66.414120.5396
21.9792-61.747325.5914	18.3218-59.314721.7548	14.3349-65.957720.7238
21.9168-64.183825.225	18.7484-61.41221.6742	14.0102-64.592420.4897
22.2035-66.507125.5948	18.7871-63.464422.1594	13.9165-63.280220.7776
20.6871-67.964925.2199	17.9581-64.563422.0355	14.0977-62.639520.4578
13.5444-64.161627.9307	12.7204-61.720823.9584	17.0348-64.437720.5598
10.6985-61.63923.1205	9.55972-60.236820.65	18.2294-65.445418.3165
9.53096-64.889622.9724	8.98949-62.737520.5804	18.6762-63.901617.9576
10.1901-67.262322.7991	10.0446-64.407820.8193	17.9432-62.882318.0269
7.51105-64.289919.2548	7.47892-62.604118.4635	19.6494-64.455516.1411

P. fredericki CMC IP66832	P. fredericki CMC IP64791	P. fredericki CMC IP70933
10.1652-60.21567.5117	11.9564-58.99024.24984	12.4612-63.88599.69478
8.88637-62.34258.71082	9.7467-61.1685.78837	11.5374-65.93610.7263
8.74787-57.80949.19929	10.2866-56.56235.47457	11.2368-62.221310.8509
8.4683-64.271613.0833	7.67943-62.744312.2103	11.3366-67.393113.6914
7.67966-62.861212.5858	7.02218-61.20510.4906	10.7158-66.489813.3898
8.12388-60.262512.7052	7.6249-58.427110.201	10.844-64.371713.679
7.64938-57.735312.8503	7.6271-55.589310.0871	10.2536-62.427213.7567
8.17889-56.590813.6549	8.49831-53.697511.7909	10.5416-61.547714.1392
9.32782-60.864921.9409	7.26198-57.782422.7784	11.453-65.081520.0915
14.3341-63.358322.3378	13.3279-60.484624.4367	15.0782-66.520220.9358
15.1932-60.333923.4387	14.1491-57.407825.0952	15.3077-64.534521.3699
14.5727-58.018822.5799	14.0511-54.833523.6383	14.7824-63.101221.1178
18.6195-60.768323.7974	18.4072-58.186926.1421	17.3959-64.753121.8788

P. fredericki CMC IP66833	P. fredericki CMC IP64794	P. fredericki CMC IP70934
11.3045-61.55149.67553	9.62951-61.974717.1679	12.5442-63.8599.64447
9.98103-63.446510.5456	10.2362-63.739118.6187	11.5349-65.874310.6818
10.2424-59.797411.0289	10.8851-60.031318.8502	11.2534-62.192510.8422
9.43079-64.821113.8116	12.1642-65.174219.8674	11.2688-67.329313.7586
9.27149-63.760413.4661	11.8122-64.263919.898	10.6985-66.445313.3563
9.61432-61.650713.4527	12.0093-62.206919.8187	10.8559-64.379613.6462
9.48831-59.628813.5635	12.2042-60.366119.9998	10.1986-62.468913.6618
9.86248-58.593514.0416	12.6524-59.639719.95	10.5626-61.457314.1379
10.1832-62.048920.1766	17.6099-62.889921.4077	11.357-65.141319.9213
14.1976-64.602120.778	19.6897-65.004218.5243	15.1436-66.560620.8979
15.2732-61.765421.5702	21.0922-62.418517.7287	15.2831-64.499721.3691
14.6227-59.712220.7625	20.1704-60.611418.1986	14.8035-63.024821.0998
18.3371-62.739921.3739	21.78-62.967715.3595	17.583-64.732521.7843

P. fredericki CMC IP70935	P. fredericki CMC IP70938	P. fredericki CMC IP70941
14.0157-63.712811.8962	15.3367-65.312413.0592	13.4195-66.425115.4415
13.2166-65.099512.9821	13.9205-66.790214.1106	12.7241-67.627716.2965
13.5808-62.261513.1637	14.3058-63.496914.019	12.8807-65.213316.5708
12.7713-66.669615.1554	13.3645-67.617616.1983	12.5235-68.151917.1018
12.5521-65.695815.2304	13.1211-66.920816.1152	12.6138-67.572217.2481
12.9753-64.121615.0322	13.2328-64.979216.1288	12.7172-66.585717.4278
12.5328-62.272615.2139	13.1775-63.24816.0502	12.6659-65.440717.5376
13.1925-61.449115.2156	13.6653-62.612216.2189	13.1387-64.81417.5422
13.5453-63.889521.2805	12.8833-64.937421.1866	12.7674-66.852819.2743
17.3337-66.366721.9875	15.7487-66.777722.5042	15.0566-68.103820.6916
18.0122-64.450122.7245	15.9976-64.999622.8623	15.4944-67.014421.1736
17.7172-62.596921.8949	15.9-63.437622.179	15.2879-65.85120.5424
20.4931-64.692723.1112	18.0355-65.200724.0582	16.7546-67.336321.3791

P. fredericki CMC IP70936	P. fredericki CMC IP70939	P. fredericki CMC IP70942
17.4794-64.125310.996	23.4878-64.28179.38873	15.3004-67.112115.7536
16.0645-65.789412.1752	22.4463-65.865610.0403	14.7113-68.239216.2207
16.5184-62.358212.4099	22.8098-62.662810.3801	14.7031-66.404716.2771
15.3576-66.883814.5522	21.5933-67.038912.5531	14.5619-68.681917.2538
15.2777-66.050414.3578	21.4423-66.126912.3626	14.4261-68.126417.0214
15.6975-64.06514.3744	21.8102-64.466212.4564	14.4733-67.263917.1035
15.5908-62.201214.6537	21.8218-62.88912.5133	14.3058-66.251117.2241
16.1498-61.428915.1734	22.5794-61.854212.9812	14.5897-65.898517.4889
16.698-64.471320.563	21.8436-65.016417.0255	14.3729-67.294418.6667
19.9224-66.525720.8341	25.6527-67.262318.2372	16.2021-68.231720.0387
20.5028-64.872121.4579	25.8033-65.250918.7898	16.5517-67.409520.2782
20.3537-63.292520.8849	26.2171-63.690318.5605	16.5424-66.430619.838
22.8261-65.204121.7506	28.3054-66.186419.1149	17.6852-67.449620.8804

P. fredericki CMC IP70938	P. fredericki CMC IP70940	P. godoni CMC IP70943
13.2068-64.727212.1071	15.6507-66.690513.331	4.67336-60.908618.7001
12.3185-66.172212.9767	14.9849-67.947314.3967	5.04228-62.650120.0022
12.3858-63.383313.191	15.1047-65.567414.4949	5.02411-59.070519.9594
11.556-67.27814.6399	14.8702-68.542415.588	10.2019-65.036823.2471
11.679-66.710914.5263	14.7805-67.793315.5638	8.55043-63.158323.6085
11.7014-65.025114.9304	14.8893-66.743315.6901	8.11053-60.976123.6752
11.406-63.371915.0509	14.8328-65.725415.6523	8.25619-58.794123.5345
11.6247-62.416515.3031	15.1888-65.065215.6948	10.1923-56.74222.9829
11.5115-65.132919.9595	14.8848-66.867317.4669	18.0073-61.222926.7195
14.5609-67.175720.8486	16.7624-68.067118.817	20.4088-63.804322.0495
14.9082-65.250321.8146	16.9909-67.132719.1827	21.1073-60.68421.948
14.5623-63.363921.191	16.7813-66.141518.647	20.2972-58.177721.8857
17.7216-65.155122.8002	18.3899-67.356319.8558	23.2881-61.186918.9096

P. godoni CMC IP70944
8.64647-61.559719.2783
9.039-63.367520.5866
9.02919-59.890520.7979
17.2221-65.50322.0628
15.5595-64.028824.0366
15.1715-61.630824.1883
15.3621-59.388124.6381
16.8446-57.262322.7387
25.1435-61.117322.9857
24.7253-63.572718.3952
25.5511-60.276518.6259
24.7813-57.964218.7466
26.274-60.371714.6811

P. godoni CMC IP70945
8.62445-60.855411.0872
8.43949-62.319312.6695
8.85934-58.874412.4917
14.4382-64.664616.7216
12.873-62.613617.0953
12.8559-60.298517.0394
13.2912-58.256516.7453
15.5726-56.591415.631
22.8005-60.588619.131
23.9816-64.3715.2821
24.9093-60.993414.1174
24.0748-58.443514.315
26.6969-61.819611.4853

P. godoni CMC IP70946
7.74117-62.849424.4559
8.24852-64.361825.7811
8.03162-61.089725.5098
15.3149-66.008229.0682
12.9867-64.519629.6746
12.4132-62.291829.553
12.5402-60.247729.4074
14.5646-58.355728.5131
21.8983-61.499531.3402
23.8038-64.582327.513
24.1537-61.439627.0358
23.1133-59.043427.147
25.8897-61.858824.3311

P. godoni CMC IP70947
16.871-63.791310.5164
15.8476-65.141710.7167
15.6654-62.312710.7204
14.3636-66.341317.534
13.3304-65.118215.6625
13.2691-63.304515.2358
13.1131-61.510615.137
14.2162-59.97416.8464
13.5675-62.53523.3707
17.0009-64.824224.33
17.2932-62.339524.5867
17.2814-60.414623.6565
19.8262-62.696325.4519

P. godoni CMC IP70948
13.321-62.437512.4413
12.6123-63.773412.7867
12.5345-61.187313.0914
11.4846-66.175918.4511
10.6792-64.625317.494
10.4892-62.681217.4702
10.4285-61.272717.7879
11.4638-59.903518.8397
11.0374-63.412723.9611
14.7293-65.644524.0396
15.3752-63.35825.2313
15.0206-61.429624.71
17.9125-63.663225.8129

P. godoni CMC IP70949
9.84812-63.53813.5609
10.0653-64.819414.9857
10.0331-62.031314.8211
14.1604-66.483317.9348
12.9439-65.153718.1232
12.6517-63.471118.0548
12.8207-61.83618.2795
14.1495-60.527517.9835
19.019-63.352320.8315
21.5169-65.409517.9689
22.1379-63.072517.8827
21.3702-61.350917.7522
24.2041-63.461615.8481

P. godoni CMC IP70950
11.6021-63.328415.6853
11.8595-64.894316.901
11.7941-61.722716.8823
16.6501-66.320419.3575
15.5544-65.102919.8781
15.3292-63.206119.9778
15.2948-61.38819.9815
16.5656-60.240419.2202
20.3858-63.241421.3092
23.6427-65.220318.243
24.3104-63.093918.2111
23.4949-61.351317.9616
26.0154-63.483116.0508

P. godoni CMC IP70951
10.7252-63.80315.3231
10.7221-65.068116.3091
10.7412-62.293316.1537
15.4581-66.282819.618
13.5613-65.109619.9267
13.4045-63.463719.8159
13.6709-61.682719.7619
15.3953-60.425319.1577
19.1626-63.211321.9155
20.8553-65.595319.3098
21.6682-63.251518.866
20.9943-61.503118.8209
23.3871-63.924517.0462

P. godoni CMC IP70952
12.8478-65.280715.8442
12.7895-66.527917.0942
13.1156-63.77617.0092
14.2098-67.527718.7148
14.0302-66.81418.5263
14.1232-65.234718.4127
14.1323-63.820518.3014
14.3446-63.078518.3346
18.1158-65.33720.508
19.7454-67.310918.6222
20.5982-65.364718.6246
20.1324-63.809118.5371
21.9897-65.901817.2403

P. godoni CMC IP70953
13.3131-65.972715.4968
13.7651-67.218816.3723
13.8825-64.778416.6082
15.3129-67.972517.4604
15.0706-67.439317.4129
14.787-66.104917.4366
15.069-64.690117.7917
15.4412-64.030717.7253
18.6033-66.078519.0997
20.5471-67.32716.9707
21.0681-65.773916.8503
20.2981-64.450717.0612
22.1391-65.891615.3353

P. godoni CMC IP70954
-0.924304-64.470521.0802
-0.567832-65.758721.9495
-0.959247-62.516421.9614
5.13616-66.849423.4651
3.65643-65.406724.3866
3.6106-63.69724.1116
3.62827-62.067724.1322
4.74825-60.589122.6727
10.4737-63.181924.3902
11.6457-65.494620.6954
12.3273-63.042720.15
11.6718-61.678220.1577
13.5565-63.624617.8079

P. godoni CMC IP70955
7.66592-64.255315.1458
8.07358-65.849915.8431
8.38924-62.830715.8482
11.3994-67.393317.4417
10.5293-66.156317.7296
10.5842-64.469717.9011
10.7807-62.859117.9599
12.0637-61.889417.7409
16.6628-65.073418.9863
17.8394-67.023516.1348
18.9505-65.101415.9529
18.3729-63.594616.1602
20.4762-65.650414.1025

P. godoni CMC IP70956
9.03207-64.901312.8523
9.00541-66.042213.5953
9.3491-63.661913.702
12.3795-67.634215.8822
11.3964-66.653715.8108
11.459-65.151115.9983
11.6691-63.862416.2648
12.5847-62.651115.6498
15.6648-65.281817.7641
17.4412-66.871215.0253
18.1014-65.271215.0376
17.4495-63.373714.8727
19.3278-65.311913.0303

P. godoni CMC IP70957
11.274-65.605116.0958
11.7108-66.781616.7839
11.7154-64.448316.8099
15.3398-67.989418.601
14.7765-67.045218.9838
14.6514-65.637818.9262
14.6219-64.524619.0353
14.7563-63.394918.385
17.7043-65.649419.7486
19.8429-67.266117.6245
20.1788-65.86717.9759
19.6011-64.131217.311
22.0873-65.827315.5711

P. godoni CMC IP70958
16.546-64.908319.932
17.1439-66.044720.9505
17.2344-63.497120.6345
20.5609-67.063121.9196
20.0161-65.954622.2163
20.0402-64.456322.0391
20.0971-63.100621.9759
20.6845-62.31821.2564
23.8814-64.563522.4148
25.2352-66.564619.9093
25.8132-64.836719.6723
25.259-63.329319.209
26.9297-65.404117.4481

P. godoni CMC IP70959
17.7863-65.469720.6214
17.9886-66.537521.7027
18.4837-64.016821.4339
20.3961-67.518823.2072
19.8712-66.733923.3117
20.0378-65.218422.8571
20.2214-63.736823.0598
20.8642-63.014722.5181
24.2942-65.623724.0833
25.459-67.274422.2012
26.1719-65.856221.5653
25.7095-64.379721.552
27.2668-66.433420.0541

P. godoni CMC IP70960
10.9385-67.121615.9046
11.6616-67.775216.8882
11.4734-65.806816.6717
12.7998-68.233317.4425
12.7984-67.886217.485
12.5096-66.703217.3582
12.4409-65.483717.2373
12.3078-64.980117.0687
16.034-66.027417.3052
16.9484-67.299715.3744
16.8796-65.890814.9886
16.3089-64.933615.1316
17.5127-66.239513.4543

P. godoni CMC IP70961
18.5847-67.229718.2265
18.9184-68.026219.0258
18.9873-66.203818.9087
19.6288-68.542819.4366
19.658-68.027919.3841
19.6586-66.987419.3249
19.6804-66.286719.3641
19.6417-65.719418.9885
21.5781-67.123619.6483
22.6233-68.239518.3017
23.1809-67.146517.7295
22.4812-66.097917.886
23.8265-67.447816.6027

P. pyriformis CMC IP70963	P. pyriformis CMC IP70966	P. pyriformis CMC IP70969
9.28032-51.05826.96487	8.16625-52.52612.6786	7.44455-53.86885.99575
10.0243-53.02858.5053	9.1312-54.331114.3693	8.66724-55.53127.40874
9.77084-49.11288.7715	9.34215-50.704114.2105	8.25412-52.0527.09206
15.4318-55.534211.2744	11.5858-55.564815.8435	10.9321-56.45268.52988
13.8726-53.539611.679	11.1406-54.503515.7307	10.5474-55.5558.49454
14.0274-51.001111.3757	11.2338-52.51415.2935	10.5771-53.69718.17798
13.5541-48.869212.1637	11.4557-50.613215.8639	9.98394-51.69898.3841
14.9194-46.976311.8889	12.3791-49.515415.764	10.1616-50.8858.20072
23.9191-50.714714.7421	18.4232-52.817118.3577	15.6516-53.43749.77721
29.5908-52.93539.02598	22.9705-55.261714.0689	19.9698-55.39925.70012
30.7924-49.63359.30426	24.2348-53.055213.9917	20.8837-53.30725.46358
28.9703-46.61848.90308	23.2076-51.369413.7422	20.27-51.35745.18911
36.658-49.44724.81778	28.2953-53.867511.497	24.146-53.49342.32281

P. pyriformis CMC IP70964	P. pyriformis CMC IP70967	P. pyriformis CMC IP70970
6.08421-52.35378.08351	6.48807-52.062413.8148	5.8076-54.21818.41458
6.9054-54.4049.58931	7.25857-53.977415.0479	6.67852-55.8069.41148
7.21029-50.82610.2264	7.45071-50.223615.149	6.79027-52.60779.41152
10.8519-56.41511.7432	10.2036-55.402216.6418	8.26474-56.653910.5882
9.74714-55.299711.8094	9.89537-54.187916.6799	8.41513-55.90710.4438
9.4924-53.026911.4972	10.1772-51.936316.2124	8.35692-54.1099.99951
9.58964-51.023312.316	9.93882-50.03816.7279	8.34791-52.350210.3441
11.1523-49.739712.3941	9.95137-48.939516.4401	8.45454-51.657610.38
17.3792-53.556915.5123	17.9849-52.18418.7529	14.7776-54.162611.9191
22.7074-55.565110.5895	22.6888-55.087913.4863	19.3227-55.88187.95883
24.0471-53.067411.3215	23.7766-52.551613.3508	20.0583-53.98967.77912
21.9501-50.21910.9676	22.6434-50.221813.1061	19.1101-52.44827.71133
28.6367-53.00167.77166	27.5984-53.37249.52411	23.2424-54.24714.91124

P. pyriformis CMC IP70965	P. pyriformis CMC IP70968	P. pyriformis CMC IP70971
8.15127-51.274810.0712	10.7037-52.74611.1628	6.98915-69.522311.1095
8.9481-53.398411.811	11.2321-54.614912.1857	7.41239-71.028612.2511
9.03494-49.576811.6477	11.865-51.075312.4886	7.69504-68.053612.1041
12.193-54.882913.976	12.8784-55.674913.4033	8.356-71.710213.2061
11.8074-53.838714.0544	12.8007-55.007113.2916	8.61463-71.176813.1268
11.9765-51.742813.8867	13.1191-53.136413.1875	8.78723-69.528412.8704
11.8462-49.499614.2225	13.4906-51.232813.7147	8.87886-68.058313.1283
12.3397-48.149513.9941	13.5483-50.495813.5167	8.80896-67.32613.0803
18.181-51.967316.4817	19.2652-54.04715.8917	14.1065-70.072715.6969
23.0222-54.740512.5222	23.7203-56.646111.8922	18.2855-72.323812.718
24.5128-52.477912.7731	25.1021-54.537811.8256	19.671-70.530912.357
23.4147-49.964412.7708	24.0061-52.37511.7204	18.7456-68.632812.0062
29.689-53.224110.1022	29.0873-55.10538.74904	23.1804-71.30979.66726

P. pyriformis CMC IP70972	P. pyriformis CMC IP70975	P. pyriformis CMC IP70978
7.86375-71.11919.93383	8.8516-71.724310.3016	11.3966-72.67710.7343
8.18874-72.282511.3125	9.45763-73.11511.2491	11.9654-73.725511.706
8.30927-69.342110.7037	9.31318-70.533811.1339	12.0212-71.333511.4074
9.2119-72.888612.7444	10.5226-73.860812.1256	12.5788-74.141712.5096
9.04552-72.377612.4752	10.7021-73.209912.1145	12.6176-73.711312.2391
9.38486-70.727211.9839	10.8428-71.741512.0066	12.7176-72.451611.9618
9.16003-68.999211.7514	10.4878-70.493612.0589	12.6362-71.342411.9831
9.27459-68.348111.5467	10.4001-69.929511.9787	12.6637-70.749211.9586
13.1655-70.349414.3841	14.7031-71.597613.4039	15.0305-72.125113.2617
16.787-72.824112.1595	18.5992-72.668311.0452	18.2998-73.362512.274
17.7768-71.122211.8125	19.2089-71.117211.0595	18.9452-72.025712.0359
16.9672-69.57811.1291	18.2403-69.742910.9199	18.2616-71.045511.7284
21.048-72.188110.0613	22.1435-70.89419.03197	21.2974-72.379510.7527

P. pyriformis CMC IP70973	P. pyriformis CMC IP70976	P. pyriformis CMC IP70979
7.3853-70.46069.01159	10.2681-72.19867.18016	11.5212-73.82039.92127
8.12216-72.138710.1423	10.8351-73.26357.97233	12.1605-74.398711.0863
8.51913-69.287810.0491	10.8308-71.06647.80148	12.0686-72.627810.458
9.5251-73.121711.1762	11.6131-73.82748.67467	12.5482-74.312211.3455
9.76407-72.258711.2552	11.596-73.14148.46613	12.5174-74.107511.2375
10.0697-70.799310.9966	11.5779-72.02978.27535	12.5304-73.361110.9141
9.79123-69.396411.2272	11.3873-70.94968.45029	12.4703-72.576810.7274
9.98118-68.591811.0612	11.3967-70.50898.38419	12.4844-72.300210.5808
13.928-70.993212.9234	15.0079-71.81339.80937	13.8655-73.169111.6646
18.301-73.06969.96888	18.8174-73.11637.03582	16.1715-74.146611.1396
19.1469-71.5119.9546	19.1625-71.68426.88503	16.6868-73.143410.8201
18.6066-70.0679.7229	18.3944-70.4586.60146	16.1709-72.344510.2941
22.548-71.92367.78885	21.7176-71.94994.64791	18.4182-73.67199.98438

P. pyriformis CMC IP70974	P. pyriformis CMC IP70977	P. pyriformis CMC IP70980
8.89591-71.5317.60593	10.9329-72.0199.49325	10.0498-73.5713.4837
9.54236-72.81388.68123	11.7294-73.219310.6337	10.5333-74.557714.1168
9.72408-69.9948.48229	11.5954-70.754910.4081	10.1746-72.624114.1052
10.7126-73.41759.9047	12.408-73.560411.0539	10.8362-74.721714.5525
10.509-72.78629.67955	12.4596-73.119611.1407	10.8195-74.516714.5213
10.5878-71.32949.34828	12.4642-71.895311.0264	10.6917-73.446514.4666
10.5928-69.76159.48009	12.4381-70.656411.1499	10.5381-72.633914.5328
10.7517-69.23139.32382	12.256-70.298811.0842	10.5-72.347814.5441
14.2661-71.054711.7085	15.194-71.816312.4174	12.7036-73.19916.143
18.4738-72.77389.87137	18.4961-73.102410.3803	15.7997-73.517315.1682
19.2172-71.22889.83126	19.0026-71.726310.3486	16.1074-72.157815.2397
18.2064-69.82289.38957	18.3994-70.676210.1635	15.4135-71.341914.6858
22.7131-71.71688.4042	21.4769-71.76648.89193	18.6433-71.941414.2692

P. spicatus CMC 70983
-3.55848-50.35799.77062
-4.3144-52.001611.1519
-3.77333-47.871211.3349
5.53683-58.420616.0548
1.60635-54.239417.1131
2.44818-50.994516.6263
2.75204-47.793617.3955
7.7018-44.901115.803
17.0145-53.043317.612
17.7021-57.932410.1298
19.3303-52.81148.72942
18.3102-49.17679.41001
19.8195-53.82963.66569

P. spicatus CMC IP70984
-6.65468-51.422211.5624
-6.58481-53.566712.8473
-6.95377-49.006612.5439
4.29717-57.792416.2206
1.19544-54.153518.5304
1.34041-51.215917.5346
0.819565-48.18218.4432
4.62742-45.026715.0631
15.8767-51.118817.3787
17.0764-56.660810.9304
18.8994-51.85159.36582
16.8148-47.54839.1938
20.9241-53.46533.62

P. spicatus CMC IP70985
-4.71107-52.866911.5943
-4.64568-55.154112.9392
-4.71632-50.755112.8187
6.52928-59.171714.9707
2.61415-55.730717.2778
2.8039-53.093816.5584
2.63653-50.562217.5661
6.53777-47.096615.3342
17.3683-53.196417.6211
17.3849-57.725210.0684
18.9121-52.5369.33048
17.5504-48.451810.1939
19.4183-52.95043.78729

P. spicatus CMC IP70986
-4.40372-52.88088.59953
-4.81493-55.056710.3794
-4.43395-50.839510.5231
3.92015-59.34413.969
0.631265-56.473615.7195
0.916147-53.79115.8941
1.04643-50.688615.9612
5.06851-48.436114.5463
13.4362-54.898618.965
15.4789-59.551312.7794
17.8521-54.783811.9431
16.5626-50.531212.537
20.4784-55.88217.21832

P. spicatus CMC IP70987
-2.61881-53.08869.20303
-3.07897-54.362510.5141
-3.11025-51.026310.6237
5.39493-59.416315.7885
1.37084-55.363416.6877
1.88149-52.705416.284
1.57304-50.041116.6441
5.00116-46.668315.3125
14.8101-52.650518.4934
15.9147-57.79111.9821
17.2528-53.130410.847
16.3829-49.148610.9643
18.1885-54.10655.82019

P. spicatus CMC IP70988
28.5387-53.884411.0946
28.585-51.909212.4916
28.6834-55.964712.1111
21.6355-48.408317.6346
24.3368-51.41218.2618
23.6209-54.002117.3144
24.1595-56.457118.2069
22.0885-59.556117.2475
11.1957-54.380422.2982
8.52352-49.584815.9601
6.68349-54.556715.3383
8.28949-58.587215.6377
4.45834-53.721910.0946

P. spicatus CMC IP70989
27.5687-55.085311.3728
27.7181-53.06212.3865
27.5393-56.938912.5787
19.4161-49.657516.1829
22.0858-52.516817.2861
22.0281-55.057116.9172
22.1699-57.518117.3494
19.8389-60.574616.4282
11.1149-55.561818.7964
9.76637-51.36213.2331
9.25061-56.220112.2111
10.6332-59.841112.8502
8.17578-55.92837.56991

P. spicatus CMC IP70990
25.6099-55.473214.6761
25.8526-53.659915.7428
25.7385-57.147515.8207
18.3993-49.692718.8623
21.6191-52.372319.8585
21.3761-55.085720.199
21.7239-57.575220.4784
19.0104-60.11419.9419
10.6313-54.613522.8769
7.89818-50.794716.1874
7.43262-55.444715.5543
8.38059-59.503816.5551
6.4261-55.498710.8524

P. spicatus CMC IP70991
24.9797-55.672415.2391
24.9143-53.951716.2234
24.8328-57.763816.186
17.5303-51.187818.0311
19.7461-53.291419.2793
19.5656-55.950719.0356
19.7981-58.343819.4071
17.6972-60.748118.0772
7.87424-56.409819.2585
7.58188-52.530913.5639
6.51344-56.708612.5787
7.33589-59.921813.2084
5.87128-56.30827.94851

P. spicatus CMC IP70992	P. spicatus CMC IP70995	P. spicatus CMC IP70998
24.6272-55.530714.1921	22.0787-58.702719.9907	11.8156-60.917912.5422
24.6516-54.037115.0049	20.9528-57.319120.5442	11.9228-62.484613.6082
24.6821-57.682815.032	21.231-60.495120.4522	11.9725-59.420313.648
17.4876-50.885517.9281	16.9521-55.544417.8835	14.76-63.74415.3119
20.5429-53.600118.8435	17.3366-57.101919.3824	13.7415-62.453715.3766
20.1529-56.02718.1106	17.6077-59.177918.6607	13.7087-60.843415.146
20.5436-58.347718.7232	17.7262-60.982418.9949	13.5417-59.218915.3918
17.9214-61.081117.6615	17.463-62.910316.5692	14.7423-58.053115.305
9.43691-56.424420.3167	12.63-59.396112.6793	18.6351-60.85417.1189
6.90058-52.189514.4481	15.9201-55.51319.75772	19.9982-63.319714.2967
5.90745-56.648813.0218	16.8725-58.63068.51404	20.9414-60.756213.6875
7.77387-60.188213.8224	16.9706-61.63279.14299	20.1514-58.771814.005
4.91373-55.7058.53324	19.4204-57.70066.65154	22.0877-61.02811.1019

P. spicatus CMC IP70993	P. spicatus CMC IP70996	P. spicatus CMC IP70999
25.893-57.785315.1356	10.3569-59.672411.14	13.7823-61.418413.7515
25.4989-56.270816.2448	10.3644-60.980712.2372	13.8651-62.75814.0449
25.414-59.54216.059	10.7284-58.050112.3961	13.8613-60.219214.3372
20.1526-53.398318.4685	14.8567-62.951214.6742	16.6392-64.239515.4107
21.8573-55.486119.0767	13.6124-61.587815.008	15.2852-63.091515.5205
21.6329-57.723318.4958	13.6924-59.712914.7898	15.3203-61.691415.5106
21.601-59.968918.8146	13.7498-57.882114.9062	15.4604-59.9515.7847
19.5754-61.806318.0936	15.7328-56.783414.6145	16.7025-58.629515.8693
12.1616-57.164819.6659	21.115-59.998416.6699	20.2653-61.9917.1179
10.9025-53.325815.0916	21.6408-62.535213.6563	21.5038-63.832514.3582
9.24709-57.502713.668	22.6153-59.699513.1333	22.3921-61.648113.722
10.4079-61.116214.4696	22.1126-57.544213.4485	21.6765-59.441214.4557
8.5908-56.91039.26321	23.0706-60.001710.2307	23.1739-61.947211.4294

P. spicatus CMC IP70994	P. spicatus CMC IP70997	P. spicatus CMC IP71000
20.0907-58.779623.4805	11.0474-59.866112.9801	11.822-61.288312.8154
19.4312-57.267824.0455	11.5212-61.225314.2977	12.0816-62.537313.6011
19.1196-60.328423.7189	11.6971-58.248213.9473	12.0372-60.007413.5467
14.5894-53.840621.5729	15.2023-62.977516.1132	14.1978-63.779115.1648
14.98-56.325122.6603	14.247-61.588416.2369	14.0355-62.819915.3252
14.853-58.449522.2234	14.417-59.792115.8013	14.0209-61.31915.3385
14.8038-60.43922.4886	14.4821-57.793716.0204	14.2167-59.674115.4945
14.2055-62.403220.3732	15.6684-56.641515.3062	14.7996-58.534515.3668
9.23176-57.378616.2403	20.4439-59.960517.4076	19.2852-61.311417.1803
12.5232-53.440711.4239	22.0681-62.95513.7018	20.7839-63.340614.6874
12.2298-57.76389.38853	23.0746-60.31712.7916	21.5415-60.910914.1912
12.6299-60.717210.1033	22.2181-58.029912.956	20.8688-59.155714.4236
15.6739-56.47436.05937	23.9583-61.00049.97491	22.438-61.376612.0895

P. symmetricus CMC IP71003	P. symmetricus CMC IP71006	P. symmetricus CMC IP71009
15.6504-61.10046.4619	13.8816-64.02678.56606	17.2652-64.761525.9003
14.3864-63.29857.48112	12.7351-65.28319.5878	16.4814-63.151225.6027
14.0297-59.2917.5296	12.7363-62.28359.89215	16.1086-65.891125.5013
13.2622-65.651412.1182	12.2855-66.632513.9264	14.2641-61.515923.368
13.0639-64.110410.8115	11.7804-65.37513.3273	14.3165-62.606823.5989
12.7168-61.661110.9585	11.7158-63.603113.1871	14.0222-64.199123.4152
12.3769-59.407711.4787	11.8023-61.929213.2368	13.7746-65.885623.5529
13.0525-57.700212.2804	12.7797-60.809313.5154	13.3676-66.931122.6597
12.2494-62.30719.869	12.5219-63.684919.9536	10.5522-63.479617.3953
18.0999-65.172622.952	17.4124-65.166423.1131	12.5611-62.420512.5625
18.3304-62.022124.2836	17.3884-63.374423.5647	12.2557-63.732711.8626
18.0296-59.424423.2518	17.4968-61.731222.259	12.5807-65.53512.5479
22.6585-62.03727.3457	21.0275-63.663125.8956	14.1927-64.00817.31184

P. symmetricus CMC IP71004	P. symmetricus CMC IP71007	P. symmetricus CMC IP71010
10.0951-62.13697.43317	11.969-63.08779.47394	17.0046-64.848825.2912
8.81479-63.93688.40082	10.6703-64.432610.7383	15.5268-63.258425.3606
9.21865-60.54748.25707	11.1525-61.457310.6655	15.662-66.296924.9218
7.51777-65.676313.3315	10.1878-66.173314.6909	13.4324-61.794723.5969
7.52495-64.171212.2804	9.90336-64.774714.4366	13.4618-62.915824.1284
7.59978-62.064412.3121	10.0001-63.086914.501	13.5159-64.754124.0463
7.5579-59.978112.5629	10.3006-61.288314.6651	13.2573-66.308623.9878
8.27318-58.508613.2356	10.7946-59.92114.9627	13.3415-67.179523.5265
6.61017-62.067119.6078	10.1755-63.246119.9665	9.72712-64.093918.9688
11.9664-65.028524.3561	15.1517-66.128423.2521	11.7298-61.920614.8656
12.6411-62.268225.6538	16.1327-63.676724.6192	11.2699-63.575713.1406
12.7321-59.981724.2563	15.8528-61.320523.2685	11.58-65.410514.0655
17.2215-63.017729.145	19.8437-64.436327.1378	12.8218-63.01859.70817

P. symmetricus CMC IP71005	P. symmetricus CMC IP71008	P. symmetricus CMC IP71011
11.9497-63.07638.85746	15.27-63.41348.59912	24.8711-65.897310.0648
10.9421-64.710810.0495	14.1967-65.40989.57485	24.0764-67.033610.8416
11.0842-61.40549.87104	14.2172-62.0529.486	24.5922-64.537110.6968
10.4012-65.981212.8598	13.269-66.599712.5974	23.8172-67.896912.8616
10.3706-65.177712.5916	12.969-65.651412.1464	23.744-67.300612.6859
10.2163-63.082712.54	13.0585-63.663612.2087	23.9663-65.744612.6665
10.2451-61.158412.7475	13.0507-61.875712.0922	24.106-64.479812.7648
10.5015-60.087913.2376	13.5772-60.624412.576	24.4237-63.768512.7674
10.9053-63.076320.2408	13.053-63.856118.8432	24.9206-65.675417.0418
15.7974-65.497622.327	17.4778-65.996321.3657	28.0971-67.227118.4651
16.7039-62.951623.6673	18.2937-63.634222.3528	29.0103-65.632319.1408
16.0895-60.748222.3127	18.0753-61.479521.3092	28.915-64.158618.1752
20.291-63.283525.057	21.2169-64.097524.261	31.7027-65.978120.6161

P. symmetricus CMC IP71012	P. symmetricus CMC IP71015	P. symmetricus CMC IP71018
4.22405-54.09399.69331	6.39305-55.920810.1038	7.93147-55.780511.4309
4.9803-55.617711.1814	7.14279-57.466710.6637	8.55233-57.287812.1636
5.21845-52.307310.9276	7.24579-54.569710.9974	8.67245-54.674912.3197
8.35016-56.781312.6686	7.91119-58.412611.2423	9.70393-58.050712.8885
7.85256-55.91512.7257	8.06028-57.583911.2659	9.61019-57.400612.8037
7.80144-54.012212.6465	8.07143-56.141511.4799	9.59791-55.999312.9163
7.88487-52.027512.4895	8.24315-54.74511.8229	9.63034-54.568113.0759
8.74211-50.983112.0693	8.24395-54.288411.8656	9.74174-54.044913.1648
15.9344-53.97313.4971	11.3229-56.503912.4817	13.0319-55.993413.8484
19.0207-56.16389.84895	14.997-58.13589.95642	16.413-57.733811.236
19.8354-54.03239.56147	15.9074-56.760910.2539	17.7201-56.095411.0893
18.8511-52.33829.08161	15.6563-54.8569.95448	16.7188-54.562911.2015
22.5586-54.73886.81458	19.0259-56.49658.27587	20.1118-55.93668.83117

P. symmetricus CMC IP71013	P. symmetricus CMC IP71016	P. symmetricus CMC IP71019
7.50478-54.93910.3865	9.17335-56.599610.1162	8.10251-71.964910.0175
8.11154-56.657411.2517	9.86032-57.51610.9316	8.35807-73.131710.5742
8.68037-53.37211.4961	9.71629-55.015410.7115	8.7193-70.78410.2936
9.77937-57.686512.1598	10.7198-58.15411.7777	8.90561-73.466411.1633
9.71501-56.809912.327	10.9904-57.64411.9006	8.99406-73.082111.1422
9.89171-55.167612.4564	10.7376-56.285811.6729	9.17959-71.722211.0394
10.1365-53.57812.563	10.453-54.910711.6617	9.51916-70.741711.0137
10.2851-52.72112.2852	10.3203-54.480511.458	9.28178-70.448510.672
14.7402-55.499113.3764	13.8237-55.80913.2357	11.9942-72.195112.2773
17.531-57.49869.93683	18.0158-56.692110.9164	15.0838-73.86411.0839
18.5133-55.9239.97867	18.3231-55.330810.9807	16.1229-72.63310.6898
17.5364-54.034210.4211	17.1679-54.098510.7713	15.3672-71.365910.4515
20.7141-55.38147.47536	20.4675-55.24199.64	18.2626-73.01919.3721

P. symmetricus CMC IP71014	P. symmetricus CMC IP71017	P. symmetricus CMC IP71020
9.33126-55.92979.95974	8.52208-55.033512.5807	8.39982-72.08553.71852
10.0056-57.194710.9874	8.88081-56.278113.4626	8.60452-73.38044.29982
10.0242-54.448610.7903	9.31923-53.913713.5835	8.67313-71.08884.39138
11.6981-58.066111.8602	10.7625-57.295814.2857	9.33614-73.99885.25404
11.3128-57.12611.7998	10.7175-56.54314.2891	9.37017-73.48495.14588
11.2484-55.853611.601	10.9063-55.171214.2792	9.35031-72.15655.26545
11.2838-54.360111.6063	11.1818-53.837214.2873	9.39236-71.0925.38078
11.389-53.65611.4719	11.2408-53.177314.1147	9.51478-70.69975.50647
14.687-55.630812.5184	16.0205-55.752914.5676	11.9687-72.3486.91077
17.758-57.16649.72608	17.1035-57.449511.884	14.8287-73.55165.90484
18.6404-55.75239.3566	17.6915-55.794611.599	15.5334-72.13286.05453
17.4958-54.12959.5253	17.2006-54.595511.5643	14.8451-71.02395.8682
20.96-55.71286.51691	19.0949-56.11169.52198	17.9455-72.24625.30407

P. symmetricus CMC IP71021	P. tulipiformis CMC IP71024	P. tulipiformis CMC IP71027
12.3714-73.41115.08668	4.35862-68.475810.5652	6.70537-68.874512.4109
12.8392-74.36825.70369	4.19751-69.875911.8973	6.63306-70.23413.5169
12.5748-72.54595.62471	4.5708-67.023211.6729	7.06618-67.280413.2278
13.1787-74.396.05417	8.0222-71.943115.0035	10.7452-72.131616.2725
13.1991-74.14986.08893	7.46443-70.186714.9899	10.1387-70.447616.5981
13.1079-73.32926.07058	7.93531-68.385914.5486	10.4574-68.835616.3697
13.1202-72.40326.17563	7.78663-66.576414.7941	10.4031-67.079316.5496
12.9832-72.10076.13824	9.01523-65.018214.327	11.6717-65.796215.9133
15.0433-73.16037.26296	14.4664-68.935916.6724	15.2392-69.226518.0711
18.0584-74.19696.32187	17.258-71.719613.4776	17.7077-72.039615.7565
18.7808-73.03336.24044	18.3665-69.239912.8751	18.8216-69.608515.2464
18.0499-71.99396.14055	17.9407-66.981113.0405	18.2359-67.57815.3633
21.1074-73.10955.50131	19.1526-69.935210.4533	20.1575-70.307213.3282

P. symmetricus CMC IP71022	P. tulipiformis CMC IP71025	P. tulipiformis CMC IP71028
11.503-73.959312.3278	5.44049-68.098211.5256	5.91189-69.45613.6694
11.7812-74.642312.9546	5.63989-69.612112.9706	6.40912-70.725414.9314
11.9047-72.957112.8778	6.01919-66.091912.7045	6.73664-67.925514.8097
12.0468-74.80213.1467	9.89649-71.511115.0118	10.1126-72.207216.9333
12.3348-74.467913.3305	9.34043-69.979115.5877	9.62981-71.001916.7994
12.3394-73.664913.2852	9.65309-68.263215.255	9.71602-69.422716.5378
12.393-73.031513.2869	9.67702-66.414815.6976	9.91472-67.891916.6375
12.3366-72.761913.2126	10.6937-65.029514.6942	10.4846-66.680516.2589
13.8479-73.67113.7913	15.7295-69.208216.8119	14.4861-69.621318.1298
15.4375-74.375412.9359	17.78-71.750712.72	18.1929-72.52615.4738
15.8372-73.682112.8075	18.7147-69.473212.3898	18.6841-70.166514.9377
15.3984-73.064412.7697	18.214-66.852212.6335	18.4593-68.11614.696
17.1358-73.692611.8565	19.4425-69.84729.41233	19.5548-70.62513.258

P. tulipiformis CMC IP71023	P. tulipiformis CMC IP71026	P. tulipiformis CMC IP71029
4.00678-68.043711.551	6.52753-69.804411.3552	7.81402-68.807713.4505
3.93554-69.558112.84	6.72076-71.280312.7138	7.84136-70.350914.3552
4.13411-66.521712.721	6.86405-68.348512.6389	8.21145-67.484614.7166
9.30934-72.334816.1518	10.4134-73.049614.9197	11.1302-72.62116.4022
8.28927-70.2216.435	9.5053-71.730614.8486	10.3084-71.044216.7149
8.49722-68.227816.1641	9.68681-69.941414.866	10.638-69.364516.6972
8.29674-66.364416.4852	9.41665-68.329614.9501	10.7829-67.979917.0992
9.60241-64.519816.141	10.6247-67.092214.8957	12.061-66.663616.6204
15.7917-68.507818.1857	14.9448-70.247716.437	15.2872-70.302118.4301
18.7299-71.042114.9309	18.2532-72.363814.2182	17.8651-72.72315.529
19.2913-68.27114.5875	18.9252-70.36113.9174	18.7656-70.387915.1215
18.534-65.968814.7949	18.3165-68.430614.0115	18.2238-68.353215.4908
20.5942-68.543412.003	20.0197-70.730311.9461	19.9224-70.755213.0808

P. tulipiformis CMC IP71030
6.72874-69.157211.7906
6.54982-70.380312.5749
6.77132-67.981912.6307
9.69729-72.499915.1753
9.2434-71.19415.4022
9.48812-69.504815.3128
9.57163-67.988515.6809
10.516-66.843815.3979
14.6872-70.417617.1719
16.4329-72.701114.6277
17.5013-70.899614.3871
17.094-68.922414.7528
18.2289-71.130212.3125

P. tulipiformis CMC IP71031
7.69825-70.45813.2874
8.14081-71.584614.7444
8.49925-69.055114.2192
11.0344-73.034216.4634
10.1952-72.034916.3284
10.4314-70.456215.9008
10.3048-68.823915.9613
10.937-68.110215.6492
14.1662-70.493417.3886
17.6518-72.980215.1336
18.416-71.014914.7959
17.7484-69.589314.7675
19.6928-71.47512.7217

P. tulipiformis CMC IP71032
7.62197-70.183512.7676
7.73308-71.503313.7303
8.1575-68.764213.9173
10.3865-73.225915.401
9.91179-72.191915.3424
10.244-70.462715.4446
10.1862-69.014415.7138
11.2964-67.915715.504
14.811-70.754916.2854
17.5481-72.672113.4799
18.083-70.935113.4425
17.7238-69.132613.4268
19.0477-70.855411.4769

P. tulipiformis CMC IP71033
8.78672-70.727714.7349
8.65561-71.876216.0594
9.05774-69.234215.6565
10.5309-72.99117.8996
10.0017-72.143617.6882
10.2431-70.556117.2245
10.2741-69.011317.3253
11.0012-68.202217.1158
13.4711-70.73718.7108
15.658-72.877216.9338
16.4012-71.127416.3983
16.114-69.730816.3253
17.3787-71.795914.7871

P. tulipiformis CMC IP71034
8.59634-71.168213.6501
9.02322-72.212315.0219
9.35808-69.604914.7183
11.197-73.031516.5385
10.7015-72.115516.3989
10.8348-70.665816.0622
10.8274-69.335516.1734
11.5052-68.343415.6043
14.4818-70.524117.4232
16.9783-72.514615.4928
17.7149-70.840714.5132
17.0117-69.294314.4929
18.577-71.555213.4064

P. tulipiformis CMC IP71035
6.60112-71.06675.46442
7.06841-72.42416.68561
7.07177-69.67926.53078
9.80986-73.37358.27565
9.16886-72.50388.19972
9.32452-71.09837.49103
8.91594-69.49758.16983
9.29941-68.76867.83475
13.1116-71.12919.78416
15.392-73.07847.99991
16.1185-71.07967.48492
15.3662-69.41117.51347
16.9776-71.57115.57529

P. tulipiformis CMC IP71036
8.48781-71.544111.2504
8.57154-72.924212.1192
8.82612-70.434712.253
10.3645-74.19113.4589
10.0016-73.509313.4766
10.2629-71.776513.4063
10.243-70.453113.8398
10.7456-69.837713.8821
14.2098-72.340314.922
15.8765-73.75412.992
16.5431-72.072512.9458
16.0424-70.743713.2282
17.3292-72.262411.4464

P. tulipiformis CMC IP71037
10.8975-71.973811.3831
11.0294-73.197712.7052
11.5667-70.773212.1805
11.806-73.660413.6004
11.7183-73.274213.3952
12.0263-71.850812.9736
11.9936-70.777312.9672
12.2153-70.18712.8206
14.799-71.653814.5792
17.0145-73.438213.3519
17.5037-72.033412.851
16.7456-70.694312.8376
18.429-72.353611.401

P. tulipiformis CMC IP71038
7.6653-71.867910.795
8.17094-73.145911.7657
8.35272-70.654111.6058
9.80748-73.949312.7678
9.53854-73.208612.6966
9.8378-71.784712.5122
9.71837-70.337212.6208
10.2419-69.770512.4046
13.4112-72.00513.1188
14.9417-73.975611.2251
15.7018-72.314510.5263
15.3674-71.006510.5985
16.2574-72.89428.94251

P. tulipiformis CMC IP71039
8.3966-72.031510.6193
9.16132-73.395911.9117
9.40758-70.701511.7799
10.8112-74.193112.9688
10.6857-73.593612.8954
10.8529-72.207612.6055
10.9632-70.838712.9066
11.069-70.068212.764
13.8823-72.273313.664
15.6786-73.597912.0019
16.3965-72.137511.4821
15.7938-70.806511.6926
17.1415-72.530110.1815

P. tulipiformis CMC IP71042
10.9014-73.83813.3682
11.1937-74.542114.0175
11.1896-72.896513.7444
11.7757-74.782714.5617
11.6966-74.559414.4579
11.7144-73.598614.2164
11.6835-72.745514.2806
11.7978-72.536314.2944
13.7772-73.305214.9917
15.0632-74.076913.8315
15.2555-73.366313.7101
14.7199-72.508213.4343
16.0557-73.491112.6213

P. tulipiformis CMC IP71040
10.072-73.552811.563
10.5216-74.476912.6379
10.3597-72.410612.2685
11.1994-75.004113.3892
11.2036-74.465213.2566
11.2033-73.28212.9568
11.16-72.097913.2669
11.0966-71.764513.1599
13.5889-73.046814.2591
15.6287-74.24413.0184
16.0277-72.918412.8504
15.45-72.00412.7179
17.176-73.063611.9335

P. tulipiformis CMC IP71041
9.05733-72.9115.9602
9.32839-73.719416.8406
9.34846-71.812316.598
9.90388-74.154317.4671
9.91247-73.833617.4322
10.057-72.80517.257
10.0384-71.780517.4401
9.99219-71.29517.2936
12.6411-72.656818.3551
14.314-74.181717.0557
14.9513-72.68616.7743
14.3901-71.743916.8849
16.0192-73.239815.7987

APPENDIX VI

CHARACTER LIST

1. Globular thecal shape Absent (0); Present (1).

2. Distal Ambulacra length/width relationship L>W (0); L>>W (1).

3. Proximal ambulacra length Short (0); Elongate (1).

4. Non heteromorphic ambulacral outline shape Parallel-sided (0); Lanceolate (1); Oblanceolate (2); Rhombiform (3).

5. Shape of ambulacra, proximal to distal Straight (0); Convex (1).

6. Abaxial surface of ambulacra Flat (0); Concave (1); Convex (2).

7. Interambulacral shape in summit view Concave (0); Convex (1).

8. Ambulacra position with respect to surrounding thecal plates Even with surrounding plates (0); Seated above surrounding plates (1); Seated below surrounding plates (2).

9. Lancet shape Button (0); Elongate (1).

10. Lancet exposed between sideplates Absent (0); Present (1).

11. Lancet-sideplate contact Sideplates overlap lancet (0); Sideplates abut lancet (1).

12. Reduced D ambulacra length Absent (0); Present (1).

13. Ambulacra project below basals Absent (0); Present (1).

14. Ratio of plates surrounding ambulacra oral > radial (0); Radial > oral (1); Approximately equal (2).

15. Radial/oral relative positions oral overlaps radial (0); Radial overlaps oral (1); oral abut radials (2).

16. Radial/oral relative size oral > radial (0); Approximately equal (1);

Radial > oral (2).

17. Aboral radial sutures Recessed (0); Flat (1).

18. Oral plate ornamentation Nodes/pustules (linear arrays) (0); Nodes/pustules (no pattern) (1).

19. Oral plate body Absent (0); Present (1).

20. Oral plate crest Absent (0); Present (1).

21. Radial Plates project above summit Absent (0); Present (1).

22. Radials project below basals Absent (0); Present (1).

23. Widest portion of radial Adoral (0); Medial (1); Aboral (2).

24. Ambulacra recumbent Absent (0); Present (1).

25. Lateral food grooves curve adorally Absent (0); Present (1).

26. Endothecal respiratory structure Absent (0); Present (1).

27. Exothecal respiratory structure Absent (0); Present (1).

28. Number of respiratory fields 8 (0); 9 (1); 10 (2).

29. Respiratory structures exposed above side plates Absent (0); Present (1).

30. Type of respiratory structure (covered by side plates) Hydrospire Cleft (0); Hydrospire Pores (1).

31. Number of individual respiratory folds/slits per field 1 (0); 2 (1); 3+ (2).

32. Number of hydrospire pores per side plate 1 (0); 2+ (1).

33. Hydrospire cleft length <50% of ambulacra (0); Approximately half length of ambulacra (1); >50% of ambulacra (2).

34. Placement of hydrospire slit Hydrospire slits on orals and radials

subequally (0); Hydrospire slits primarily on orals (>50%) (1); Hydrospire slits primarily on radials (>50%) (2).

35. Hydrospire ducts Absent (0); Present (1).

36. Position of azygous basal AB interray (0); DE interray (1).

37. Epideltoid (O1) Exposed (0); Concealed (1).

38. Epideltoid (O1) borders anus No (0); Yes (1).

39. Cryptodeltoid Absent (0); Present (1).

40. Cryptodeltoid size Small (0); Large (1).

41. Anus bordered by hypodeltoid (O7) and epideltoid (O1). Hypodeltoid (O7) bordering >50% (0);Hypodeltoid (O7) and epideltoid (O1) bordering subequally (1); Epideltoid (O1) bordering >50% (2).

42. Anus bordered by hypodeltoid (O7), epideltoid (O1), and cryptodeltoids All deltoids expressed at surface (0); Hypodeltoid (O7) and epideltoid (O1) expressed at surface (1); Hypodeltoid (O7) and cryptodeltoids expressed at surface (2).

43. Anus bordered by hypodeltoid (O7) and radials Absent (0); Present (1).

44. Inflated hypodeltoid (O7) Absent (0); Present (1).

45. Oral plate project above summit Absent (0); Present (1).

46. Anus position with respect to spiracles Anus confluent with spiracle(s) (0); Anus separate from spiracle(s) (1).

47. Non-anal side spiracle manifestation Single (0); Paired (1).

48. Distal basal shape (basal view) Circular (0); Triangular (1); Pentagonal (2).

49. Columnal type Flat (0); Elongate (1).

VITA

James (Will)iam Atwood was born in Danville, Kentucky to Jerry and JoAnn Atwood. Will was raised by his parents in the neighboring town of Stanford, Kentucky. Will's only sibling is his older brother Jay Atwood. Some of his favorite memories growing up were of playing pinochle with his family and being outside.

Will graduated From Lincoln County high school in 1994. After high school he worked and did nothing fruitful with his life until he joined the United States Navy in 1997. While in the navy, as a quartermaster (navigation), Will excelled making rank as well as teaching himself celestial navigation. He was honorably discharged from the navy in 2001 with two Navy and Marine Corps achievement medals.

After a small hiatus Will started his undergraduate degree at Morehead State University, in the fall of 2002, where his brother was going to school. Not knowing what to choose as a major, he enrolled in classes that just seemed appealing. While in his first semester at Morehead, he did well enough in his astronomy class that he was offered a job at the astronomy laboratory as a telescope operator. Will switched his major to space science by the next week. By the time he graduated in the fall of 2008 he was the primary telescope operator for the 21m radio telescope conducting research on the microvariability of active galactic nuclei and had taken two field excursions to the high-arctic to study the geology of an impact crater in conjunction with NASA and the CSA. As an undergraduate Will received nine academic awards at Morehead, three for meeting presentations (national and regional) and six departmental.

After graduating from Morehead, Will went to the University of Tennessee to study aerospace engineering. Once at the university he had a change of heart and by chance was given a teaching assistantship in the geology department. Will had taken geology classes at Morehead so

the decision to become paleontologist was an easy one. While at Tennessee Will joined the Assembling the Echinoderm Tree Of Life team being able to contribute a section on echinodermata. In the August of 2012, Will was given a chance to join a group of international paleontologists to investigate Devonian rocks in Mongolia. As a result, he went on to spend almost a month in Western Mongolia doing research. After returning from Mongolia Will moved to Lexington Kentucky to be near loved ones and has no idea what the future holds. He wins.